5-2021

Gravel Geology and Muskoxen Paleontology of a Late Pleistocene Fossil Site in Saltville, Virginia

Nickolas A. Brand
East Tennessee State University

Gravel Geology and Muskoxen Paleontology of a Late Pleistocene Fossil Site in Saltville, Virginia

---

A thesis

presented to

the faculty of the Department of Geosciences

East Tennessee State University

In partial fulfillment

of the requirements for the degree

Master of Science in Geosciences, Paleontology

---

by

Nickolas A. Brand

May 2021

Dr. Blaine W. Schubert, Co-Chair

Dr. Chris Widga, Co-Chair

Dr. Michael J. Whitelaw

Keywords: Saltville, Pleistocene, muskoxen, gravel, debris flow

ABSTRACT

Gravel Geology and Muskoxen Paleontology of a Late Pleistocene Fossil Site in Saltville, Virginia

by

Nickolas A. Brand

Two distinct studies within the Saltville Valley of southwestern Virginia revealed insights into local Pleistocene geology and paleontology. A variety of analytical techniques were applied to gravel deposits within the paleontological site of SV-5/7 that revealed this unit is very poorly sorted, has a subangular matrix, and contains significant components of silt and sand in addition to rounded cobbles. These results suggest that rather than being deposited by fluvial processes as previously suggested, these gravels were likely the result of one or many debris flows. Additionally, the identity of fossil muskoxen from Saltville was reassessed using cranial and dental material. The results of the comparative anatomy of *Bootherium* and *Ovibos* specimens suggest that it may be possible to distinguish between fossil muskoxen genera using teeth, and to a lesser extent, cranial measurements. This analysis reaffirms that *Bootherium* is the only muskoxen definitively known from the Pleistocene of the Saltville Valley.

DEDICATION

This thesis is dedicated to all those who have stood by me through the process of completing this project, as well as to those giants whose shoulders provided the foundation for its completion.

ACKNOWLEDGEMENTS

This thesis could not have been completed without the support of others. Dr. Chris Widga has truly been an invaluable asset during the last few years — guiding me, pushing me, and always being willing to entertain distracting conversations about science or otherwise. Your mentorship, and friendship, will always be highlights of this endeavor. Dr. Blaine Schubert has been there through every step of this thesis and is the one directly responsible for pointing me towards Saltville gravels and muskoxen. You have always made sure that my project was both meaningful and grounded, and your feedback and discussions have made me twice the scientist I was before. Dr. Michael Whitelaw deserves thanks for joining an already fast-moving project, and always making time to help me despite an incredibly hectic schedule. I thank Matthew Miller of the National Museum of Natural History, Adam Pritchard of the Virginia Museum of Natural History and April Nye of the Gray Fossil Site & Museum for access to specimens. Additionally, I have had the privilege of working for and learning from April in the Gray Fossil Site collections and am grateful for having been given such an opportunity.

I sincerely thank my friends and family. Mom and Dad, thank you both for listening to me ramble and rant about rocks and fossils. I couldn't have done this without your support. My friends and colleagues from ETSU have made this experience all the better. I'll miss movie nights, museum trips, and Thursday night card games for years to come. Matthew Inabinett, your friendship has been crucial through these three years and I'm not sure I'd have made it out sane without you. Austin Gause, you saved this thesis with your help at the NMNH and kept my card skills sharp. I'm honored to call you my friend. Finally, I would like to thank Amanda Wilkinson. No typed words can express the impact your companionship has had during these last few years.

TABLE OF CONTENTS

LIST OF TABLES

LIST OF FIGURES

CHAPTER 1. INTRODUCTION

Introduction

Overview

This master's thesis addresses two very different aspects of the prehistory of Saltville, Virginia. Hypotheses of the depositional environment in which a gravel layer at site SV-5/7 formed are tested, and the identity of muskox fossils from the Saltville Valley is also assessed. The town of Saltville is located in southwestern Virginia (Fig. 1.) and is well known for its exceptional vertebrate fossils and historically important salt and gypsum deposits. Like the twofold nature of the town's natural history notoriety, the research contained and detailed within this thesis tackles two Saltville questions, one paleontological and one geological.

This first chapter reviews Saltville geological and paleontological research and provides a historical context for the research questions proposed in later chapters. This introductory chapter discusses relevant sites and discoveries and helps familiarize the reader with localities that are referenced throughout the thesis. It also reviews basic information about the time period represented by these fossils and provides a brief background on paleontological and paleoecological research that has occurred in the valley.

The second chapter focuses on the geology of the gravel layer at site SV-5/7. Historically, this gravel has been hypothesized to be the remnants of an ancient river, though recent observations suggest this may not be the case. A multidisciplinary study of the properties of this gravel is presented, with the goal of determining the mode of deposition.

The third chapter focuses on the paleontology of fossil muskoxen from Saltville. Muskoxen are a relatively common part of the Saltville paleofauna but there is some uncertainty in their generic and specific relationships. The available fossil material afforded the opportunity

to address two separate muskoxen questions at the same time. This chapter will provide identifications for indeterminate muskox material from Saltville. The steps taken to address this question make it possible to then examine morphological differences between two co-occurring North American muskoxen genera, *Bootherium* and *Ovibos*.

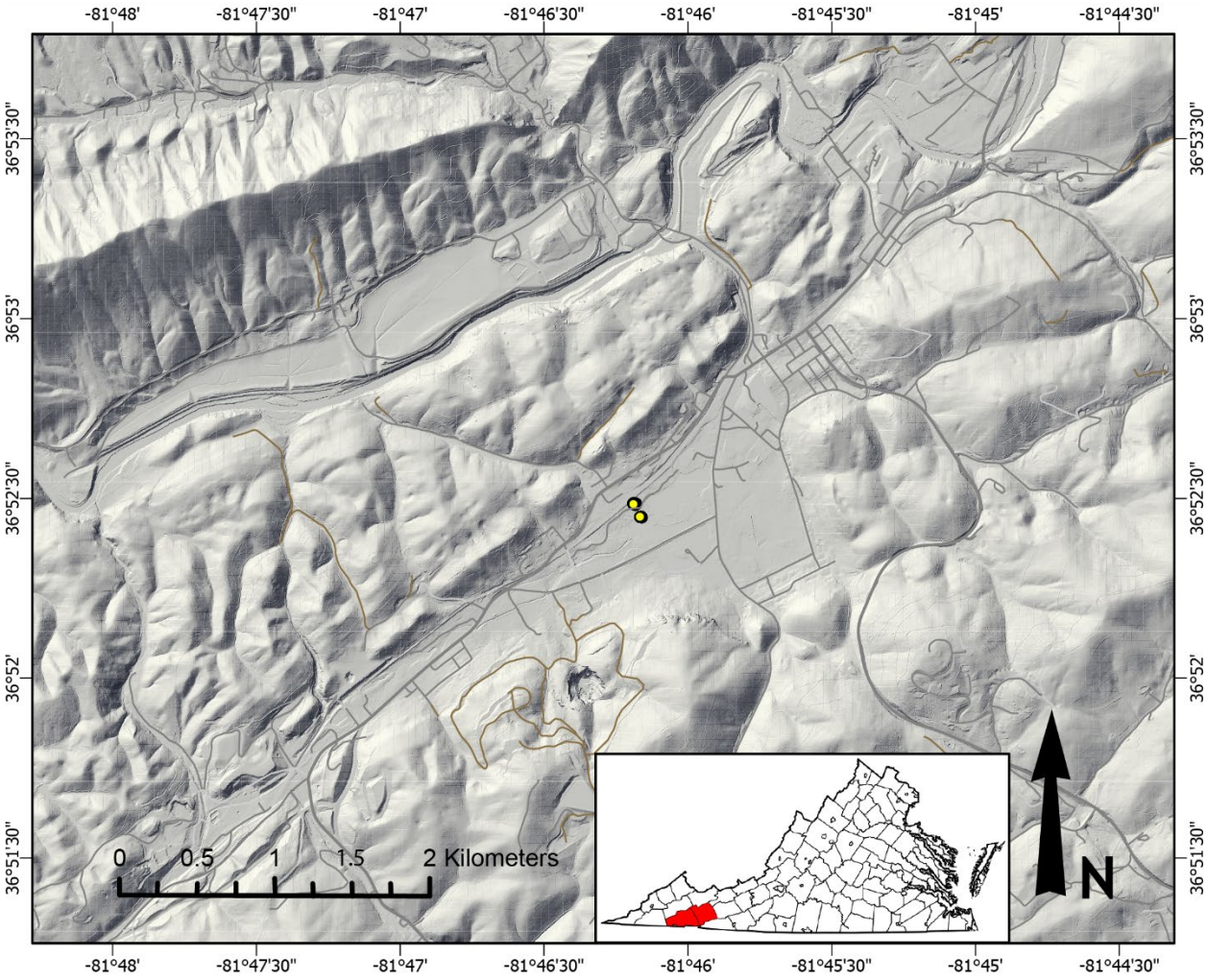

Figure 1. Hillshaded LIDAR map of the Saltville Valley. Inset shows location of Smyth County, Virginia. Yellow circles indicate active excavation sites (SV-5/7 and SV-10)

Saltville: A History of Salt and Fossils

The geological legacy of Saltville, Virginia extends back two and a half centuries to when former president Thomas Jefferson reported salt-brine and fossil remains from the area around Saltville (Jefferson 1781). Workers expecting to access a supply of salt water in 1840 created a deep shaft in the valley and discovered the first bed of rock salt in the eastern U.S. (Watson 1907). More wells quickly followed, and large-scale salt production began at Saltville. This Smyth County and Washington County town would go on to play a role in shaping the politics of the United States, as Saltville became a strategic target for the Union due to its salt production for the Confederacy during the Civil War (Whisonant 1996). Though the salt which gave the town its name would later be used to produce sodium hydroxide and sodium bicarbonate (Watson 1907), it also spurred an interest in the geologic history of the Saltville Valley.

Excavation History

Pleistocene fossils have been documented from Saltville, Virginia since at least the 18th century when Thomas Jefferson noted the occurrence in his book, *Notes on the State of Virginia* (1781). Saltville fossils were not professionally studied until the 20th century when Olaf August Peterson published the first paper on fossil remains from the valley (Peterson 1917). These remains were recovered from strata that were exposed when a well operated by Mathieson Alkali Works collapsed. The fossils from this recovery included *Mammut*, *Megalonyx*, and *Cervalces*, which hinted at the late Pleistocene age which would later be confirmed for valley fossil-bearing deposits (Peterson 1917; McDonald 2000; Schubert and Wallace 2009).

Decades later, paleontologists from the Smithsonian National Museum of Natural History

worked with scientists from the Virginia Polytechnic Institute to describe Quaternary faunal and floral remains from Saltville (Ray et al. 1967). Additional work was performed by Jerry McDonald, who collaborated with Charles Bartlett Jr., to describe an extinct muskox (McDonald and Bartlett 1983), before publishing numerous papers on the geology and paleontology of the Saltville Valley (McDonald 1983; McDonald 1985a; McDonald 1985b). McDonald would also excavate a purported archeological locality, making a case for Pre-Clovis human activities within the valley (McDonald 2000). McDonald began a numbering system to designate excavation localities in the valley, and he applied SV-1 to the muskox locality and SV-2 to the locality he interpreted as archaeological (McDonald 2000; Schubert pers. comm. 2020).

Excavations were continued by Ralph Eshelman from 1999 to 2003 for the Museum of the Middle Appalachians (MoMA) and he added SV-3 through SV-10 as excavation localities (Schubert pers. comm. 2020). Steven Wallace of East Tennessee State University (ETSU) continued excavation of SV-10 in 2003 and 2004 for MoMA. Blaine Schubert (ETSU) developed an agreement between MoMA, the town of Saltville, and ETSU so that excavated fossils would be curated in the ETSU Museum of Natural History collections (ETMNH). From 2008 on, Blaine Schubert has been in charge of ETSU's expeditions to Saltville to recover fossils, and he brought in Jim Mead and eventually Chris Widga (in 2016) to help lead excavations and research. SV-5, SV-7, and SV-10 (Fig. 2) have all been the subject of paleontological research in recent years, though significant changes were made to some of the localities. In particular, SV-5 and SV-7 were relocated and expanded by the ETSU crew under Blaine Schubert and have been combined into one locality now called SV-5/7 to differentiate it from the previous excavations. Table 1 summarizes the localities relevant to the thesis, as well as principal investigators responsible for excavation.

Table 1. Paleontological Localities Within the Saltville Valley. Includes Only Localities Discussed in the Text

Locality	Principal Investigators
SV-1	McDonald / Bartlett
SV-2	McDonald
SV-5	Eshelman
SV-7	Eshelman
SV-10	Eshelman / Wallace / Schubert
SV-5/7	Schubert / Mead / Widga

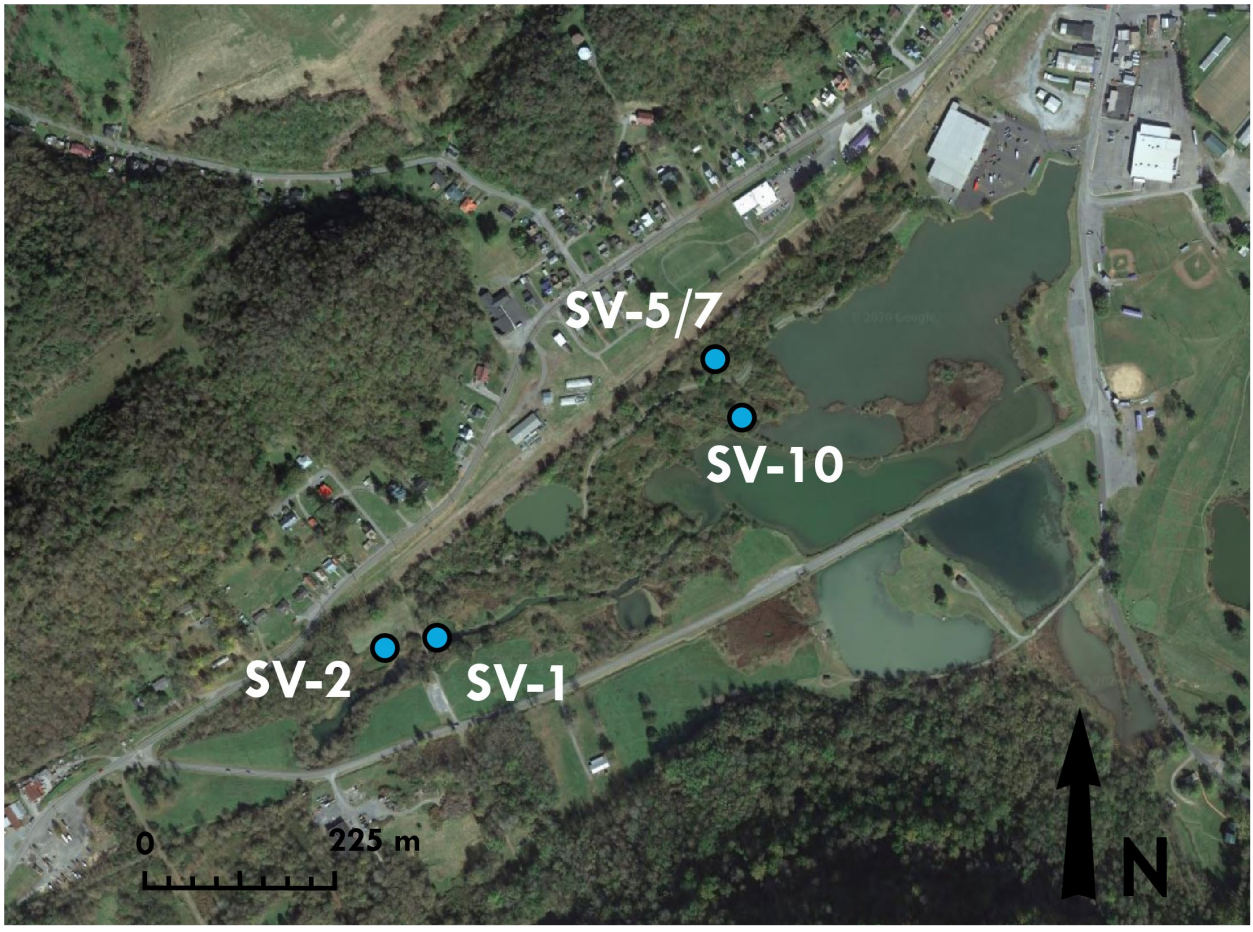

Figure 2. Google Earth satellite image of the Saltville Valley. Locations of relevant fossil-bearing localities are shown

Quaternary Fossils: Flora and Fauna

Within the Saltville Valley, most paleontological materials are concentrated within two geologic units. Fossils are found both in a gravel layer that spans much of the bottom of the valley (W4), and also in overlying silty and sandy sediments (W3) (McDonald and Bartlett 1983; Holman and McDonald 1986; Schubert and Wallace 2009). Some fossils contained within the gravel deposit are highly abraded, though many also have areas that are virtually unworn (Silverstein 2017). In contrast, some fossils recovered from above the gravel are incredibly well preserved (e.g., mammoth from SV-10), with little to no abrasion damage (Schubert pers. comm. 2020).

Pleistocene taxa that have been recovered from excavations at Saltville localities include: *Arctodus*, *Mammut*, *Mammuthus*, *Megalonyx*, *Cervalces*, and *Bootherium* (Schubert and Wallace 2009). Artifacts suggesting an early human presence have been reported as well (McDonald and Bartlett 1983: McDonald 2000). Vertebrate remains are primarily found in W3 and W4 and have been interpreted as representing a boreal fauna (Ray et al. 1967; McDonald and Bartlett 1983; Holman and McDonald 1986). A diverse herpetofauna containing salamanders, snakes, and turtles has been noted from units W2 and W3 (Holman and McDonald 1986). These are all taxa that are present in the valley today and it is not known if they were contemporary with megafauna found in W3 and W4.

Palynological analysis of sediment sampled from a fossil muskox cranium from Saltville by Ray et al. (1967) revealed that the paleoenvironment at the time of deposition was dominated by spruce and pine trees, but remained wet, and possibly flooded, year-round. Isotopic analyses of Saltville fossils have been performed by France et al. (2007) to examine megafaunal paleo-diets. Specifically, this study examined nitrogen and carbon stable isotope values of Saltville

megafauna, wherein they determined that the tested individuals were eating mostly C3 plants, that tend to do well in cooler, wetter climates (France et al. 2007). Further isotopic research utilizing fossil ungulate material from Saltville suggests that the paleoenvironment during the time of deposition contained an open forest habitat, and that temperatures were not particularly variable throughout the year (Simpson 2019). A recent thesis by Gause (2020) examined both the late Pleistocene and modern ostracode faunas from sites in the Saltville Valley, and hypothesized that the standing water within the valley was not always highly saline.

CHAPTER 2. GENESIS OF THE SV-5/7 GRAVEL DEPOSITS

Introduction

Overview

The concept for this thesis was introduced to the author when he attended a paleontological conference field trip to Saltville in 2017. The SV-5/7 site was visited during this trip, and the origin of the gravel unit was of primary interest to those working on the site. Collaborating with these researchers to understand this gravel unit became a primary goal of this thesis once work began. While previous researchers had interpreted these gravels as being deposited by an ancient river, paleontologists working at Saltville had seen no evidence for this at SV-5/7. Thus, this portion of the thesis was designed so that competing depositional models could be tested against each other to see which best matched the available data.

In order to provide the background knowledge necessary to understand the deposition of the SV-5/7 gravels, this chapter begins with a generalized discussion of the geology of the Saltville Valley. The Maccrady Formation, the most widespread bedrock formation across the bottom of the valley, is discussed, as are relevant Pleistocene sediment units which include the SV-5/7 gravels. After this section, a detailed research history of the gravels in the Saltville Valley is provided, with a section then focusing specifically on what is known of SV-5/7 and the gravels at that site. The introduction concludes with a description of potential depositional processes that are being tested in this thesis.

This review is followed by the methods section which covers how data were collected and analyzed, as well as a results section which relays the findings of those studies. A discussion section follows which details how the depositional models fit the results, how certain parts of the

study may be useful to continued research, and what limitations existed with this study. The most important results are presented in a short conclusion section which closes the chapter.

Geology of the Saltville Valley

The town of Saltville is located in southwestern Virginia and is a part of the Valley and Ridge Province of the Appalachian Mountains. The Valley and Ridge is characterized by a series of unmetamorphosed, folded and faulted, Paleozoic rocks that consist largely of epicontinental sea deposits (Kulander and Dean 1986). These laterally extensive layers form long, northwest trending ridges separated by valleys that give the province its name. As a part of this province, the basic geologic structure of the 1.5-mile-wide Saltville Valley is that of lower Mississippian shales and carbonates that have been folded into a syncline. The southern slope of the valley contains the Saltville thrust-fault, which thrusts Cambrian rocks of the hanging wall over Mississippian footwall rocks (Cooper 1966).

Cooper (1966) conducted the most detailed mapping and descriptions of the geologic units of the Saltville Valley, although the groundwork for his study was laid by Butts (1933). The large Greendale syncline forms the floor of the Saltville Valley, and consists of the folded Lower Mississippian strata (Cooper 1966). The geologic formations known from Saltville Valley, in order from oldest to youngest, are the Parrot Formation, Price Formation, Maccrady Formation, Little Valley Formation, Hillsdale Limestone, Ste. Genevieve Limestone, and the Gasper Limestone, all of which are Mississippian in age (Cooper 1966). On the north facing slope of the southern ridge of the valley, the Saltville Thrust has pushed much older Cambrian rocks over the Mississippian Maccrady Formation and caused extensive brecciation (Cooper 1966). Cambrian rocks on the northern slope of the Saltville Valley, from youngest to oldest, are the Honaker

Dolomite, Nolichucky Formation, and the Knox Dolomite (Cooper 1966). Resting atop the units of the valley floor is a covering of unlithified late Pleistocene sediments (Peterson 1917; McDonald and Bartlett 1983; McDonald 2000).

Of these rock units, the Maccrady Formation and the overlying Pleistocene sediments are the most relevant to the goals of this thesis. Geological and paleontological samples examined during the course of this study are contained within the Pleistocene deposits, which are underlain by the Maccrady Formation. Therefore, both the Maccrady Formation and the Pleistocene sediments are described in more detail in the following sections.

The Maccrady Formation

The Maccrady Formation is of particular interest to this study because it underlies Pleistocene sediments which have been the focus of recent geological and paleontological research. The Maccrady is a highly variable geologic unit and has been noted as being one of the most locally variable formations in the entire southern Appalachian Mountains (Cooper 1966). Within the Saltville Valley, this formation is particularly thick, with total bed thicknesses up to 1700 feet (Cooper 1966). The formation can be divided into 3 general units: (1) a basal sandstone and siltstone member, (2) a middle dolomite member, and (3) an upper, plastic shale member (Cooper 1966; Nelson 1973).

The sandstone and siltstone members are defined by the presence of red or maroon sandstone, siltstone, and shales. The base of the Maccrady is defined as the first maroon sandstone unit (Nelson 1973). The dolomite member is characterized by the presence of shaly dolomite that contains marine fossils (Cooper 1966) and is known to contain a small amount of quartz (Nelson 1973). The upper member, the plastic shale member, is characterized by red and green colored shales, containing gypsum and salt deposits in some areas, especially in the

vicinity of the town of Saltville (Cooper 1966).

Salt and gypsum deposits are only known to occur in the overturned Maccrady beds on the southern limb of the Greendale Syncline (Cooper 1966). The Saltville Fault thrusts Cambrian rocks over the Maccrady Formation, and some research suggests that the plastic nature of the shales may have facilitated this movement (Cooper 1966). In the Saltville area, it is the Honaker Dolomite that has been thrust over the Maccrady, although northeast of the town the Rome Formation is encountered as a poorly preserved unit (Cooper 1966).

At SV-5/7, the site of this study, the Maccrady Formation is represented by wet, disintegrating, colorful red and gray clays, which are intermixed with evaporite deposits. The lithology of the Maccrady at SV-5/7 has yet to be described in detail.

Pleistocene Sediments

Pleistocene and Holocene sediments overlying Paleozoic rocks in the Saltville Valley were first described by Peterson (1917). These sediments were identified as alluvium and described as an upper black soil underlain by a sticky clay with a gravel pavement base which frequently contained fossils (Peterson 1917). Subsequent excavations would provide better stratigraphic resolution for the Pleistocene sediments, as multiple fossil and potential archaeological localities in the valley were examined in more detail (Ray et al. 1967; McDonald and Bartlett 1983; Holman and McDonald 1986; McDonald 2000). The culmination of these studies provided a synthesis of the named stratigraphic units for the sediments. The following unit descriptions are largely adapted from the work of McDonald (1984b and 2000). The units were given designations based on their position and depositional age so that stratigraphic units with a "P" prefix were deposited in the Paleozoic, units with a "W" prefix have been interpreted as being deposited during the Wisconsin glaciation, and units with an "H" prefix were deposited

during the Holocene. It is important to note that all units are not necessarily of uniform distribution or depth throughout the valley. The following unit descriptions are based on observations that took place primarily at SV-1 and SV-2 (McDonald and Bartlett 1983; McDonald 2000), and may not be representative of the same units at other localities.

Unit P1 is the Maccrady Formation of Mississippian age. The lithology of the unit varies throughout the valley, although it usually consists of steeply dipping, weathered shales which have been interpreted as being scoured by Pleistocene erosional processes in some places.

Unit W4 is a gravel deposit which was interpreted as being of fluvial origin by Peterson (1917) and more specifically a fluvial lag gravel by McDonald (1984b) and McDonald (2000). This unit is known for containing abundant Quaternary fossils throughout the valley (McDonald and Bartlett 1983; McDonald 1984b; McDonald 2000; Schubert and Wallace 2009).

Unit W3 is a heterogenous unit consisting of silts, sands, and thin gravels, which has a characteristically sharp boundary with the underlying gravel of unit W4 (McDonald and Barlett 1983; McDonald 1983; McDonald 2000). Vertebrate bones are found in W3, and are common at the base of the unit, just above the contact with the W4 gravels. Radiocarbon dates on fossils recovered from units W3 and W4 indicate that they were deposited during the late Pleistocene (McDonald 2000). Schubert and Wallace (2009) examined potential scavenging traces on mammoth bones recovered from W3 in the nearby SV-10 locality, identifying *Canis* (perhaps *C. dirus*) and another large carnivoran (most likely *Arctodus*) as the likely agents of modification. This indicates that at least some bones contained within unit W3 were available for scavenging or feeding at some point before burial. The bones of a fossil muskox from SV-1 were also recovered from W3 and were reported to have “green” breaks (smooth-edged fractures which usually occur only on fresh bone), which was interpreted as being potentially indicative of

carnivore feeding activity (McDonald and Bartlett 1983). Additionally, the bones appeared to contain fossilized egg cases of a flying insect, which would indicate that they were above water and unburied long enough for them to be cleaned of soft tissue and the eggs to be laid (McDonald and Bartlett 1983). In both cases, parts of animal carcasses must have been accessible to local scavengers for some amount of time after death, suggesting that burial of organic matter was not an immediate process.

Unit W2 is a medium gray to brown and black mud, interpreted by McDonald (2000) as likely being deposited in lentic, or standing water conditions during the Pleistocene. This unit has been reported to have a thickness of up to 120 cm in some areas (McDonald 2000), and contains microvertebrate and plant remains (McDonald 1984b).

Unit W1 is a thinner, organic soil deposit ranging from 6 to 15 cm, and has been radiocarbon-dated to the latest Pleistocene at around 10,000 ^{14}C years before present (McDonald 1984b; McDonald 2000). In some places the boundary with W2 is sharp, and in other places it is disturbed and less well-defined (McDonald 2000).

Unit H2 is a medium gray lentic mud with darker blotches and streaks. It is differentiated from W1 by a sharp boundary and varies in thickness from a little over half a meter to nearly two meters (McDonald 2000). Almost no plant or animal remains are recovered from this unit (McDonald 1984b).

Unit H1 is the most recent sedimentary deposit in the valley and is the historic surface (McDonald 1984b; McDonald 2000). Thickness of this unit varies from 0.1 to 1.0 m. Mechanical removal of over-burden and historic land-use activities have removed this unit from parts of the valley and it is no longer present at all paleontological localities within the valley.

Research History and Hypotheses of Saltville Gravel Deposition

The first geologic description of Pleistocene gravels in the Saltville Valley was prepared by O. A. Peterson in 1917, when he visited a fossil site exposed by a salt mine well collapse. The gravel layer at this locality was identified as potentially Pleistocene in age based on embedded fossils of *Mammut*, *Megalonyx*, and *Cervalces* (Peterson 1917). Described as "a pavement of coarse gravel, pebbles and cobble-stones, some of considerable size..." (Peterson, 1917 p. 470-471), the deposit was interpreted as having been left by a river of substantial size based on the similarity of the gravels to those seen in streambeds (Peterson 1917). This river was believed to have picked up and redeposited the fossils that had been discovered at the well site.

Decades later the hypothesis that the Saltville Valley gravels were fluvially deposited was expanded upon and supported by a description of sediments from the site of a fossil muskox skeleton discovery (McDonald and Bartlett 1983). McDonald and Bartlett (1983) interpreted the gravels from this muskox locality (later named SV-1) as being from an active stream of at least moderate size. This interpretation was based on rounded rock clasts in the gravel, which formed a tightly fitting pavement. Additionally, it was noted that many of the bones that had been found as inclusions in the gravel layer displayed different degrees of abrasion (McDonald and Bartlett 1983), which is consistent with Peterson's interpretation of fluvially reworked deposits. These authors named this hypothesized ancient river the Saltville River, and it was proposed to have been a tributary of the North Fork of the Holston River (McDonald and Bartlett 1983), which runs through the Saltville Valley today.

Continued work by McDonald (2000) examined the gravel layer in a locality to the west of the muskox locality. This was designated the SV-2 locality and was reported to contain late Pleistocene archaeological materials. During the study of this locality, the gravels of the valley

floor were given the unit designation W4 (McDonald 1984a; Holman and McDonald 1986). Present at SV-1, SV-2, and other localities throughout the valley, the gravels were interpreted as being fluvial lag gravels (McDonald and Bartlett 1983; McDonald 2000), although no explanation was given as to how this conclusion was reached aside from a quote in a field trip guide to Saltville… "... its distribution and composition suggest that it is primarily of fluvial origin" (McDonald 1984b, p. 17). The ancient Saltville River was hypothesized to originate in the southwest of the valley and flow into the North Fork of the Holston River until 13,500 years before present when it was pirated by McHenry Creek (McDonald and Bartlett 1983; McDonald 2000). This piracy event was hypothesized as an explanation for the loss of the ancient Saltville River and subsequent deposition of colluvium at site SV-2 (McDonald 2000) because stream piracy is relatively common in the modern valley (McDonald and Bartlett 1983).

While the Saltville River hypothesis is prominent in the literature, other hypotheses for the origin of the gravel unit in the Saltville Valley should also be considered. A study of the contact between the valley gravel layer and the underlying Maccrady Formation found that it was not always conformable and was in some cases irregular (Ray et al. 1967). Ray et al. (1967) suggested that the large fossils preserved just above the gravels could not have been transported by the same forces that moved the lithologic clasts without being broken and, therefore the fossils must have arrived sometime after the layers overlying the gravel had already been deposited. In this model, animals walked out over the "muck", before becoming mired in the wet silts and clays (Ray et al. 1967). This process was also invoked to explain the gravel layer, with transported clasts supposedly sinking through the mud and silt to rest atop the Maccrady Formation. The presence of frail and thin bivalve shells within the layers immediately above the gravel is potentially problematic for this model, although it was assumed that this meant

conditions must have been “exceedingly fluid,” (Ray et al. 1967, p. 613), with no geological mechanism for this condition provided.

The SV-5/7 Site

Currently exposed sediments at SV-5/7 (Fig. 3) only include three of the named units found within the valley. The basal layer at SV-5/7 is interpreted as a red to gray shale member of the Paleozoic Maccrady Formation, due to the color of the rock, as well as the Maccrady Formation’s position as the Saltville Valley floor. The presence of evaporites observed intermixed with the clays also point towards this layer being the Maccrady Formation (Schubert pers. comm. 2020). This basal layer has been designated as unit P1, and according to McDonald (2000), it has been scoured by Pleistocene depositional processes in some locations.

Above this is a gravel unit consisting of large rock clasts and fossils in a fine matrix. This has been designated as unit W4 and is a primary focus of this thesis. This unit was hypothesized to be fluvial in origin when first described (Peterson 1917), an interpretation that has been widely applied across the valley (McDonald and Bartlett 1983; Holman and McDonald 1986; McDonald 2000). At SV-1, these gravels have been reported as being up to 15 cm thick, though the presence of this gravel unit and its thickness varies across the valley (McDonald 2000).

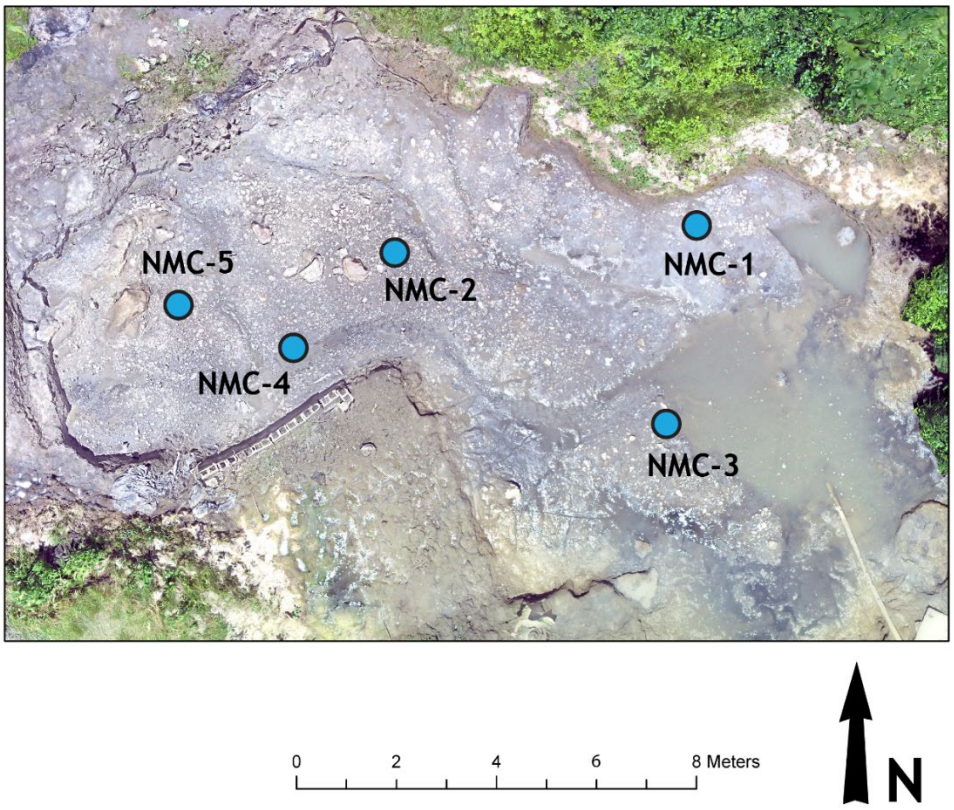

Figure 3. Aerial sitemap of SV-5/7. Locations of the five sampling locations are shown

The gravel unit is overlain by finer-grained sediments also dating to the late Pleistocene. These have been interpreted as belonging to McDonald's W3 unit, which consists of a mixture of silt and sand layers, and occasional finer grained gravel deposits (McDonald 2000), although this last component has not been observed by subsequent excavators (Schubert pers. comm. 2020). At site SV-1, the W3 layer reached a maximum thickness of 15 cm (McDonald 2000). Vertebrate megafauna remains are frequently found in this layer and much of the fossil material excavated from SV-5/7 is from the lowermost portion of layer W3 or the upper part of the W4 gravel layer. Recovered fossils from SV-5/7 by ETSU include but are not limited to *Arctodus*, *Mammuthus*, *Mammut*, *Cervalce*s, *Rangifer,* and bivalve shells (Schubert pers. comm. 2020).

While one valley-scale geological description has been published (Cooper 1966), and some smaller site-specific descriptions exist (Peterson 1917; McDonald and Bartlett 1983; McDonald 2000), no detailed sedimentological analysis of the gravel unit at SV-5/7 has been previously reported.

The SV-5/7 Gravel Unit

The SV-5/7 gravel unit occurs in the same stratigraphic position as fluvial gravels noted across the Saltville Valley at other fossil sites, in that it is a gravel layer of variable thickness which is overlain by finer grained sedimentary units, and directly underlain by the Maccrady Formation. Because of this, it is likely it is the local equivalent of the valley wide W4 unit. While these W4 gravel layers have been repeatedly interpreted as being of fluvial origin, this interpretation has not been subjected to quantitative sedimentological analyses. McDonald (2000) noted that some of the gravels from the SV-2 locality were imbricated, though these were not figured. Continued excavation of the SV-5/7 locality over many years has opened a large window to the surface of the gravel unit and no imbrication has been observed. This led researchers to question whether the fluvial origin for these deposits is viable and to consider if other depositional hypotheses may have better explanatory power for the SV-5/7 gravel unit.

Since fossils from Saltville were first described, researchers have noted variable preservation and taphonomic histories. Some are abraded to the point of being unidentifiable, while others are relatively pristine (Peterson 1917). These taphonomic differences could be the result of a fluvial depositional environment where fossils go through cycles of deposition, reworking, and redeposition (Peterson 1917). Some of the fossils recovered from the gravel layer appear to show signs of fluvial taphonomic processes such as abrasion (Silverstein 2017).

Carbonate concretions commonly form around the Saltville fossils, which may insulate some bone areas from abrasion while exposing others (Silverstein 2017).

Because the gravel unit is important for understanding the age and taphonomic history of SV-5/7, correctly identifying its depositional origin is of the utmost importance for site interpretation. Given the lack of evidence for a fluvial origin, the lack of imbrication within the SV5/7 gravel unit, and its unsorted appearance, quantitative sedimentological analyses of the gravels was undertaken in order to assess the validity of the assumed fluvial depositional model. The results of gravel grain size distribution analyses and evaluation of clast sphericity and rounding serve as a framework to begin assessing the depositional processes that resulted in the SV-5/7 gravels. Once this basic data is acquired, it can be compared to other potential depositional models such as a braided river, a meandering river, and debris flow events.

Potential Facies Models for the SV-5/7 Gravels

Within this study, three primary depositional facies models are considered as candidates for the deposition of the SV-5/7 gravels. These three models (braided river, meandering river, and debris flow) were chosen because they are well represented in the literature, and identification of the deposits they leave behind is relatively straightforward. While other depositional processes could be responsible for the gravel deposition, these facies models have either been previously proposed for the gravel units within the valley or seemed to fit the earliest data and observations of current researchers working at SV-5/7.

Fluvial regime is determined largely by energy (Pettijohn 1975). Generally, it is possible to characterize lower energy and higher energy streams of two different types. Braided rivers represent high energy systems, while meandering rivers tend to represent a lower energy environment. The braided river is a fluvial endmember facies characterized by high energy,

which can transport large clast sizes (Miall 1977; Collinson 1978). Within mountainous regions, this type of river typically occurs on steeper gradients and is often associated with alluvial fans and other areas where vegetation is unable to stabilize slopes against erosional forces (Pettijohn 1975). The primary characteristics of a proximal braided river are their namesake low sinuosity and multiple channels, high and variable discharge levels, and a consistently coarse-grained bedload (Smith 1970; Miall 1977). Generally, the presence of alternating massive gravel layers, stratified gravels, and either laminated or crossbedded sands are considered indicators of a braided river environment (Miall 1977; Bryant 1983). Of particular importance are sedimentary structures such as crossbeds, lamination, ripple marks, and imbrication, as these ordered structures indicate an environment with at least occasionally consistent flow (Miall 1977; Lancaster et al. 2010). Recognition of alternating gravel and sand facies, created by multiple channels moving laterally within a valley, are also very important for identifying braided river deposits. During periods of high stream discharge coarser gravels are laid down as longitudinal bars, channel lags, or channel fills in areas where the carrying capacity is high (Miall 1977). Sandy sediments are abundant, and frequently infill the void spaces between large clasts in gravel deposits. The sandiest horizons are typically considered to represent sandbars, minor channel or scour hollows, and flood deposits (Pettijohn 1975; Miall 1977). Silt and clay horizons are rare within braided river deposits and represent only a small portion of total sediment volume (Pettijohn 1975; Miall 1977). Because energy tends to be higher in this depositional environment and reworking of recently deposited sediments is so common, silt particles are usually unable to settle, and are only present as mud drapes and channel fills within inert channels during times of flooding (Miall 1977; Hein 1984). Overall, braided river deposits tend to be dominated mostly by coarse gravel and sand layers, when closest to their source, and dominated by alternating

layers of massive or stratified sands and gravel lags as a result of the high energy, highly variable, environment in which they form. While particle size analysis of braided rivers is an uncommon practice, some research suggests a distinct lack of silt and clay in the high energy upstream reaches of rivers (Kodama 1994). If a braided fluvial system were responsible for the deposition of the SV-5/7 gravel unit, the expected stratigraphy of the gravels would be that of alternating imbricated gravels with stratified, crossbedded sand horizons, and very little silt or clay.

A meandering river is the other fluvial endmember under consideration, and generally reflects a lower stream gradient, and therefore lower energy, than that of a braided stream (Smith 1970; Pettijohn 1975). These rivers exhibit a higher sinuosity than their counterpart and tend to deposit a wider variety of grain sizes (Collinson 1978). Whereas the primary identifier for braided river deposits is the abundance of sandy channel fills and pebbly/gravely lags and a lack of silts and clays, meandering river deposits are defined by cyclical fining upwards sequences (Smith 1970; Pettijohn 1975). These fining upwards sequences are the result of a more orderly shifting of channel location caused by downstream meander migration, in contrast to the frequent channel shifting of a braided river. The highest energy environment represented in a meandering river is the channel floor, which deposits conglomerates, gravels, or coarse sands, scouring into an erosional surface (Pettijohn 1975). The intermediate energy environment within the meandering river deposits cross-bedded sands overlain by rippled sands and silts and is interpreted as having been deposited on the point bar of the river (Pettijohn 1975). The uppermost portion of the cycle is representative of overbank deposition, which occurs primarily when flood events bring water to higher levels which overflow existing banks (Hicken 1993). In this zone, silts and clay are deposited farther away from the channel on the river's floodplain

(Pettijohn 1975). The thickness of these layers varies greatly from deposit to deposit, with single cycles ranging from 3 to 20 meters in total thickness, though in a single cycle the order from bottom to top is always coarse conglomerate/sand, crossbedded sand, rippled sands and- silts, and finally overbank silts and clay (Smith 1970; Pettijohn 1975). Thus, if a meandering river were responsible for the deposition of the SV-5/7 gravels, we would expect to observe a well-defined, fining upwards sequence from coarse gravels to sands and silts and clays.

The third depositional environment to be considered is a debris flow, or mass flow deposit. Debris flows are defined as the mass movement of sediments as a viscous fluid and are triggered by the addition of enough water to cause the fine-grained sediment (sand and mud) fraction to create a high-density fluid that can suspend or float, large clasts as they flow downhill (Blackwelder 1928; Prothero and Schwab 1996; Costa 1994; Scott and Yuyi 2004). Nearly all particle sizes, including massive boulders, can be transported by debris flows, and speeds of up to 10 meters per second are possible, making them dangerous events (Scott and Yuyi 2004). Because of this unusual mode of transport, grain sizes are not sorted as they are in fluvial deposits. Debris flow events deposits are typically poorly sorted (Prothero and Schwab 1996; Costa 1994), unstratified (Costa 1994; Scott and Yuy, 2004), have angular grains due to their short transport times (Lancaster 2010), and are characterized by a matrix which usually supports the larger clasts (Scott and Yuyi 2004; Lancaster et al. 2010). Scott and Yuyi (2004) list four identifying characteristics of debris flows in the field: (a) a fine-grained, muddy matrix surrounding the large clasts, (b) bimodal grain size histograms, (c), poor sorting with a large range of sediment sizes, and (d) having a massive/unstratified lithology. Importantly, the grain size histogram of debris flow deposits tends to be bimodal, trimodal, or polymodal. (Needham and Stuart-Smith 1987; Blair and McPherson 1992; Saula et al. 2002). Thus, if the SV-5/7

gravels are representative of debris flow deposition, we would expect the presence of very poorly sorted sediments containing clasts sizes of cobbles and larger, that have a large proportion of finer grain sizes as matrix.

While this study will focus exclusively on these three facies models, it should be noted that these are not the only modes of deposition that could potentially have resulted in the SV-5/7 gravels. Hypothesis testing in this study, while targeted, is by no means exhaustive, and even if one model fits the data well it does not rule out other untested modes of deposition. Additionally, it is possible that a combination of these models was responsible for the SV-5/7 gravels. For example, debris flow deposits have been known to rework fluvial deposits and vice versa (Lancaster et al. 2010), and thus it is possible that two or more of these depositional regimes could have acted on the examined sediments over time.

In order to distinguish these three depositional models from one another, a varied and multidisciplinary approach was used. First, the gravel was sampled via digging, and the stratigraphy of sample areas within SV-5/7 was recorded. The stratigraphy allows for direct comparison with the three facies models and is likely to be informative given the major differences between the facies models. Particle size analysis is an essential step in determining the depositional environment. In combination with the stratigraphy, this method can potentially distinguish between facies on the basis of grain size histograms. This analysis aids in distinguishing between depositional environments, as sorting is a key component in identifying some of the facies models. Roundness of sand and finer materials was documented in thin section. These data correlate with transport distance and further assist in the determination of the depositional environments, in conjunction with other data. Long axis clast orientation on large clasts (> 5cm) was collected in the field. Analysis of these data will help assess flow direction.

This will aid in comparison between facies models and inform the direction of future research. Lithology of gravel clasts was determined by response to HCl acid and physical observations. Lithology of fine-grained samples was determined by loss on ignition of organics and carbonate minerals in bulk sediment samples. No prior lithological research has been conducted on the SV-5/7 sediments, and while this only serves as a general analysis, it may have implications for the provenance, and thus possible history of the gravels.

Methods

Sample Collection, Stratigraphy, and Preparation

Rock hammers were used to sample the gravel layer in five locations at SV-5/7. Care was taken to remove large gravel clasts intact. With one exception (described below) the entire thickness of the gravel layer was sampled at each collection location, and the stratigraphy of each site was measured and recorded. Sample weights (Tab. 2) range from 6503 g to 12,113 g (in initial mass). All five wet samples were collected and stored in heavy duty ziplock bags until processing could begin. Prior to processing, small portions of the bulk samples were set aside for later analyses and were not included in analyses presented in this thesis. These samples were all given the designation of NMC, which stands for Nick/Mick Collection (Referencing collection by Nickolas Brand and Michael Whitelaw), followed by an identifying number so that the first sample is NMC-1, the second NMC-2, and so on.

Samples were allowed to air-dry, then oven dried at 50° C. Once dry, the samples were weighed on a digital scale. The volume of the bulk samples required multiple individual weight measurements to be summed in order to calculate the total weight for each sample. After

weighing, the samples were picked by hand to identify clasts over 1 cm in diameter, which were removed and stored separately from the fine fraction. Large clasts were washed with deionized water and brushed clean. The residual sediment was recovered and returned to the fine-grained fraction. Once dried, the large clasts were weighed individually.

Table 2. Gravel Samples Mass and Thickness. Initial Dry Mass of Collected Samples, and the Thickness of the Gravel Layer for Each Sample Collection Site. Reported Mass Does Not Include the Un-Used Subsamples. *Represents Thickness From Top of Upper Gravel Layer to Bottom of Lower Gravel Layer, Including Sand and Clay Layers in Between.

Sample Number	**Initial Mass (g)**	**Gravel Thickness (cm) ***
NMC-1	8647	10
NMC-2	10859	31
NMC-3	10625	>40
NMC-4	7538	12
NMC-5	5609	9

Particle Size Analysis - Dry and Wet Sieving

After allowing the sediments to settle and dry, 10-15% of the remaining fine-grained fraction was subsampled for particle size analysis. Coarse-grained (> 2 mm) material was separated using a combination of wet and dry sieving. Fine-grained (2 mm and below) material was separated by wet sieving. The stickiness of the clays within the samples made dry screening impractical for separation of smaller material. The samples were screened one size class at a time in 5-gallon buckets partially filled with deionized water.

Fine-grained samples were wet-screened using 8-inch diameter nested sieves held directly on the surface of the water and agitated by hand. This resulted in the smaller grains collecting in the bottom of the bucket where they could be recovered and used in the next finest-screen sieve. Sediments adhering to the side of the bucket were scraped off or removed with a deionized water squirt bottle until the sample bucket was completely clean and could be used to repeat the next step.

Recorded sieve sizes include: 128+ mm (-7 ϕ), 64 mm (-6 ϕ), 32 mm (-5 ϕ), 16 mm (-4 ϕ), 8 mm (-3 ϕ), 4 mm (-2 ϕ), 2 mm (-1 ϕ), 1 mm (0 ϕ), 0.500 mm (1 ϕ), 0.250 mm (2 ϕ), 0.125 mm (3 ϕ), and 0.063 mm (4 ϕ). Clast sizes well above 128 mm were noted in the field but were not collected. Sieving times were greater for the smaller fractions because the clays flocculated and clogged the mesh. In these instances, the sediment would either need to be scooped carefully away from the center of the mesh to allow for water to re-enter the sieve, or split into smaller, sievable portions to be processed. After sieving of the fine-grained fraction was completed, the sieved fractions were transferred to 50 mL tubes and centrifuged at 3000 rpm for 15 minutes. This ensured that water could be decanted to allow for air drying with minimal loss of sediment. These samples were dried at 50° C under vacuum.

The mud particles too small to be sieved easily (silt and clay), were allowed to settle and dry, and were not further separated for this study. This remaining fine fraction retained moisture for weeks even after standing water was removed, and the delicate use of a hair dryer on low heat and power at a distance (so as to not send particles airborne) was required to complete the drying process, as the COVID-19 pandemic rendered laboratory ovens temporarily unavailable. Once dried, the fine fraction was weighed on a digital scale.

The weights of each size fraction for each subsample were recorded in a Microsoft Excel spreadsheet. The final recorded weight for all coarse-grained material was subtracted from the total weight of each sample in order to determine the total weight of fine material. The weight percentage for each size class of the fine-grained material was multiplied by the total weight of fine material to estimate the total weight of each fine-grained size class for each sample. Charts showing the cumulative weight, in percent of each particle size fraction, were created in Microsoft Excel, along with histograms showing the proportion of each grain size fraction for all five samples.

Lithologic Description

After sieving was complete, each size fraction (excluding silt and clay fractions) was analyzed to assess rough lithology, for all five samples. Dilute hydrochloric acid was used to test for the presence of carbonate, and if there was little to no effervescing, the clast was scratched (or many fine-grained clasts were crushed) and acid treatment was performed again to test for the presence of acid resistant grains, specifically. Where possible, clasts were identified by lithology (carbonate, sandstone, siltstone, shale, etc.), and notes were compared across the samples to determine the consistency of lithologies across location and grain size.

Thin Section Analysis and Roundness

Thin sections of the fine-grained fraction of each gravel sample were created for analysis. Subsamples (~1 cm^3) were randomly selected from the bulk samples and placed into small plastic containers. The containers were then filled with epoxy resin (Epson 30-minute slow cure epoxy) and swirled with mixing sticks to create a random distribution of grains. The resin was

allowed to cure for 2 hours before being removed from the plastic containers with the use of a saw.

An Ingram model 65C saw/grinder was used to make thin sections close to finished thickness. Thin sections were finished by hand on a glass grinding plate with 80/220/500 grit and checked by using the petrographic properties of quartz grains as a relative control for standard thickness. Two thin sections were prepared for each sample, for a total of 10 thin sections.

Roundness of individual sediment grains (angular to well-rounded) was recorded following Pettijohn (1975) using a petrographic microscope. Random slide transects were performed and roundness recorded for each grain in the transect until 100 grains from each slide had been characterized. This resulted in 200 grains per sample. Any grains large enough for roundness to be characterized were included.

Sediment Sorting

An initial estimate of sediment sorting was carried out by visual examination of each gravel sample in the field. In the lab, after sediments were weighed, these visual estimates were compared to the grain size fraction distribution of the sieved fractions. The Inclusive Graphic Standard Deviation of the cumulative weight formula, "StdDev = ((ϕ84% - ϕ16%) / 4) + ((ϕ95% - ϕ5%) / 6.6)))" from Folk (1980) was used to calculate the relative sorting of each sample. A standard deviation within a range of values indicates a level of sorting as seen in Table 4.

Table 3. Sorting Calculation Values. Calculated Sorting Standard Deviation Values and Their Associated Sorting Levels. (After Folk, 1980.)

Calculated Value	**Indicated Sorting**
Below 0.35ϕ	Very well sorted
Between 0.35 ϕ and 0.50 ϕ	Well sorted
Between 0.50 ϕ and 0.71 ϕ	Moderately well sorted
Between 0.71 ϕ and 1.0 ϕ	Moderately sorted
Between 1.0 ϕ and 2.0 ϕ	Poorly sorted
Between 2.0 ϕ and 3.0 ϕ	Very poorly sorted
Over 4.0ϕ	Extremely poorly sorted

Orientation of Gravel Clasts

During the 2019 paleontological field season, the orientations of *in situ* clasts from the exposed SV-5/7 gravel surface were measured to assess preferred orientation. The orientation of the long axis of each grain was determined as an azimuth using a Brunton compass. Within a 2-meter square area the orientation of every grain visibly larger than 5 cm in any dimension was measured until a sample size of 50 long axis orientations had been collected. Although the small sample size precludes rigorous estimates of orientation, it is adequate for field analysis of grain orientation (Karatson et al. 2002).

Because each clast could have the long axis oriented in either direction (180 degrees apart), an opposing orientation was calculated for each measurement as is standard in long axis orientation analyses. A rose diagram of this dataset was created using the freeware program GeoRose 0.5.1 (Yong Technology Inc. 2014; http://www.yongtechnology.com/georose/), in order to quickly assess the potential for preferred orientation. Visually, there is a preferred

orientation, however these data were further subjected to statistical analyses in order to quantify the presence or absence of a preferred orientation within the gravels.

A variety of tests are available to statistically test for the presence of a preferred orientation within a circular dataset. The standard for assessing orientation preference in circular data within paleontological and geological analyses is the Rayleigh test, and has been utilized consistently for decades across both disciplines (Hein 1984; Karatson et al. 2002; Domingo et al. 2017). The underlying assumptions of the Rayleigh test are that the data are not diametrically bilateral, and that they are assumed to be unimodal (Landler et al. 2019). Because the Saltville gravel resulted in a bilateral (peaks 180 degrees apart) and strongly polymodal (3 or more peaks) distribution of orientation, the Rayleigh test is inappropriate for this dataset. Therefore, other tests are required if the possibility of preferential orientation is to be quantitatively assessed.

Other tests that can be used to assess uniformity within circular data are the Pycke test, and the Hermans-Rasson test. Recent, robust, statistical analyses have been performed that have illustrated the utility of the Hermans-Rasson test when attempting to assess uniformity within a multimodal sample (Landler et al. 2019), and thus this test is most appropriate for the current analysis. The Pycke test is another tool that was developed to address the weaknesses of the Rayleigh test in properly analyzing multimodal samples (Pycke 2010). When compared to the new Hermans-Rasson test, trials suggested that the Pycke test performed similarly, although it tended to have greater power with larger sample sizes (Landler et al. 2019). This power appears to have come with the trade-off of being less powerful compared to the new Hermans-Rasson test if the data were not concentrated tightly around the modes (Landler et al. 2019). For comparative purposes, the Rayleigh test was performed, but only the results of the Hermans-

Rasson tests and the Pycke test will be treated as accurate and informative if discrepancies arise between the results.

All tests were run using RStudio and the R package "circular," (Agostinelli and Lund 2017) which handles circular statistics. This package included a built-in function for the Rayleigh test. R code provided in supplemental data by Landler and colleagues (2019) was used to craft and execute the Pycke, and Hermans-Rasson tests.

Loss on Ignition

As a method for determining the volume of siliciclastics relative to organic and carbonate content of the fine-grained (2 mm and smaller) fraction of the sediments, weight loss on ignition (LOI) was used. This method is often used in paleolimnological studies to estimate the percentage of organic carbon and inorganic carbonate within a sediment sample (Heiri et al. 2001; Wang et al. 2010).

A small (~1.5 mg) subsample was collected from the fine-grained (2 mm and smaller) fraction of each gravel sample, homogenized in a crucible, and weighed prior to processing. An oven was heated to 500 C°, and the crucibles were placed inside for one hour. The crucibles were then removed, and the specimens allowed to cool to room temperature before being weighed to determine how much organic carbon had been burned away (% ORG). The oven was then heated to 900° C and the crucibles were once again placed inside for one hour. Then samples were allowed to cool to room temperature before being weighed in order to determine the percentage by weight of inorganic carbonate (% CO_3) that had been removed by heating.

Results

Sample Collection, Stratigraphy, and Preparation

The gravel unit at SV-5/7 was examined both on the surface and in cross section in the five collection sites designated NMC-1 through NMC-5. Gravel deposits at most of the sampling locations were determined to be dominantly clast supported, although some areas appeared to be matrix supported. No vertical grading was observed nor did there appear to be any dominant clast orientation. For all but one location, where samples were collected, the gravel unit was unstratified throughout its entire thickness (Fig. 4). Stratification was only apparent in NMC-2. Vertical contacts, where present, were measured from the gravel surface.

The gravel at NMC-1 was 10 cm thick. Surface gravels and matrix were gray while the layers beneath had a matrix with clouds of reddish and gray colors. No internal structure was observed during collection. The total weight of collected sediment for NMC-1 was 8.97 kg.

NMC-2 was excavated to a depth of 31 cm. This collection site displayed stratification, where the uppermost gravels rested atop a thin sand layer, a set of red and gray bedded clays, and then another gravel layer with notably angular clasts. As in NMC-1, the surface of the gravels was a dark gray color, while the gravels beneath were embedded within a reddish and gray matrix. The NMC-2 sample weighed a total of 12.11 kg.

The NMC-3 collection site was dug >40 cm deep but did not encounter the Maccrady Formation. The gravel here was visually sandier in some areas than seen in NMC-1 and NMC-2. The gravels at the surface and uppermost section of the sample site tended to be larger, while the gravels immediately below were smaller (but still poorly sorted). The contact between the gravel units was sharp suggesting that the layers may represent separate horizons, rather than a single

heterogeneous one. The gravel matrix appeared mostly grayish, with little to none of the red coloration seen at depth in the other sites. The total bulk weight of sample NMC-3 was 11.85 kg.

At NMC-4, the gravels were similar to those seen at the surface of the other NMC sample sites. These gravels were 12 cm thick and rested atop at least 14 cm of red clay interpreted to represent the Maccrady Formation. A bulk sample of 8.70 kg was collected from this site.

Site NMC-5 was located 12 centimeters southeast of a large boulder resting on the top of the SV-5/7 gravels. At this site the gravel was 9 cm thick, and underlain by a layer of sand and clays for at least another 23 cm. The Maccrady was not reached here, but a 6.50 kg bulk sample of the gravels was collected for study.

All samples had large amounts of gravel present, and all remained sticky and extremely difficult to separate by either dry or wet sieving methods. Therefore, a subsample of the bulk sample was selected to permit quicker screening. Future work may benefit from the use of chemical disaggregation. As sample processing began NMC-1, NMC-2, and NMC-3 were all a gray color, while NMC-4 was a darker gray with reddish-brown areas, and NMC-5 was a lighter gray than the other samples. When processing finished, the silt and clay fractions for NMC-1, NMC-2, and NMC-4 were all dark gray. The NMC-3 clays and silts ended processing with a reddish-brown color, while the NMC-5 clays and silts were a light gray color. The final colors may have been produced by oxidation, as the wet sieving process required specimens to remain wet or in water for large amounts of time. Unfortunately, Munsell color charts were not available during field collecting and early processing. Future work may benefit from a more quantitative analysis of sediment color.

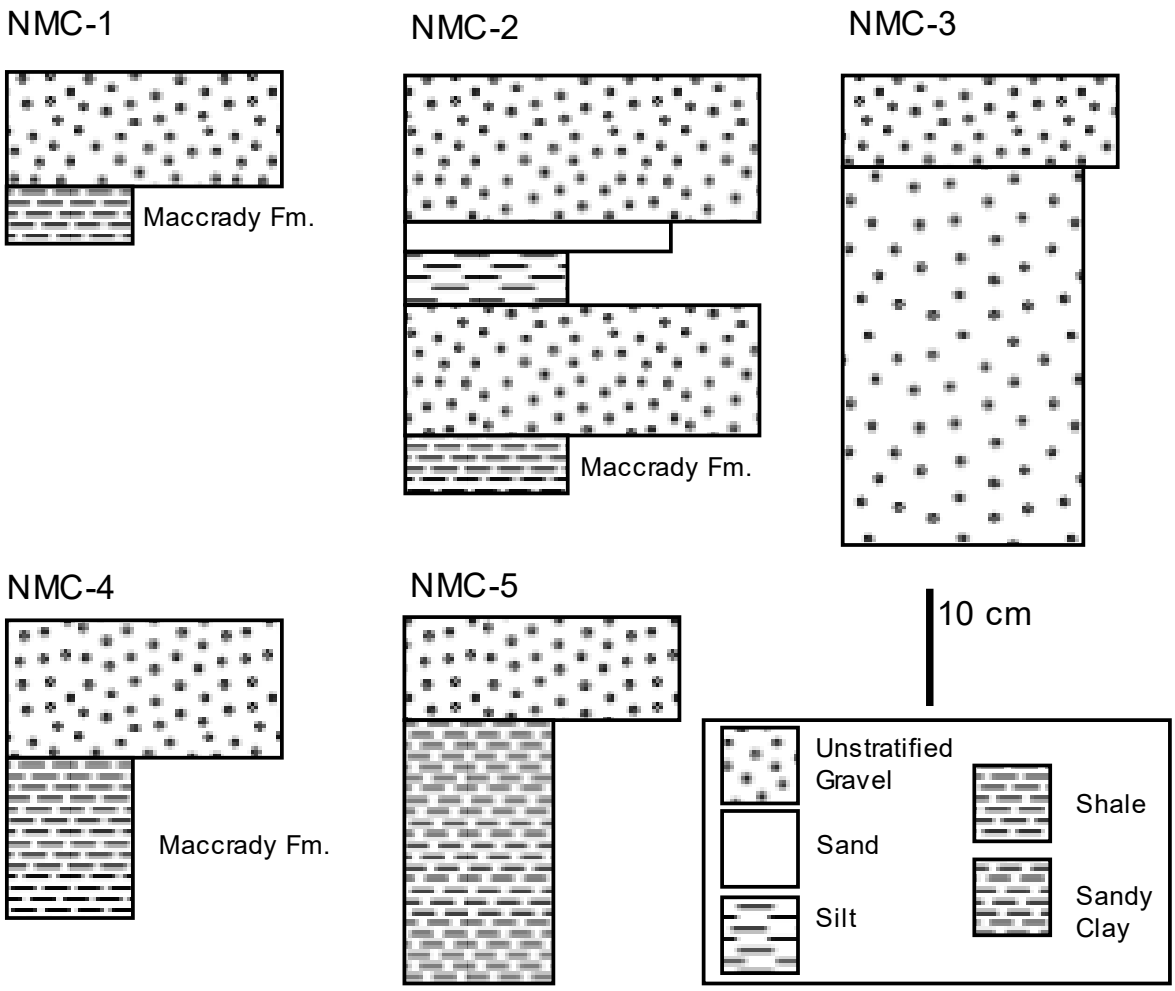

Figure 4. Stratigraphic columns for each NMC sample. Thickness of uppermost gravel layers may vary due to history of repeated excavations and removal of pond scum via spraying

Particle Size Analysis - Wet Sieving

When sieving was complete, the percentage by weight of specific phi size ranges were collected for each subsample. The ranges were < ϕ -1 (pebbles and larger grains), ϕ0 (very coarse sand), ϕ1 (coarse sand), ϕ2 (medium sand), ϕ3 (fine sand), ϕ4 (very fine sand), and > ϕ5 (silt and clay). The sediment fractions by weight (and total weight) are reported in Table 4. When interpreting the histograms, any local maximum where the bin was higher than the bins to either side was treated as a peak. If two adjacent bins were both taller than the surrounding bins, they are treated as one peak.

By weight, NMC-1 was 65 % gravel, 10 % sand, and 25 % silt and clay (Fig. 5). Very coarse sand made up nearly the entirety of the sand fraction, accounting for 9.0 % of the total sample weight, and 86.5 % of the sample's sand weight. Compared to the other samples, NMC-1 had the highest percentage of gravel, and the lowest total percentage of sand. The histogram for NMC-1 shows a trimodal distribution with peaks at the -7 ϕ/-6 ϕ (cobble), 0 ϕ (very coarse sand), and 5+ ϕ (silt and clay) sizes.

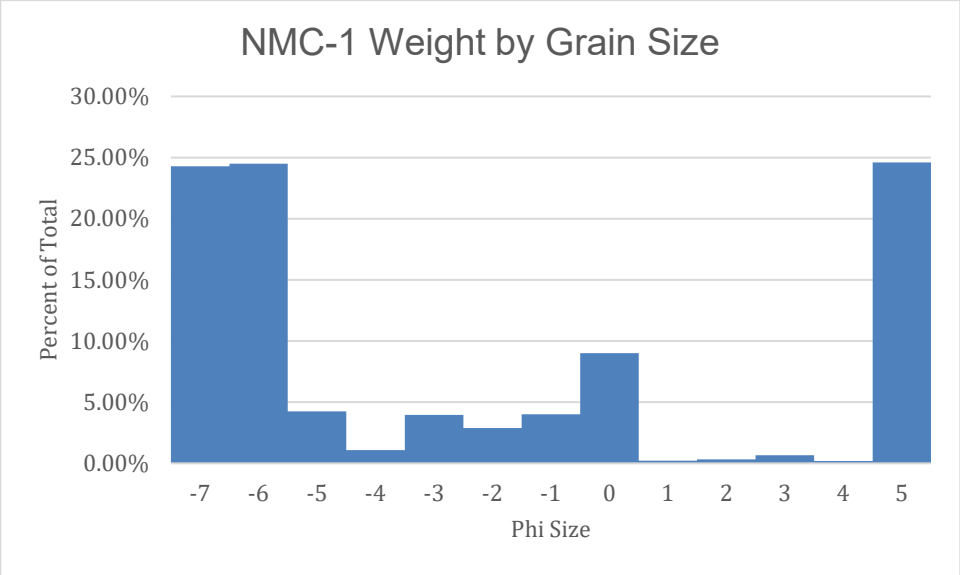

Figure 5. Histogram of grain size frequency by percentage of weight for NMC-1

The NMC-2 subsample contained 53 % gravel, 32 % sand and 15 % silt and clay (Fig. 6). The contribution to weight of the very coarse grains was less in this sample than in NMC-1, while the smaller sand sizes were well represented in the subsample. The histogram for NMC-2 was strongly trimodal with peaks at -7 ϕ (cobbles), 0 ϕ (very coarse sand), and 5+ ϕ (silt and clay) sizes.

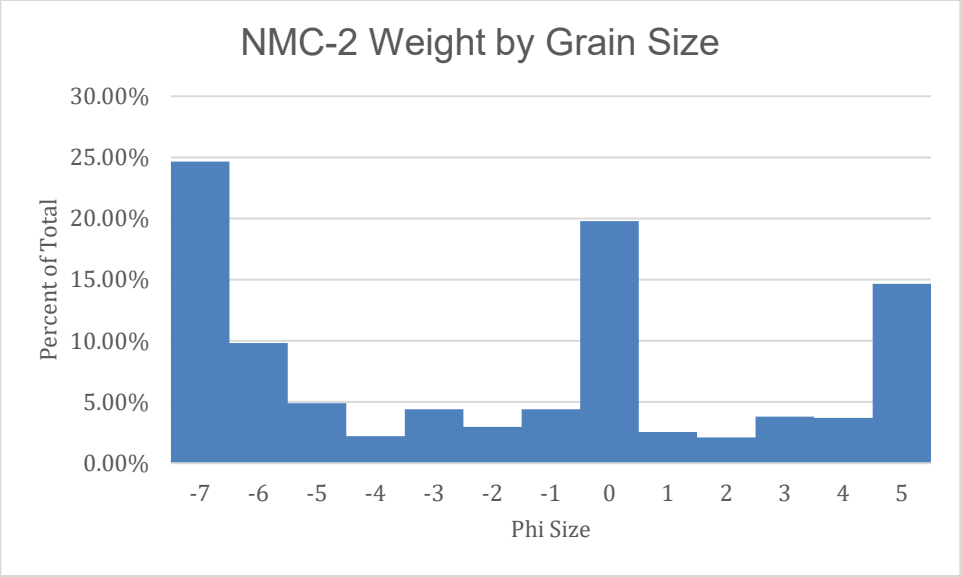

Figure 6. Histogram of grain size frequency by percentage of weight for NMC-2

NMC-3 consisted of 50 % gravel, 35 % sand, and 15 % silt and clay (Fig. 7). Within the sand fractions, very coarse sand was much more abundant while medium sand was less abundant than the other sand particle sizes. Compared to other samples, this sample contained the most sand (35 % of total weight) by a large margin and was the only sample where a sand size (specifically very coarse sand) fraction was the single most dominant clast size by weight. These measurements are in agreement with the field observations that recognized a high sand content in NMC-3. The histogram for NMC-3 displayed a polymodal distribution with peaks at the -6 ϕ (cobble), -3 ϕ (medium pebble), 0 ϕ (very coarse sand), and 5+ ϕ (clay and silt) sizes.

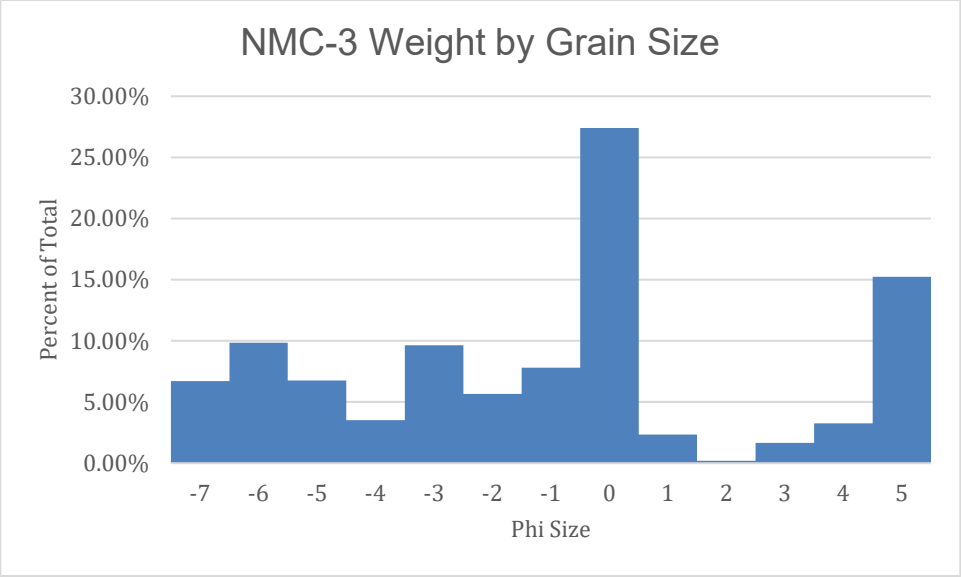

Figure 7. Histogram of grain size frequency by percentage of weight for NMC-3

NMC-4 contained 55 % gravel, 35 % sand, and 10 % silt and clay by weight (Fig. 8). The sand fraction of this sample was the second largest by percentage of all samples and contained by far the largest percentage of fine sand (27.1 % of sample sand weight). Additionally, NMC-4 contained the lowest percentage of silt and clay of all five samples. The histogram for NMC-4 was polymodal with 4 peaks at -6 ϕ (cobbles), -3 ϕ (pebbles), 0 ϕ (very coarse sand), and 5+ ϕ (silt and clay) sizes.

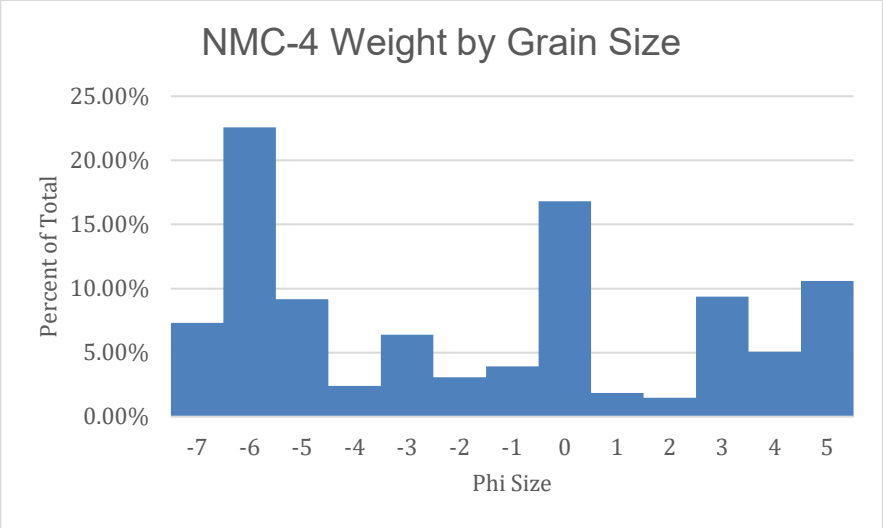

Figure 8. Histogram of grain size frequency by percentage of weight for NMC-4

By weight, NMC-5 was 46 % gravel, 24 % sand, and 30 % silt and clay (Fig. 9). The sands were dominated by the very coarse sand fraction (88.7 % of sand sized grains by weight). Compared to the other samples, NMC-5 has the highest proportion of silt and clay, as well as the smallest percentage of gravels. The histogram for NMC-5 was strongly trimodal with peaks at -6 ϕ (cobbles), 0 ϕ (very coarse sand), and 5+ ϕ (clay and silt) sizes.

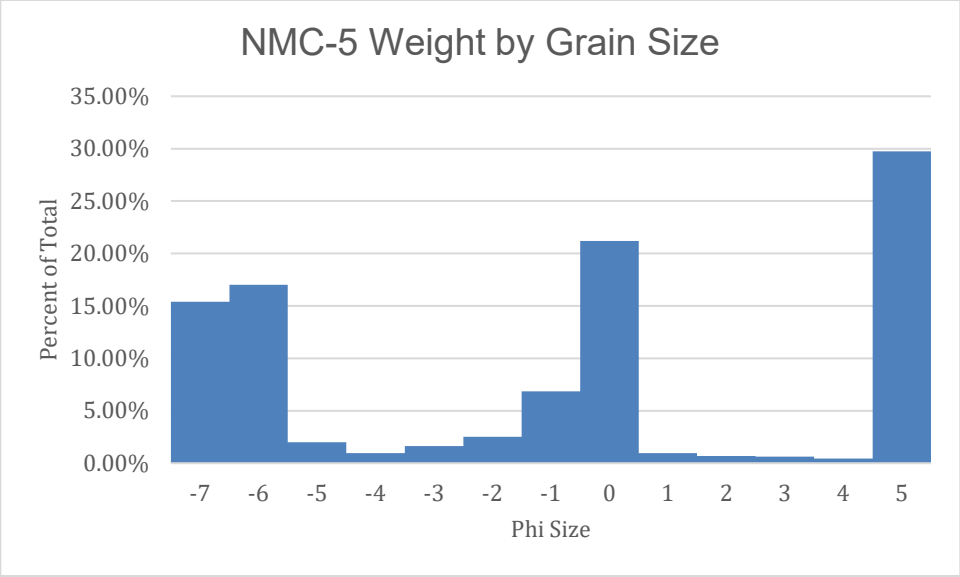

Figure 9. Histogram of grain size frequency by percentage of weight for NMC-5

Histogram of grain size frequency by percentage of weight for NMC-5

While the samples were quite varied, there are multiple trends that can be observed in the grain size distribution data. The most readily apparent pattern is the heterogeneity of the NMC samples. Ranges of percentage by weight vary by up to 19% for the gravel sized fractions, 25% for the sand sized fraction, and 19% for the silt and clay sized fraction. NMC-1, 2, 3, and 4 had an overall higher percentage of sand than silt and clay, and NMC-1 and 5 had a higher overall percentage of silt and clay than sand. NMC-3 contained the largest proportion, by far, of very coarse sand (0 ϕ), and NMC-4 contained a similarly disproportionate amount of fine sand (-3 ϕ) when compared to the other samples. Given that each sample was collected only a few meters away from each other, there is high variation in the grain size composition across the relatively small SV-5/7 study area.

Commonalities across the samples were also noted. The most common grain size category by weight was gravel (larger than sand) for all 5 samples. Additionally, the histograms for all samples showed peaks at the 0 ϕ (very coarse sand) and 5+ ϕ (silt and clay) grain sizes.

Peaks were present at either -6 ϕ or -7 ϕ in all samples, though this trend was noticeably less pronounced in NMC-3. All histograms showed a bimodal, trimodal or polymodal (NMC-4 has 4 peaks) distribution, though the relative strength of the peaks varied significantly across samples. These patterns indicate a large amount of grain size variation across short lateral distances in the SV-5/7 gravel. This variation is unlikely to be due to sampling different horizons, as all NMC samples were collected from similar elevations.

Table 4. Percentage of Grain Size by Weight for Each Subsample. Total Weight of Sediments

Listed in Parentheses

Phi Size & Category	**ϕ-7 (Cobbles)**	**ϕ-6 (Cobbles)**	**ϕ-5 (Very Coarse Pebbles)**	**ϕ-4 (Coarse Pebbles)**	**ϕ-3 (Medium Pebbles)**	**ϕ-2 (Fine Pebbles)**	**ϕ-1 (Very Fine Pebbles)**	**ϕ0 (Very Coarse Sand)**	**ϕ1 (Coarse Sand)**	**ϕ2 (Medium Sand)**	**ϕ3 (Fine Sand)**	**ϕ4 (Very Fine Sand)**	**ϕ5 (Silt and Clay)**
Metric Size	128 mm	64 mm	32 mm	16 mm	8 mm	4 mm	2 mm	1 mm	0.5 mm	0.25 mm	0.125 mm	0.063 mm	Smaller than 0.063 mm
NMC-1	24.3 % (2101 g)	24.5 % (2117 g)	4.30% (368 g)	1.10% (945 g)	4.00% (343 g)	2.90% (249 g)	4.00% (347 g)	9.00% (779 g)	0.20% (19 g)	0.30% (28 g)	0.70% (58 g)	0.20% (16 g)	24.59% (2126 g)
NMC-2	24.70% (2677 g)	9.80% (1066 g)	4.90% (534 g)	2.20% (240 g)	4.40% (479 g)	3.00% (324 g)	4.40% (478 g)	19.80% (2148 g)	2.50% (276 g)	2.10% (229 g)	3.80% (415 g)	3.70% (401 g)	14.70% (1592 g)
NMC-3	6.70% (713 g)	9.80% (1046 g)	6.80% (718 g)	3.50% (373 %	9.60% (1025 g)	5.70% (602 g)	7.80% (829 g)	27.40% (2911 g)	2.30% (248 g)	0.20% (21 g)	1.70% (176 g)	3.30% (345 g)	15.20% (1618 g)
NMC-4	7.30% (551 g)	22.60% (1703 g)	9.20% (691 g)	2.40% (181 g)	6.40% (482 g)	3.10% (232 g)	3.90% (295 g)	16.80% (1266 g)	1.80% (139 g)	1.50% (111 g)	9.40% (706 g)	5.10% (383 g)	10.60% (798 g)
NMC-5	15.40% (864 g)	17.00% (954 g)	2.00% (113 g)	1.00% (53 g)	1.60% (91 g)	2.50% (141 g)	6.90% (385 g)	21.20% (1189 g)	1.00% (54 g)	0.70% (38 g)	0.60% (35 g)	0.40% (24 g)	29.70% (1668 g)

Lithology

Within NMC-1, the -7 ϕ, -6 ϕ, and -5 ϕ grain sizes were dominated by rocks of a dark gray color, which did not readily react to dilute hydrochloric acid unless deeply scratched, which identified them as acid resistant carbonate clasts. Concretions present in these size classes effervesced vigorously when exposed to HCl, as did lighter gray colored carbonate clasts and thus are interpreted to be limestone. The -4 ϕ, -3 ϕ, -2 ϕ, and -1 ϕ grain sizes all contained clasts (possibly siltstone) that did not react when treated with acid, in addition to carbonate clasts. The 0 ϕ to 4 ϕ size fractions had both clastic and carbonate clasts present, although as grain size decreased, a larger percentage of clasts reacted, and with increasing vigor. The silt and clay size fraction effervesced slightly when exposed to HCl.

NMC-2 was dominated by carbonate clasts in almost all of the grain size classes. The larger sized (-7 ϕ and -6 ϕ), concretion fragments effervesced readily when exposed to HCl, as did some carbonate clasts. Some carbonate cobbles displayed an iron sulfide coating (possible marcasite or pyrite), and this coating was determined to be surficial when some of these clasts were broken open. Many of the acid resistant carbonate clasts within the -6 ϕ size contained crisscrossing veins of a white mineral. The acid resistant carbonate clasts were generally more abundant in the sizes from -7 ϕ to -4 ϕ, and the lighter colored and more readily reactive limestone clasts were more abundant in sizes -3 ϕ and smaller. Dark colored fossil bone fragments (unidentifiable) were found in both the -3 ϕ mm and -2 ϕ size samples but were limited to one specimen in each. The 0 ϕ size group and below contained some reddish rock clasts that effervesced strongly when exposed to hydrochloric acid, as well as the dolomite and limestone clasts. All of the NMC-2 sand particles effervesced vigorously when exposed to HCl

acid (and thus must be carbonates), although the silt and clay sized fraction reacted only slightly to the HCl.

NMC-3 had larger size groups dominated primarily by carbonate, with acid resistant carbonate being less abundant throughout the -7 ϕ to the 1 ϕ sizes. The -4 ϕ sample contained a carbonate clast which bore a brachiopod fossil, and the -3 ϕ sample contained a fossil bone fragment. The -2 ϕ sample, while being carbonate, also contained at least a few very fine-grained clastic rock fragments with well-defined flat surfaces, which are interpreted as being shale clasts. The -1 ϕ and 0 ϕ sizes contained a few siltstone clasts as well. The 1 ϕ and smaller sizes contained reddish grains that reacted strongly to hydrochloric acid. This red lithology comprised about 1/10, 1/3 and 1/4, and 1/2 of grains at the 1 ϕ, 2 ϕ, 3 ϕ, and 4 ϕ size classes respectively. The silt and clay fraction reacted moderately to the HCl but noticeably more than the silts and clays in samples NMC-1 and NMC-2.

NMC-4 was similar to NMC-3 in displaying a pattern of effervescent carbonate as the most common lithology, and acid resistant carbonate as the next largest constituent throughout most of the class groups (-7 ϕ to -1 ϕ). A minority of shale clasts were observed within the -3 ϕ mm and -1 ϕ sizes only, while a fossil bone fragment was present within the -2 ϕ mm size class. -1 ϕ, 0 ϕ, and 1 ϕ mm size classes displayed the reddish clasts, though most abundantly in the 0 ϕ fraction. As with NMC-3, these reddish clasts reacted strongly to hydrochloric acid. Additionally, the 1 ϕ fraction contained Pleistocene fossil shell fragments. The 2 ϕ and smaller size classes all were light gray in color with only minor red areas present. When exposed to HCl, the silt and clay fraction of NMC-4 reacted vigorously, as the sample was notably more reactive than samples NMC-1, NMC-2, and NMC-3.

NMC-5 was dominated by acid-resistant carbonate within the larger size classes. At -7 ϕ only veined resistant carbonate clasts were present, and their clasts were more common than the reactive carbonate grains in the -6 ϕ to -4 ϕ fractions (where veins were also observed in the resistant carbonate). From -3 ϕ and smaller, reactive carbonate became the most common clast lithology, with resistant carbonate making up the rest of most of the samples where lithology could be determined. The -1 ϕ fraction contained a small amount of shale clasts. Interestingly, the 1 ϕ to silt and clay fractions all bore a tan color rather than the strong red or gray color present in the other samples. All size classes reacted strongly to the hydrochloric acid, including the silts and clays.

Despite the observed textural differences between the samples, the lithology of the gravels was somewhat consistent across samples. Acid resistant carbonate tended to be more prevalent in larger clast sizes (and to be covered in iron sulfide within the -7 ϕ sample), and reactive carbonate to be more prevalent within the smaller fractions. While all samples were dominated by carbonate lithologies at most, if not all, sizes, shale and siltstone clasts could also be present, and possessed no apparent pattern of distribution other than being more common in smaller (-3 ϕ and below) size fractions. Color and reactivity to hydrochloric acid varied greatly within the fine-grained (2 mm and smaller) fractions. Similar to the particle size analysis, these results suggest a strongly heterogeneous deposit and help to underscore the variability of these gravel deposits within the excavation pit.

Thin Sections and Roundness

Opaque and translucent grains were both present in the finished thin sections, with the former being more common in all. Previous studies have reported chert within gravels in the Saltville Valley (McDonald and Bartlett 1983; McDonald 2000), and it is possible that fragments

of chert are present as some of the opaque grains observed in the thin sections. Many of the non-opaque grains were pleochroic, meaning that they changed colors as the slide was rotated. Based on the lithologic analysis opaque grains likely represent shale, pyrite, or opaque silicate clasts.

Results of the roundness analysis are reported in Table 5 and Figure 10 below. For most of the samples, subangular and subrounded grains are the most common, while well rounded grains were either absent or poorly represented within the sample.

Table 5. Roundness in Thin Section by Subsample. Percentage of Each Roundness Class Encountered in Two Thin Sections Created from Each Sample (N= 200). Total Number of Grains in Parentheses. Percentage Rounded Up to the Nearest Whole Percent.

	NMC-1 Total Count (%)	**NMC-2 Total Count (%)**	**NMC-3 Total Count (%)**	**NMC-4 Total Count (%)**	**NMC-5 Total Count (%)**
Angular	44 (22%)	51 (26%)	58 (29%)	39 (20%)	33 (17%)
Subangular	75 (38%)	78 (39%)	77 (39%)	87 (44%)	100 (50%)
Subrounded	45 (23%)	55 (28%)	56 (28%)	64 (32%)	64 (32%)
Rounded	32 (16%)	15 (8%)	8 (4%)	9 (5%)	3 (2%)
Well Rounded	4 (2%)	1 (1%)	1 (1%)	1 (1%)	0 (0%)
Count Summary	200 (101%)	200 (102%)	200 (101%)	200 (102%)	200 (101%)

Because only grain sizes smaller than -1 ϕ (2 mm and smaller) were included, the following discussions of roundness pertain only to this fraction, and do not represent the roundness of clasts larger than -1 ϕ. The grain roundness classes for NMC-1 were dominated by subangular grains (38%), with angular, subrounded, and rounded grains also being common, though the latter to a lesser extent. Well-rounded grains were present, but in small numbers. Compared to the other samples, NMC-1 had a much higher count of rounded and well-rounded grains.

NMC-2 was dominated by the subangular grain class (39%). Angular, subangular, and subrounded grains were all present in percentages greater than 25%. NMC-2 had a slightly higher representation of angular grains than NMC-1.

NMC-3 displayed a grain roundness class distribution similar to NMC-2, with subangular grains representing the mode. Angular and subrounded grains were present in high percentages, while rounded and well-rounded grains made up <5% of the clasts.

NMC-4 was consistent with the other samples in having subangular clasts as the mode, and an abundance of angular and subrounded grains. Rounded and well-rounded grains were present in small percentages.

NMC-5 was characterized by having half of the grains identified as subangular (50%). Subrounded grains were the next abundant clast type, angular grains being a somewhat distant third. Rounded grains were present in small numbers, and no well-rounded grains were observed in the sample.

Subangular grains were the most common roundness class across all samples, accounting for 38-50 % of the grain population. Well-rounded grains were rare, and only NMC-1 contained >10% of rounded plus well-rounded grains. While not analyzed in the same detail as

the matrix grains, the large gravel clasts (-5 ϕ and larger) tended to be either rounded or well rounded.

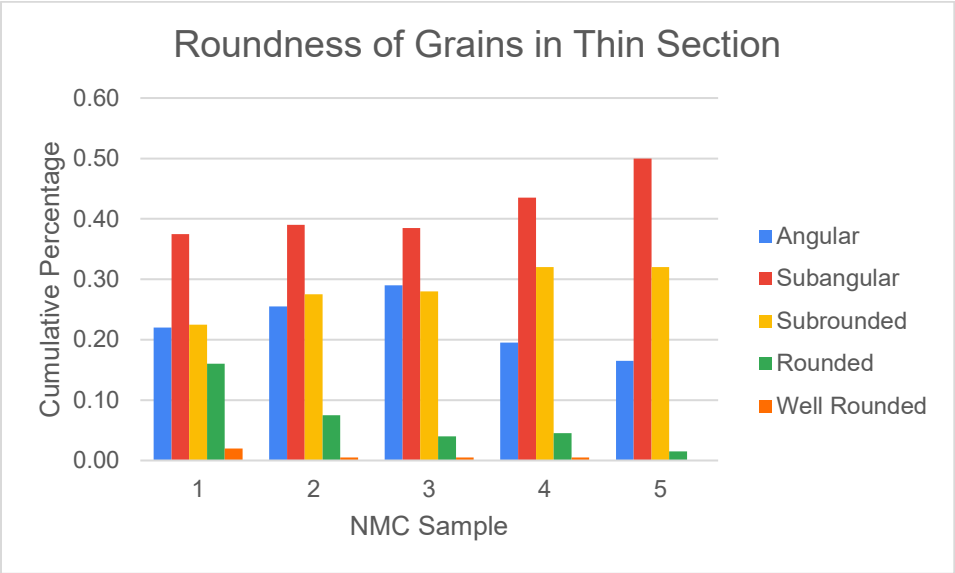

Figure 10. Cumulative percent chart for roundness classes. Percentage of each roundness class for thin sections of each sample

Sorting Calculation

Sorting was estimated in the field, by visual inspection, to be poorly sorted to very poorly sorted for all five samples, using the standard sorting visual comparator published by Longiaru (1987). The measured weights for each grain size category were used to create cumulative weight curves for each sub-sample (Figs. 11-15). In order to mathematically calculate the sorting of the sediments, the inclusive graphic standard deviation (Folk 1980) was calculated for each sample and these values are reported in Table 6. It is important to note that because a limited number of phi sizes were used by binning all silt and clay grains, that the actual values for all samples skew more poorly sorted than suggested.

Table 6. Inclusive Graphic Standard Deviation Results for All Samples

Sample	**Inclusive Graphic Standard Deviation**
NMC-1	4.42 ϕ
NMC-2	4.16 ϕ
NMC-3	3.91 ϕ
NMC-4	3.66 ϕ
NMC-5	4.16 ϕ

Using the cumulative percent curve for NMC-1 resulted in a value of 4.42 ϕ. This corresponds to extremely poor sorting of the gravels in this sample. The curves for NMC-2 and NMC-5 resulted in a value of 4.16 ϕ, which is also indicative of extremely poor sorting of sediments. The curves for NMC-3 and NMC-4 resulted in calculated values of 3.91 ϕ and 3.66 ϕ, respectively, which indicate a very poor sorting for the gravels. Though the level of sorting varied slightly between samples, all samples displayed characteristics of an unsorted grain population.

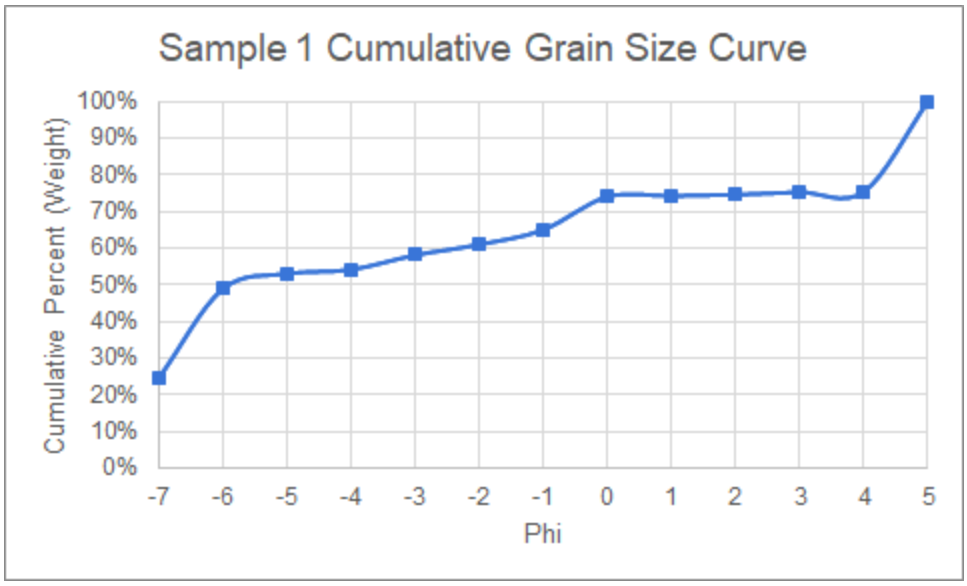

Figure 11. Cumulative percentage curve of weight for NMC-1. Phi sizes > 5 are grouped together

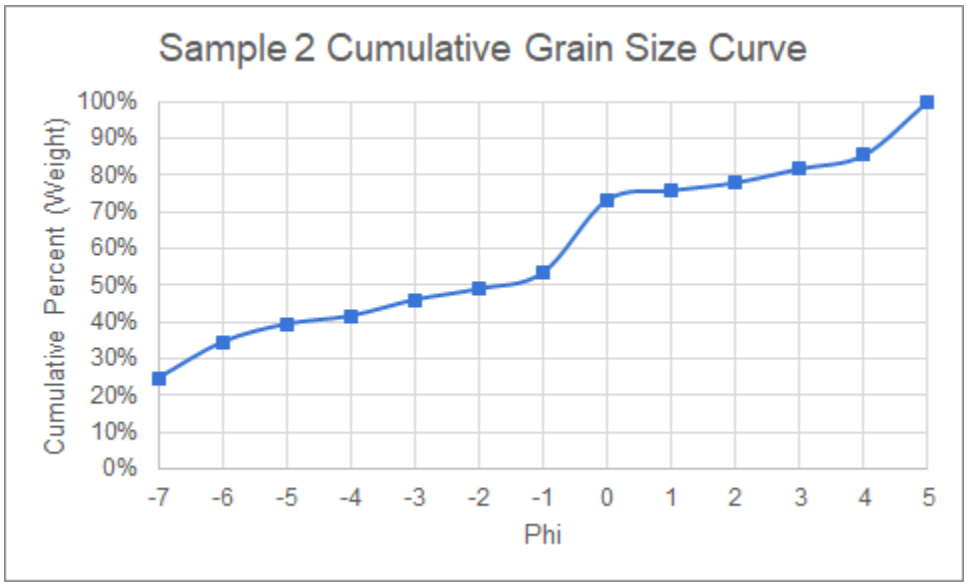

Figure 12. Cumulative percentage curve of weight for NMC-2. Phi sizes > 5 are grouped together

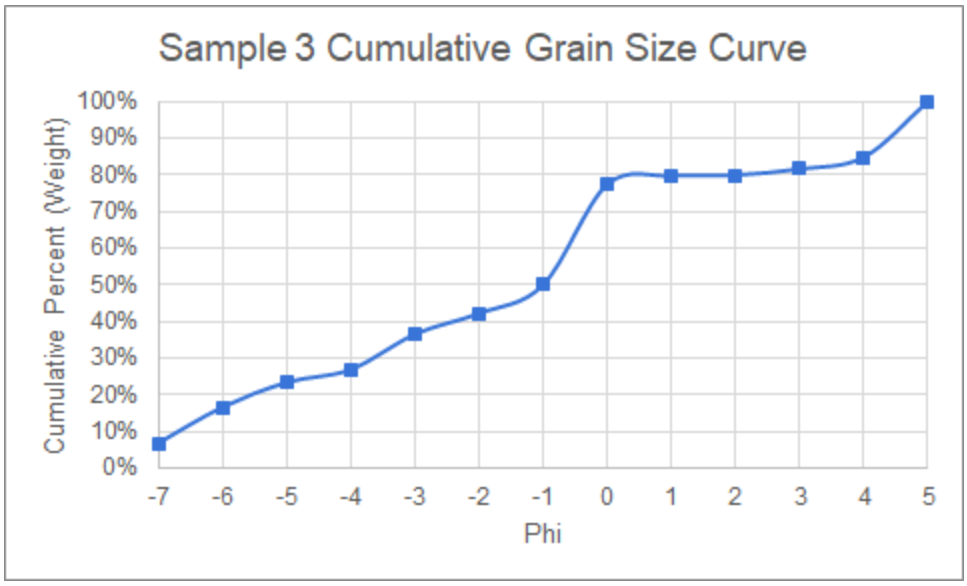

Figure 13. Cumulative percentage curve of weight for NMC-3. Phi sizes > 5 are grouped together

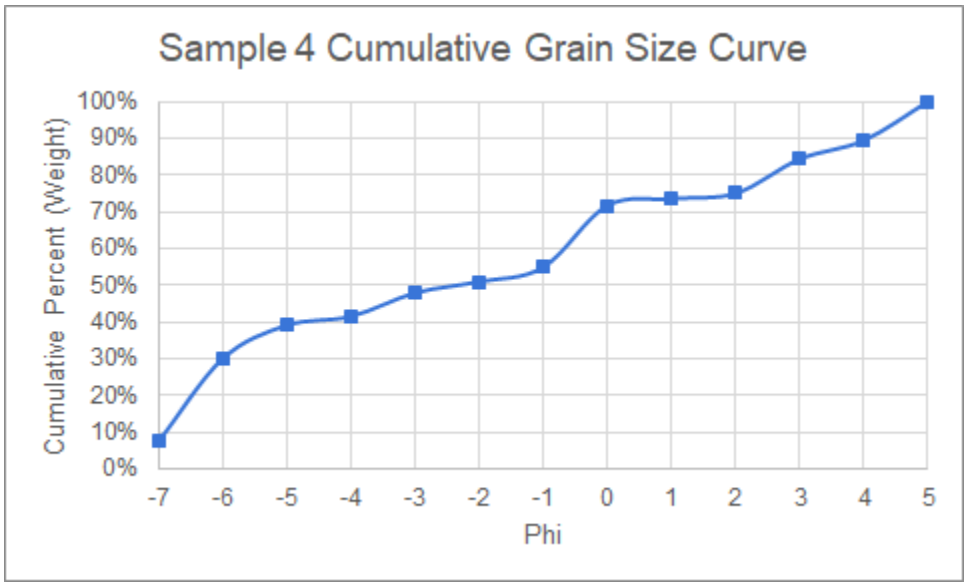

Figure 14. Cumulative percentage curve of weight for NMC-4. Phi sizes > 5 are grouped together

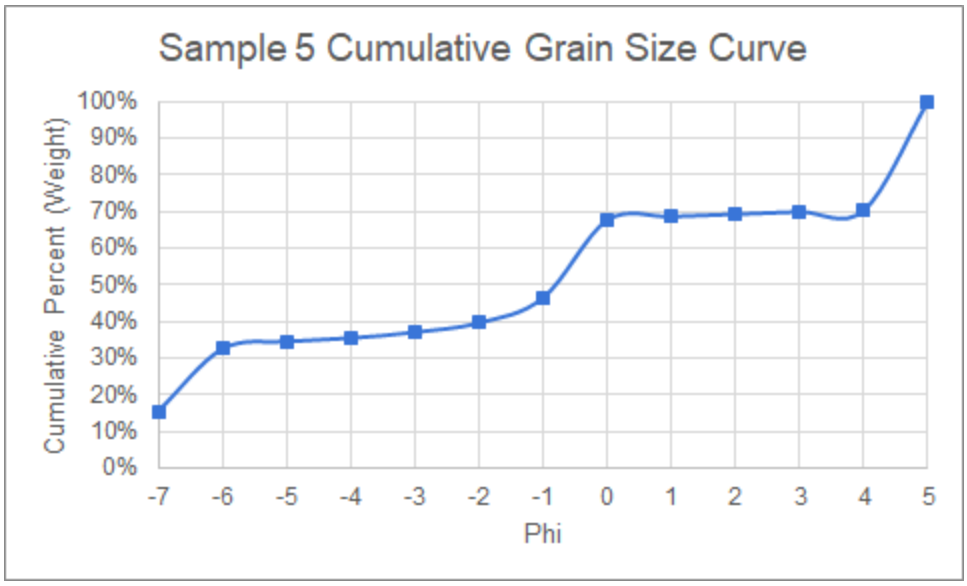

Figure 15. Cumulative percentage curve of weight for NMC-5. Phi sizes > 5 are grouped together

Orientation of Gravel Clasts

The 50 measured orientations of the gravel clasts are reported in Table 7. The mirrored version of this dataset is plotted on a rose diagram with a bin size of 10°. These initial results suggest that there may be at least some directionality (Fig. 16), though almost every bin had at least one grain fall within its bounds. The two strongest peaks are at 120°-°130/300°-310°, while subpeaks are present in multiple bins. These orientation data are certainly multimodal, and this was taken into consideration when attempting to statistically determine if there was a preferred orientation within the measured clasts. Importantly, while a sample size of 50 is sufficient to assess whether there is a preferred orientation of clasts, it is insufficient to determine orientation strength (Karatson et al. 2002).

Table 7. Gravel Clast Orientation Measurements. Lists the Collected Orientation Measurements from Clasts Exposed at the Surface of the Gravel Unit in SV-5/7. Only Grains with a Long Axis Greater Than 5 cm Were Measured.

Record ID	Trend (o)	Record ID	Trend (o)	Record ID	Trend (o)
1	59	**18**	162	**35**	279
2	93	**19**	105	**36**	130
3	56	**20**	172	**37**	339
4	136	**21**	184	**38**	305
5	126	**22**	274	**39**	31
6	318	**23**	120	**40**	85
7	44	**24**	110	**41**	156
8	55	**25**	227	**42**	122
9	114	**26**	322	**43**	154
10	64	**27**	229	**44**	131
11	147	**28**	262	**45**	129
12	135	**29**	302	**46**	7
13	151	**30**	272	**47**	304
14	61	**31**	151	**48**	274
15	149	**32**	209	**49**	93
16	82	**33**	116	**50**	129
17	193	**34**	145		

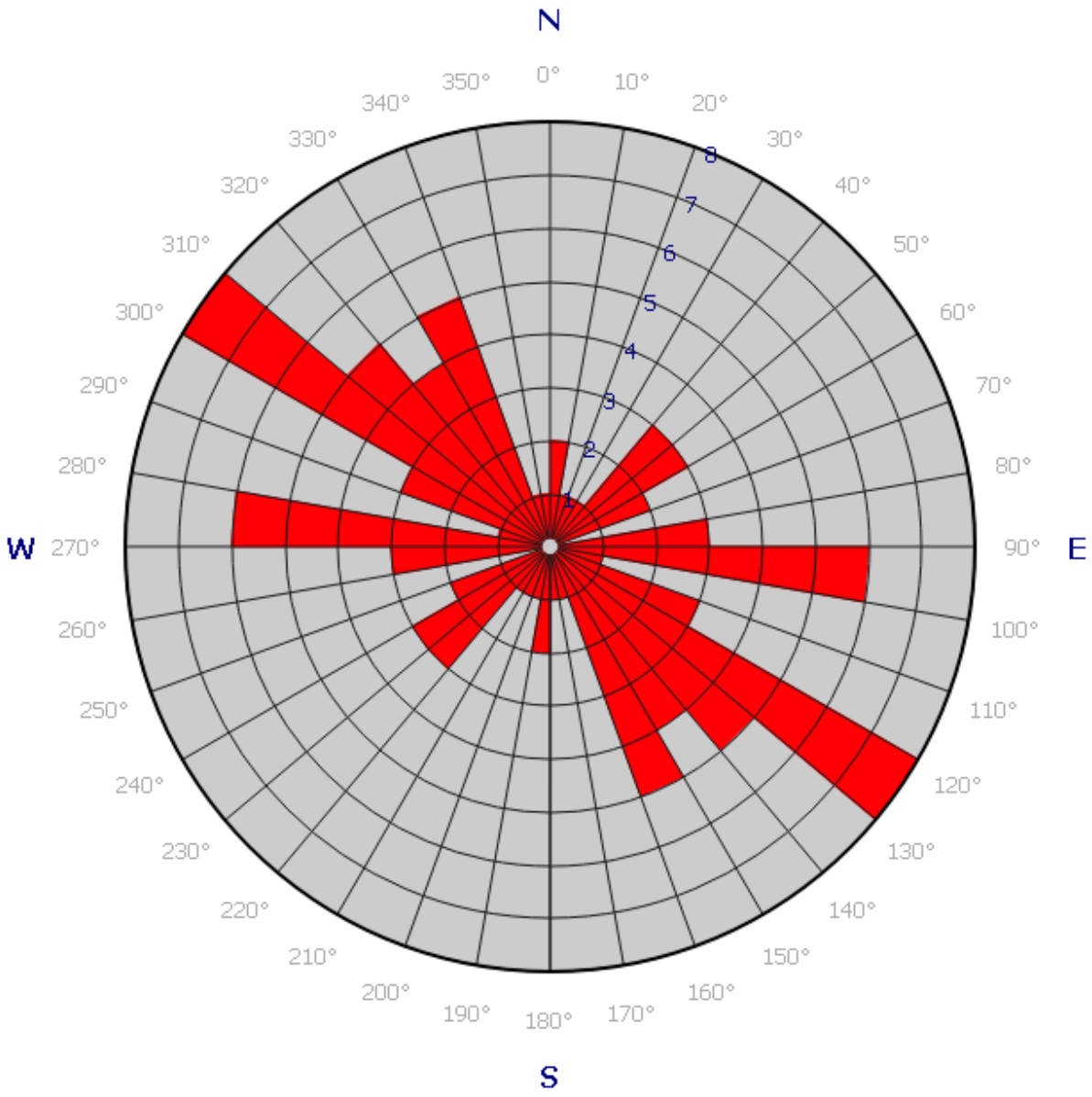

Figure 16. Rose diagram illustrating mirrored orientation data of SV-5/7 gravel clasts. Recorded clasts were greater than 5 cm in their longest dimension, and collected from the same, small area

To improve the interpretive rigor of the rose diagram, statistical analyses were used to assess directionality within the collected dataset. Tests performed include the new Hermans-Rasson test from Landler and colleagues (2019), the original Hermans-Rasson test, the Rayleigh

test, and the Pycke test. Each test was used to evaluate both the SV-5/7 dataset collected for this study, as well as a constructed, perfectly evenly distributed dataset (Table 8).

The Rayleigh test failed to reject the null hypothesis of uniformly distributed circular data in both the perfectly even and SV-5/7 datasets. This result is not entirely surprising, given the previously noted difficulty of this test handling multimodal datasets.

Both the new and original Hermans-Rasson tests failed to reject the null hypothesis of uniform data distribution for the perfectly even dataset but did reject this null hypothesis for the SV-5/7 dataset with p-values of 0.0006 and 0.0001 respectively. The Pycke test returned similar results, with a failure to reject the null hypothesis of uniformly distributed circular data in the perfectly even dataset, and a rejection of this null hypothesis in the SV-5/7 dataset. Both Hermans-Rasson tests returned smaller p values, though this may be due to the smaller sample size rendering the Pycke test less powerful, or due to there being less concentration of the orientations around the modal orientations.

Given the demonstration of successful analyses of multimodal data from these tests, the results of these tests are accepted. The orientation dataset that was collected from the center of SV-5/7 for this study is not uniformly distributed and does display at least some preferred orientation. This preferred orientation appears to be 130/310°.

Table 8. Gravel Orientation Statistical Tests. P-Values from Statistical Tests Performed on the Clast Orientation Dataset. Significant Test Results are Indicated With the (Reject Null) Label.

Test	Even Dataset p-value	SV-5/7 Dataset p-value
Hermans-Rasson (New) Test	1	**0.0006 (Reject null)**
Hermans-Rasson (Original) Test	1	**0.0001 (Reject null)**
Rayleigh Test	0.9811	0.5775
Pycke Test	1	**0.0058 (Reject null)**

Loss on Ignition

The small (1.5 mg) subsample collected from the fine-grained (sand and smaller) fraction of the gravel samples were subjected to loss on ignition (LOI) analysis. Loss on ignition results (Table 9) were mostly consistent across the samples. After 60 minutes at 500°C, NMC-1 lost 1.45% total weight, NMC-2 lost 2.88% total weight, NMC-3 lost 3.58% total weight, NMC-4 lost 2.39% total weight, and NMC-5 lost 3.17% total weight. Thus, the samples averaged around 2.69% ORG within the fine-grained fraction of the gravels. After the 900°C treatment for 60 minutes, each sample lost a significantly higher percentage of total weight. NMC-1 lost 10.66%, NMC-2 lost 9.61%, NMC-3 lost 9.90%, NMC-4 lost 12.13%, and NMC-5 lost 27.18%.

The average for samples 1-4 is a loss of 10.58% carbonate content per sample. NMC-5 lost more than twice this percentage of carbonate, which could possibly indicate a sampling bias. Alternatively, this could be an accurate representation of NMC-5 having a much higher carbonate content within the fine grain sediments, as other tests have demonstrated a high degree of heterogeneity between grain sizes. It is interesting however, that NMC-5 contained the highest

overall percentage of silt and clay sized grains, and the lowest overall percentage of gravels. According to the lithologic analyses, it appears that carbonate is more abundant in the larger grain sizes, and so this anomalous value may be an indication that further analysis of lithology is needed in future studies.

Table 9. Loss On Ignition Analysis Results

Sample	**Initial Mass**	**% Org (Organic Mass)**	**% $CaCO_3$ (Inorganic Carbon)**
NMC-1	136.3 mg	1.45% (1.98 mg)	10.66% (24.53 mg)
NMC-2	112.22 mg	2.88% (3.23 mg)	9.61% (10.78 mg)
NMC-3	95.71 mg	3.58% (3.43 mg)	9.90% (9.48 mg)
NMC-4	113.89 mg	2.39% (2.72 mg)	12.13% (13.82 mg)
NMC-5	88.09 mg	3.17% (2.79 mg)	27.18% (23.94 mg)

Discussion

Debris Flow Origin of the SV-5/7 Gravels

Although research occurring in the Saltville Valley in the last few decades has assigned a fluvial origin for the W4 gravel layer (McDonald and Bartlett 1983; Holman and McDonald 1986; McDonald 2000), there have since been indications that the gravels at SV-5/7 may not be consistent with a model of fluvial deposition. Prior excavations at the locality have yielded no evidence of imbrication within the gravels (Schubert pers. comm. 2020), and field observations during this study similarly found no instance of imbrication. Given the importance of imbrication in identifying alluvial gravel deposits (Prothero and Schwab 1996; Yagashita 1997; Schlunegger

and Garefalakis 2018), this lack of such a crucial structure over such a relatively large area within the SV-5/7 locality is what lead to the re-evaluation of the fluvial hypothesis by those working at the locality. This was the impetus for the geologic portion of this thesis.

In particular, the results of the particle size analysis offer support for a debris flow hypothesis, while arguing against a strictly fluvial deposition. The trimodal/polymodal patterns in all samples suggest a significant silt and clay component within those samples. Silt and clay sized grains are known to represent a small percentage of the deposits within braided river deposits (Pettijohn 1975; Miall 1977). Fluvial gravels tend to be clast supported (the gravel clasts were deposited by themselves, and then filled in with smaller grained particles afterwards) (Miall 1977), and the SV-5/7 sediments share this feature. Despite this similarity, numerous examples of clast supported debris flow deposits have been reported (Costa 1994; Blair and McPherson 1998; Sohn et al. 1999; Church and Jacob 2020), and the presence of a clast supported deposit does not rule out a debris flow origin. The problem with a fluvial interpretation then is not the presence of matrix, but the makeup of this matrix. While braided river systems can produce thick, cobble layers when located close to an alluvial fan source, these deposits still retain an abundance of sand sized grains within the matrix, and a minimal amount of silt and clay. While there are hills relatively close to the north and northeast of SV-5/7 it is not in close proximity to a large alluvial fan. Despite this, the shale and carbonate rich Paleozoic rocks that form the valley and underlie portions of it (and would likely have been exposed when the SV-5/7 gravels were deposited) would provide ample source material for a matrix of the lithologies observed. Thus, the large percentage of silt and clay within the matrix of these gravels is strong evidence against a braided river deposition.

Additional support for the debris flow model is provided by the results of the sorting

calculations. The field observation of poor sorting was confirmed, and even surpassed by the quantitative results which also indicate that the samples are either very poorly sorted or extremely poorly sorted. This extremely poor level of sorting is evidence against the fluvial and for the debris flow model. Very poor sorting of a massive gravel may be the best identifier of a debris flow deposit (Scott and Yuyi 2002; Lancaster et al. 2010), and fluvial deposits are known to have more sorted gravels (Lancaster et al. 2010).

The stratigraphy of the sample locations generally revealed a massive, unstratified gravel until the Maccrady Formation was reached. NMC-3 may have contained two separate horizons, although the only indicator of this was a difference in the largest grain sizes and, given that no gravel horizons were seen in the other samples, it seems most plausible that this represents meter-scale spatial variability in the heterogenous gravel deposit. NMC-2 was the only sample where there was more than one gravel layer, where two massive gravel layers were separated by a narrow horizon of red and gray bedded clays. The layered nature of this clay horizon suggests that it was not simply a case of a clay lens within the gravels. A possible explanation for this horizon could be that there were multiple debris flow events over time, and that it is simply reworked fine sediment that accumulated on top of an older gravel surface before it was covered over but not completely destroyed by a second pulse or additional debris flow. Alternatively, the surfaces of debris flow deposits are not always low relief (Karatson 2002), and it is possible that small clay layers accumulated and were sheltered from the scouring and reworking of later debris flow events.

Results of the particle size analysis and sorting calculations strongly support a debris flow as the depositional model for the gravels. Field observations and sorting calculations resulting from the grain size analysis indicate that all samples are very poorly sorted to extremely

poorly sorted. In addition to being more poorly sorted than fluvial gravels, all gravel samples contained significant portions of silt and clay sized material. The relatively high percentage of muds and bimodal to polymodal grain size distribution more strongly support a debris flow origin over a fluvial one.

In summary, the most likely origin for the SV-5/7 gravel unit is one or more debris flow events. Debris flows have been documented in the Blue Ridge (Wieczorek et al. 2004), and the Valley and Ridge regions (Eaton et al. 2003) of the Appalachian Mountains, so the acceptance of this model for the SV-5/7 gravels would not invoke a novel occurrence of this depositional mode in the region.

While not a common occurrence, fossils have been described from debris flow deposits (Rogers 2005; Domingo et al. 2017), so finding fossils on the surface of and embedded in the gravel deposit does not preclude a debris flow origin. They may simply be additional sedimentary clasts, albeit exotic ones, incorporated into debris flow sediments. Though it may initially seem at odds with a mass flow event, the smooth pavement of pebbles over deeper gravel deposits could be the result of reworking of the original debris flow deposit. This could also explain how so many fossils with abrasion damage (Silverstein 2017) came to rest on the same gravel surface. Debris flow deposits are often reworked by other debris flows (Costa 1994), and debris flows can also rework material from fluvial deposits (Lancaster et al. 2010). Thus, it is also possible that the larger, more rounded cobbles and fossils within the uppermost layer of the gravels had been deposited by a stream or river before being reincorporated into the debris flow and floated with the rest of the larger clasts.

The fluvial model of the Saltville River was tested using two end-member river facies models against a debris flow facies model. Ultimately, the meandering river hypothesis and

braided river hypothesis do not adequately explain the results of this study. Conversely, the debris flow is more consistent with the results, though more extensive excavations and descriptions will be needed to further test this hypothesis. Based on these data, the proposed Saltville River (McDonald and Bartlett 1983; McDonald 2000) does not seem to have been responsible for depositing the gravels at SV-5/7, and that hypothesis may need to be re-examined throughout the valley.

Orientation and Transport History of Gravel Clasts

While not supporting any of the tested hypotheses over the other, results of the orientation analysis offer additional insight into the transport history of the SV-5/7 gravels. Both meandering river and braided river deposits are known to contain gravel clasts which are oriented with flow, even within massive gravel units (Miall 1977). While a random orientation is frequently observed with debris flow deposits, it is also common to observe a preferred clast orientation parallel to flow, as this position is the least resistant to flow (Karatson et al. 2002). Given that the other data support debris flow deposition rather than braided or meandering fluvial deposition, it seems sufficient to comment only on the implications of the preferred orientation for the debris flow model. If this preferred NW/SE clast orientation is both an accurate representation of the gravels as a whole, and also represents a flow driven pattern rather than a random one (as is supported by the results of the statistical tests), then the data support either a northwest or southeast flow direction for the debris flow event. Given the nearby slope, it seems likely that the flow direction was towards the southeast, although this hypothesis will need to be tested more rigorously. In order to further assess this potential flow direction, a thorough, more widespread analysis of gravel clast trends should be undertaken.

The results of the roundness data are harder to interpret without first embarking on a detailed analysis of valley-wide lithology and potential source rocks. While this is beyond the scope of this thesis chapter, roundness observations may inform the direction of subsequent provenance analyses. Overall, the low roundness of the matrix points to a short transportation history, although it is important to note that fluvial rounding of fine-grained silicate clasts is an extremely slow process, even at the scale of hundreds of kilometers (Russell and Taylor 1937; Pettijohn et al. 1973; Pettijohn et al. 1975). Despite this, larger clasts can be rounded quickly, and rivers in the Appalachian Mountains have been known to round down pebbles (especially carbonate clasts) in as little as a couple of miles (Whitelaw pers. comm. 2020). Although small grains were more angular, the larger clasts tended to be rounded. This trend is consistent with experimental and observational studies suggesting larger grains become rounded at a greater rate than small grains (Pettijohn et al. 1973; Pettijohn 1975), and thus does not preclude (nor confirm) the gravel clasts and matrix having been transported a similar distance.

Results of the orientation data may offer insights into the transport history of the gravels, however. As figured by McDonald (2000), the hypothesized Saltville River would have flowed east-northeast through the valley. The orientation data recovered in this study suggest instead, a flow direction of either northwest or southeast for the SV-5/7 gravels. SV-5/7 is close (a little over a couple hundred meters) to a major hillside (Fig. 1), with an opening in this hillside directly northeast. It is possible that this may be a direct source for this material given the proximity and direction to the site, although this will certainly require additional analyses to test.

While these results will hopefully prompt other projects, they are difficult to interpret without applying data from other areas of the valley, and caution should be exercised when trying to reconstruct transport distance and depositional history of clasts from a limited dataset.

Study Limitations and Future Directions

Future efforts to characterize the origin of the SV-5/7 gravel would benefit from a spatially widespread excavation program that is focused on acquiring cross-sectional data on the gravel deposits in multiple locations throughout the valley. Specifically, comparisons to the gravels reported by McDonald and Bartlett (1983) and McDonald (2000) may be beneficial to researchers studying Quaternary paleontology or geology at Saltville. Describing transects of these units, as well as larger studies of clast orientation seem like clear next steps.

Another major objective in determining the depositional history would be determining the provenance of the matrix grains as well as the large clasts. The analysis of sediment provenance is beyond the scope of this thesis. However, determining the source areas for this gravel deposit should be a high priority for future geologic investigations. Previous work has suggested that some chert and sandstone clasts from the SV-1 gravels could have been sourced from Stonemill Creek and McHenry Creek (McDonald 1984b). While not strictly necessary to test the depositional models of the site, determining the provenance of these sediments would necessarily have implications for the types of depositional processes that could have deposited them, and will increase the robustness of future assessments. Source rocks from far away are less likely to represent debris flows deposits than fluvially transported grains, for instance, and being able to source a specific unit to the sediments may assist in determining flow direction or properties if the debris flow origin continues to be supported by future data.

Such a project utilizing similar and more advanced methods could identify source areas for the sediments, and thus further inform us as to the path, distance and nature of the depositional events responsible for the SV-5/7 gravels. Additionally, it might prove fruitful to investigate other areas in the valley with reported fluvial gravels, in order to see if they match the

patterns seen at SV-5/7 or are truly different. Moreover, while the presence of the Saltville Fault was briefly mentioned in this chapter, it was not analyzed in detail. This feature seems like an obvious candidate for future explorations of source rock material of the SV-5/7 and the rest of the Saltville Valley gravels.

Conclusions

Overall, these results provide evidence for a massive gravel deposit that is poorly sorted, has a primarily subangular fine-grained matrix, and displays a bimodal to polymodal grain size distribution. The most abundant clast sizes within the bulk samples by weight are cobbles, coarse sand, and silt/clay. Silt and sand contributed a large component to the bulk sample. The traditional fluvial interpretation of deposition by the "Saltville River" for the W4 layer within the Saltville Valley is not supported at the SV-5/7 site. These data instead suggest a debris flow model of deposition at SV-5/7. Debris flows are well documented in the Appalachians, especially on steep slopes after rainfall events, and so the presence of a debris flow at SV-5/7 and within the Saltville Valley does not seem surprising.

CHAPTER 3. IDENTIFICATION AND ANATOMY OF FOSSIL MUSKOXEN

Introduction

Overview

In order to diversify this thesis and incorporate a vertebrate paleontology component, unanswered questions about the Saltville paleofauna were explored. Of particular interest to the author was the presence of bovid fossil material from Saltville that had been identified as indeterminate muskoxen. Because the material had not yet been identified to the genus level, generic identification of Saltville muskoxen became a goal of this thesis. The identification of most fossil muskoxen focuses on horncores and crania, and many of the Saltville ovibovine specimens are isolated teeth or postcrania, in addition to some cranial material. Differential diagnosis of potential muskoxen genera and subsequent identification of Saltville muskoxen remains was a primary objective of this project.

In order to provide a framework to accomplish that goal this chapter begins with a review of muskox taxonomy and phylogeny. Next, the fossil muskoxen of North America are discussed, followed by a discussion of the muskox material collected from Saltville. This review is followed by the methods and materials of this comparative study which, in turn, is followed by the accompanying results and discussion. Potential future directions and a summary of the comparative study concludes this chapter.

The Ovibovini – Muskoxen

While the extant tundra muskox (*Ovibos moschatus*) is now understood to be closely related to goats and sheep, most researchers prior to the modern evolutionary synthesis

considered them to be most closely grouped with “oxen” or cattle (Harlan 1825; DeKay 1828; Leidy 1852), evident by the species having been originally described as *Bos moschatus* by Zimmerman (1780). Blaineville (1816) erected the genus *Ovibos* to differentiate it from cattle, although some authors continued to refer to the muskox as *Bos mochatus* (DeKay 1828; Allen 1913). Upon naming the muskox, Blainville noted that the animal had more in common with sheep than with oxen (Blainville 1816), although some of the characters he used to do so (e.g., the presence of only two mammaries, and the lack of a muffle or naked portion of the muzzle) have been declared erroneous (Allen 1913). The prevailing belief that the muskox was a type of cow was so strong that Owen (1856) attempted to name it as a species of cape buffalo, *Bubalus*. Despite this, some authors continued to push for the position as close to sheep, or at least intermediate between sheep and cattle citing osteological characters to support this. Dawkins (1867) noted the tapering of the facial portion of the skull, prominent orbital protrusion, “verticality of the facial plate of the maxillary,” shape of the basisphenoid, occipito-parietal suture, and multiple dental characters as evidence for a closer association with sheep than with *Bos*. In his 1913 examination of muskoxen skull and horn ontogeny, which remains the most extensive published record of muskoxen skull and tooth morphology, Allen argued that many of these features were present in bison, and therefore Dawkins must be mistaken (Allen 1913).

The concept of a distinct muskox group (rather than inclusion within *Bos*) was developed when the similarity between the extant muskox (*Ovibos*) and the extant takin (*Budorcas*) was noted by Gray (1872), wherein the group “Ovibovidae” was proposed. Interestingly, the same name was also proposed later in Gill (1872), and the name is occasionally attributed thus. In Gray’s publication, which appears to have been published first, these taxa were linked as morphologically similar to the family Antelopidae based on sharing the characters “Nose ovine,

covered with hair, without any or only a rudimentary muffle." While many of the characteristics of the Ovibovidae used to group the muskox and takin were soft tissue, skull characters were also noted. These included a large nasal opening, short intermaxillaries that don't reach the nasals, the lack of a suborbital fissure or fossa, and well-developed molars with supplementary lobe (Gray 1872). The closeness of *Budorcas* to *Ovibos* became a controversial issue, with publications supporting (Matschie 1898) the *Ovibos*-*Budorca*s connection, and others vehemently rejecting it (Lönnberg 1900; Knotterus-Meyer 1907), or even openly mocking and questioning the methodology behind the conclusion (Allen 1913).

Genetic analyses in the 20th and 21st century proved useful for resolving these controversies and reversed the trend in muskoxen taxonomy and phylogenetic systematics. Multiple genetic studies using different techniques suggested that *Ovibos* and *Budorcas* do not form a monophyletic clade (Groves and Shields 1996; Groves and Shields 1997; Hassanin et al. 1998). Additionally, the morphological observations of Blainville (1816) and Dawkins (1867) would be supported as mounting genetic evidence positioned *Ovibos* within the goat and sheep subfamily clade of Caprinae, as a sister group to the gorals *Naemorhedus* and the serows *Capricorni*s (Groves and Shields 1997; Hassanin et al. 1998; Hassanin et al. 2009; Shi et al. 2016). Moreover, the group formed by these three genera have been assigned the rank of subtribe and the accompanying name of Ovibovina (Hassanin et al. 2009), which is the nomenclature used for this study.

Despite the tribe originally being defined by *Ovibos* and *Budorcas*, it is now generally accepted that the group of muskoxen that form a clade containing *Ovibos*, but to the exclusion of *Naemorhedus* and *Capricornis*, is called Ovibovini (Cregut-Bonnoure and Dimitrijevic 2006; Shi et al. 2014; Lazaridis et al. 2017). It should be noted that despite being named as a tribe, this

grouping no longer retains this rank, and thus may need to be renamed to better conform with taxonomic conventions. Given that the rank of tribe is now occupied by Caprini, and the subtribe is occupied by Caprina (Hassanin et al. 2009), the group of animals forming a monophyletic clade with *Ovibos* to the exclusion of *Capricorni*s and *Naemorhedus* cannot rank as a tribe or subtribe. Ovibovini as used in the literature clearly refers to a group that is meant to be a rank below the subtribe of Ovibovina and would thus be an infratribe. For sake of clarity, the traditional name of the "tribe" Ovibovini is used herein, although it should be noted that the current taxonomic classification for the group is inadequate.

Despite the clarity that genetic evidence has given us about the relationship of the muskox within Bovidae, there are many fossils of interest which exceed an age in which aDNA is currently able to be extracted. Collectively referred to as the "late Miocene ovibovine like bovids," these various genera from across Eurasia (*Tsaidamotherium*, *Parumiatherium*, *Shaanxispira*, *Palaeoreas*, *Criotherium*, etc.) are tentatively referred to as belonging to Ovibovini, though it is acknowledged that these may just be convergent forms. Many have spiraling horns such as those seen in *Shaanxispira* or *Parurmatherium* (Solounias 1981; Shi et al. 2014), or strange horn-core complexes with no known analogs (Shi 2013). Despite enigmatic origins, these fossil forms share important characteristics with *Ovibos* that have been used to erect a suite of traits that encompass characters of Ovibovini. These include: (a) short occipital condyles that are more deeply attached to the skull, (b) accessory surfaces on the lateral surfaces of the occipital condyles, (c) thickening of the basicranium, (d) rugosity/exostosis of the horn core plate, (e) semi-hypsodont premolars and molars, (f) robust cervical vertebrae, and (g) a stronger attachment of the atlas and cranium (Bohlin 1935; Geraads and Spassov 2008; Shi 2013; Shi et al. 2014). Potentially informative is that these characters are all focused on the area of

articulation of the atlas and cranium and are widely considered to be likely related to combat behavior (Geraads and Spassov 2008; Shi et al 2013). It is known that cervical vertebrae characteristics can be correlated with intraspecific combat behavior in artiodactyls (Vander Linden and Dumont 2019). Some other ruminants who engage in ramming behavior similar to muskoxen (such as *Syncerus* and *Connochaetes*) do not possess these same characteristics (Geraads and Spassov 2008) and thus it is possible, yet unproven, that these characters may serve as useful indicators of the ovibovine clade.

North American Fossil Muskoxen

Ovibovine fossils are found across the northern hemisphere in Asia, Europe and North America (McDonald and Bartlett 1983; Martinez-Navarro et al. 2012). The first known fossil of a North American ovibovine was recovered from Big Bone Lick, Kentucky, in the form of a partial cranium consisting of the occipital region, horncores, frontals and partial orbits (Wistar 1818). Though the specimen would later be identified as the helmeted muskox *Bootherium* (Leidy 1852), it initially proved to be of enigmatic origin. Comparisons to the genus *Bos* were made immediately, though Wistar noted major morphological distinctions such as the closeness of the horns to the orbits, and distance of horns from the 'occipital surface," as well as the prominent convexity of the cranium in the horn attachment. This latter character was recognized as occurring in goats, sheep and deer, and it was noticed that the horns were not deciduous like those of deer (Wistar 1818), and that author suggested the animal must be "closely allied to the bison". This publication did not reference comparisons with modern muskoxen. Subsequent work by Richard Harlan would provide a taxonomic name to the cranium, creating *Bos bombifrons* (Harlan 1825). The cranium was contrasted with that of *Bison* listing many clear

differences, and the presence of isolated teeth resembling those of *Bos*, albeit more robust, prompted assignment to the genus *Bos* when describing the specimen (Harlan 1825).

A second cranium, from New Madrid, Missouri, was examined in 1828, and was recognized as being most similar to a modern muskox (DeKay 1828). Important characters indicating this similarity were horns that are both flattened and curved and horncores that are parallel to each other and not set at an angle. The presence of a large depression separating the horns, which DeKay believed to be a natural appearance and not simply a completely degraded frontal, as well as different proportions in the pterygoid region, excluded the specimen from being assigned to *Ovibos moschatus* (DeKay 1828). The specimen was provisionally given the name *Bos pallasii*, and noted as clearly being allied to the extant muskox, but probably distinct (DeKay 1828). Joseph Leidy would go on to describe the genus *Bootherium* in 1852 based on characteristics that he felt differentiated it from both *Bos* and *Ovibos*. These included: (a) the frontal forming prominent processes which give rise to the horn cores, (b) horn cores positioned posteriorly and superiorly to the orbits, but well anterior to the inion, (c) horns curve downwards and do not recurve dorsally as seen in *Ovibos* and (d) the presence of well-developed lachrymal depressions (Leidy 1852a). While still considered to be a type of ox, and thus allied to bison and cattle, Leidy noted that "The genus [*Bootherium*] occupies a position intermediate to *Bos* and *Ovis*" (Leidy 1852b p. 12). The genus was split into two species, *Bootherium cavifrons* (bearing a rough exostosis-like process between the horns), and *Bootherium bombifrons* (bearing a smooth surface between the horns) (Leidy 1852a).

Unfortunately, many of these characteristics would later be realized to be shared with *Ovibos*, and thus the diagnosis for the genus was not actually diagnostic (McDonald and Ray 1989). The lack of truly diagnostic characters differentiating *Bootherium* from *Ovibos* (aside

from the latter having horncores that do not meet over the midline of the cranium), as well as a failure to adequately understand the anatomy of *Ovibos* for comparison, would lead to years of confusion. *Ovibos* and *Bootherium* were sometimes synonymized based on minimal material and unverified assumptions (Richardson 1952), and sometimes split despite the support of erroneous characteristics (Leidy 1854). New species of *Ovibos* (Rhoads 1897; Richardson 1952) and entirely new genera (Osgood 1905a; Gidley 1906) were erected while trying to wrestle with the variation present in a relatively limited fossil sample.

A major development in North American fossil muskoxen taxonomy was Osgood's (1905a) description of *Scaphoceras*. This genus name was found to be preoccupied and changed to *Symbos* shortly after by Osgood (1905b). The holotype cranium was mostly complete, and is missing only the nasals, one lateral half of the premaxilla, the right premolars and first molar, and left 1st molar. *Symbos* was defined by: (a) horn cores smaller than *Ovibos* that are less compressed at the base and more divergent at the tips, (b) the skull displaying heavy exostosis between the horn cores deepest in the medial plane, and with an anterior rim, (c) orbits that protrude laterally less than in *Ovibos* (d) the facial portion of the skull being almost as wide as the cranial portion, (e) a basioccipital without a tall median ridge, and (f) large and broad teeth with a quadrate m1 and m2 (Osgood 1905a). This specimen was identified with the new species *Symbos tyrelli*, while the Leidy holotype was assigned to *Symbos cavifrons* on the basis of the former being smaller than the latter, with smaller horncores, a deeper but less extensive exostosis and a more shallow braincase area (Osgood 1905a). Another genus of Pleistocene North American muskox was erected from a partial cranium by Gidley (1906) called *Liops*, though this name was invalid and was eventually replaced by *Gidleya* (Cossmann 1907). A new species of *Symbos* (*S. australis*) would also be named from six isolated teeth and non-associated postcrania,

although the main character difference was total size (Brown 1908; McDonald and Ray 1989). Throughout the 1900s, several new genera and species of North American muskoxen were erected based on fragmentary cranial and dental remains with minor variations present between them (McDonald and Ray 1989). The species *Bootherium nivicolens* (Hay 1915), *Symbos promptus* (Hay 1920), *Symbos convexifrons* (Barbour 1934), *Ovibos giganteus* (Frick 1937), and *Bootherium brazosis* (Hesse 1942) were all erected from either partial crania with horncore, or isolated teeth. Because these species were erected on poor material upon features that are now known to be highly variable within the modern muskox *Ovibos*, there was little consensus over which names were valid, which should be synonymized, and based upon which characters (McDonald and Ray 1989).

A hypothesis that had been previously posed but not well received by late 19th century and early 20th century researchers was resurrected by Hibbard and Hinds (1960), when they suggested that *Symbos* was the male woodland muskox (one of the common names attributed to the *Bootherium/Symbo*s group), while *Bootherium* was the female form. The authors pointed to the fact that all known *Symbos* described in the literature were believed to be male individuals and found that scenario unlikely (Hibbard and Hinds 1960). Subsequent opinions varied from keeping *Symbos* and *Bootherium* split (Harington 1961), to agreement with synonomy (Harington 1977; Nelson and Madsen 1987), and even the hypothesis that only some *Bootherium* species were female *Symbos* (Semken et al. 1964). Discussion and comparison would eventually lead to McDonald and Ray's (1989) publication wherein the genera *Bootherium*, *Symbos*, and *Gidleya* (the remaining "valid" names of the time) and their species were examined in detail. Characters including lacrimal fossa depth, horncore morphology, and absolute size were

examined, as well as the purportedly important character of Osgood (1905a), the degree of flexion between the basioccipital and basisphenoid (McDonald and Ray 1989).

Lacrimal fossa depth was found to be highly variable between individuals, but the fossa tended to be both more defined and larger in *Symbos* when compared to *Bootherium* (McDonald and Ray 1989). Differences in horn core morphology between the two taxa were attributed to sexual dimorphism of a higher degree than exhibited in *Ovibos*, and it was noted that greater sexual dimorphism in horn cores was present in some Pleistocene taxa when compared to their Holocene relatives (McDonald and Ray 1989). Differences in absolute size of *Symbos* and *Bootherium* were compared with those seen in male and female *Ovibos*, and it was concluded that the proportional differences were within the realm of modern muskoxen sexual dimorphism for the fossil forms (McDonald and Ray 1989). The angle of flexion between the planes of the basioccipital and basisphenoid had been noted to be potentially significant by Osgood in 1905. McDonald and Ray tested this by measuring these angles in individuals of both woodland muskox and female and male *Ovibos*. Their results suggested that the angles were correlated with age and sex in modern muskox, and that these trends were congruent with *Symbos* being the male form of *Bootherium* (McDonald and Ray 1989). In addition to laying out a strong and consistent case for synonymizing the genera into *Bootherium*, the authors suggested that continuous variation observed within the genus served as evidence that there should only be one species of North American woodland muskox, *B. bombifrons* (McDonald and Ray 1989). Subsequent publications have largely accepted this conclusion (Richards and McDonald 1991; Guthrie 1992).

Additional North American muskoxen that are worth noting include *Euceratherium*, *Soergelia,* and *Praeovibos* (Kurtén and Anderson 1980). *Euceratherium*'s known distribution is

limited to the western United States (Kurténn and Anderson 1980; Feranec 2009), and their horn cores are characteristically large and forward-curving (Stoval 1937; Kurtén and Anderson 1980). *Soergelia* is known from sites in Eurasia and North America (Stock and Furlong 1927; Kolfschoten and Vervoort-Kerkhoff 1999; Cregut-Bonnoure and Dimitrijevic 2006), and are characterized by a size even larger than that of *Euceratherium* (Kurtén and Anderson 1980) and a diagnostic "open v" horn core shape (Guthrie 1992). Given their large size and distinct horn morphology, both *Euceratherium* and *Soergelia* are easily distinguished from *Bootherium* and *Ovibos* if reported from cranial material, especially that of the posterior crania and horn sheath attachment area. The presence of either genera at Saltville would invoke significant range extension and their inclusion within the Saltville paleofauna seems unlikely at this time.

Praeovibos is another genus of Pleistocene muskox, that like *Soergelia*, was primarily distributed in Europe and Asia (Mol and Reumer 1999). Additionally, specimens have been recovered from North America, but are limited to Alaska (Mol and Reumer 1999; Campos et al. 2010). This ovibovine is differentiated from the morphologically similar *Ovibos* through the former's larger size and less flattened horncore bases (Mol and Reumer 1999; Gentry 2000). Recent genetic analysis of North American muskoxen genera resulted in a phylogenetic tree which placed the four successfully sampled *Praeovibos* entirely within the diversity observed in ancient *Ovibos* (Campos et al. 2010). Because of these results and the lack of definitive characteristics distinguishing the two genera, the authors concluded that *Praeovibos* may be an earlier, more generalized morphotype of *Ovibos* (Campos et al. 2010). Due to the combination of recent doubt of the genus' validity and the exclusively Beringian distribution within North America, it seems extremely unlikely that *Praeovibos* would be present within the Saltville paleofauna.

The advent of ancient DNA analysis techniques has been somewhat unsuccessful for revealing relationships between Pleistocene fossil muskoxen. The aforementioned examination of four of the five "valid" Pleistocene muskox genera (*Ovibos*, *Bootherium*, *Euceratherium*, and *Praeovibos*) resulted in a phylogeny that supported a close association between *Praeovibos* and *Ovibos* where the former fell completely within the diversity of the latter, with the authors interpreting this as good reason to conclude that *Praeovibos* is actually just a more ancient morphotype of *Ovibos* (Campos et al. 2010). This interpretation is bolstered by the known lack of genetic diversity of modern *Ovibos* (Groves and Shields 1997; MacPhee and Greenwood, 2007). Additionally, the aDNA and protein analyses of Campos and colleagues (2010) supported a clade where *Bootherium* and *Euceratherium* were more closely related to each other than other muskox taxa. This was not supported by a subsequent study of *Bootherium* and *Ovibos* complete mitochondrial genomes by West (2016), who recovered the two taxa as sister groups, though notably did not include other fossil muskoxen in the analysis. A follow up mitochondrial genome analysis tested seven *Bootherium/Symbos* samples and one *Euceratherium* sample against other Caprini species and once again recovered *Bootherium* and *Ovibos* as sister taxa (Bover et al. 2018). Importantly, the analyses of Bover and colleagues (2018) demonstrated a strong molecular similarity between *Bootherium* and *Symbos* and agreed with their synonomization into *Bootherium*. Although this analysis resulted in maximum support for an *Ovibos* and *Bootherium* clade, the *Euceratherium* sample failed to produce aDNA, and could not be analyzed (Bover et al. 2018). The authors tested the *Euceratherium* sequence fragment from the Campos et al. (2010) study, and found it to fall within their own *Bootherium* diversity with only one nucleotide difference between the 78 base pairs (Bover et al, 2018). This was interpreted to mean that the identity of the 2010 *Euceratherium* sample (which came from a coprolite) was in question, as it

was plausible that this could have been a misidentified *Bootherium* coprolite (Bover et al. 2018). While attempts to use molecular analyses to inform relationships between the ovibovines have met with both success and failure, a larger and more comprehensive sample of muskoxen ancient DNA must be collected and analyzed to improve phylogenetic resolution.

The Saltville Muskoxen

Fossil remains of muskoxen from Saltville have been reported in the literature since 1967, when Ray and colleagues (1967) published on a pair of muskox crania, one attributed to *Bootherium* and one to *Symbos*. In 1980, associated postcranial material attributed to at least one Pleistocene ovibovine was recovered from SV-1, and included much of the axial skeleton, a scapula, and fragments of the limb elements (McDonald and Bartlett 1983). The material was well preserved, but the scarcity of published muskoxen postcranial descriptions limited the identification of the material to ovibovine, based on the wide spacing of alar foramina, and the ventral ridge on the caudal margins of the articular surfaces of the vertebrae (McDonald and Bartlett 1983). The authors noted that the fossils were likely either *Symbos* or *Bootherium* (McDonald and Bartlett 1983) due to their previous identification in the Saltville paleofaunal community, although it was noted that the atlas was missing the surfaces that articulate with the accessory condyles seen in at least one *Ovibos* (McDonald and Bartlett 1983). Skeletal elements of USNM-M-261802, the male modern *Ovibos* which was used for comparison, were reported as smaller and less robust than those of the fossil specimen (McDonald and Bartlett 1983). Despite the larger size of the fossil specimen, it was noted that the vertebral foramina were proportionally and sometimes absolutely smaller than those in the *Ovibos* USNM-M-261802 (McDonald and Bartlett 1983).

Fossil muskoxen from Saltville are curated at a number of museums. The United States National Museum of Natural History (USNM) paleobiology collection houses material from Saltville, including two partial crania and at least two isolated teeth representing muskoxen material. The Virginia Museum of Natural History (VMNH) collection also contains fossil ovibovine material collected from Saltville, including an abundance of isolated teeth, a partial cranium, and the material recovered by McDonald and Bartlett (1983). The East Tennessee Museum of Natural History (ETMNH) collections contains Saltville specimens tentatively identified as "musk ox?" or ovibovine. This includes isolated postcrania, an isolated tooth (ETMNH 19793), and an associated series of 3 cheek teeth (ETMNH 15423). Due to the fragmentary or isolated nature of most of the muskox material from Saltville, generic identification is currently unclear.

While *Euceratherium* and *Soergelia* are not known from the eastern United States, both *Bootherium* and *Ovibos* have been recovered as fossils. Despite a broad overlap in the geographical range of the two genera in North America, *Ovibos* does not extend as far into the southern or southeastern United States (Nelson and Madsen 1978; McDonald and Davis 1989). Importantly, *Ovibos* is currently, and has in the past been associated with areas of perennially frozen ground (i.e., permafrost) during the Wisconsin glaciation (McDonald and Davis 1989). The traditional interpretation of the environmental conditions of the Saltville fossil sites is that of a periglacial environment with boreal forests or spruce parklands in the lowlands where the fossils are found, and alpine environments at the higher elevations (Ray et al. 1967; Delcourt and Delcourt 1988). Recent studies have suggested that, at times, the alpine permafrost may have extended far down into the Southern Appalachians and the Saltville sites (French and Millar 2014), and that periglacial conditions are supported for this area, and north for the Appalachian

Mountains (Clark and Ciolkosz 1988, Nelson et al. 2007). Given this association, *Ovibos* becomes a reasonable potential candidate for the identification of Saltville muskoxen specimens.

While indeterminate ovibovine fossils have been recovered from Nashville, Tennessee (Guilday 1977), the southernmost confirmed *Ovibos* materials are currently far to the northwest of Saltville. While unfigured and undescribed teeth attributed to *Ovibos* sp. have been reported from Big Bone Lick State Park in northern Kentucky (Schultz et al. 1963), the southernmost, well-documented occurrence of *Ovibos* is a partial cranium from Hamilton County, Ohio (McDonald and Davis 1989). The Nashville muskox occurrence references the First American Bank Cave locality, with a publication that identifies a lone phalanx as "Musk Ox? — Ovibovini?" (Guilday 1977).

While ovibovine material from Saltville is curated in a number museums, many of the fossils are postcrania or isolated teeth and have thus been only tentatively identified and remain undescribed and unpublished. There is a major deficit of postcranial skeletal anatomy of extinct and extant ovibovines in the scientific literature, although descriptions of fragmentary cranial material are relatively common. This study focuses on the cranial and dental anatomy of muskox remains, with the goal of refining differential diagnoses of isolated *Bootherium* and *Ovibos* elements. If that goal is achieved, then assessing the identification of ovibovine material from Saltville should be possible.

Methods

Eight modern *Ovibos* skulls (crania and associated mandibles) were analyzed along with eight extinct muskox partial crania, and ten specimens that were isolated teeth or fragmentary mandibles with teeth were measured. Additionally, 12 previously measured and published fossil teeth from Richards and McDonald (1991) were incorporated into the dataset, as well as digital

measurements of 10 figured muskox skulls (nine fossil and one modern) from the literature. The full dataset thus consists of measurements of eight modern *Ovibos* crania, 18 fossil muskox crania, 22 isolated fossil teeth, and a partial fossil mandible with four teeth

Modern *Ovibos* specimens from the USNM mammalogy collections were chosen to reflect specimen completeness and biological and morphological diversity within the sample population. Four males, three females, and one specimen of unknown sex were selected for measurement. All but one specimen retained horn sheaths, and specimens represent a variety of adult ages based on tooth wear. Additionally, specimens of different sizes were selected to better reflect size-related morphological changes.

Extinct muskoxen identified as *Bootherium*, *Symbos*, and ovibovine indet. were selected for analysis based on availability of material. Specimens from the USNM, VMNH and ETMNH were examined. To avoid possible complications due to ontogeny, juvenile specimens were avoided when collecting measurements from physical specimens and from specimens reported in the literature. These specimens included eight partial crania, one partial palate, a partial left mandible, and multiple isolated teeth. Measured specimens from Richards and McDonald (1991) were incorporated into the dataset as well, which consisted of two partial crania and twelve teeth.

Measurements reflect the goal of recovering as much overlapping morphological information as possible between complete modern skulls and fragmentary fossil remains. Linear measurements were collected using both a small and large set of Fowler digital calipers, as appropriate for the distance being measured. Angular measurements were collected using a Cen-Tech goniometer. All measurements (Table 4.1) were replicated twice and averaged for analysis. The primary source of measurements for this analysis was von den Driesch (1976) with the majority of measurements from the *Bos* cranial measurements section. This was the source for

listed measurements unless specified otherwise. These were preferred over the *Ovis*/*Capra* measurements due to the convergent nature and similar size of *Ovibos* and *Bos* skulls, and the similarity of the positions of the horns on the skull. Other measurements were created as needed with the goal of capturing potentially significant data, including linear distances and angles. Where appropriate, left and right-side measurements were collected separately.

The measurements denoted as digital were collected using the Linux distribution of imageJ image analysis software, ImageJ 1.53c (Schneider et al. 2012). A digital scale was set using a photographic scale included in the photograph, and then distances were measured by plotting a line and measuring its distance based on the scale. While the scale was set below the plane of features being measured, these measurements themselves were on the same plane and were examined exclusively as ratios with each other. Thus, while the raw measurements themselves may be slightly inaccurate, the unitless ratios should remain an accurate representation of anatomical trends. Measurements are detailed in Table 10 and illustrated in Figs. 17, 18, 19, 20 and 21. The measurements are listed along with the exact definition of the measurement.

Table 10. Muskoxen Measurements. Names and Descriptions of Measurements Provided.

1	Distance from prosthion (anteriormost tip of nasal bone) to akrokranion (posteriormost point on the vertex of the cranium).
2	Distance from prosthion to posteriormost extent of occipital condyle.
3	Distance from prosthion to the basion (anterior-most margin of the foramen magnum).
4	Distance from the premolare (median point of line connecting the anteriormost points of the premolar alveoli) to the basion.
7	From the nasion (median point of the nasal/frontal suture) to the prosthion.
16	Distance from infraorbitale (most posterior point of infraorbital foramen) to prosthion. Measured both left and right.
20	Total length of cheektooth (premolars and molars) row. Measured both left and right.
21	Total length of molars row, from anterior alveoli to posterior alveoli. Measured both left and right.
22	Total length of premolars row, from the anterior alveoli to the posterior alveoli. Measured both left and right.
25	Greatest mastoid breadth. Measured from otion to otion.
26	Greatest breadth of the occipital condyles, including ovibovine accessory surface.
26A New measurement	Greatest breadth of standard articular surface only of occipital condyles (does not include ovibovine accessory surfaces).
27	Greatest breadth at the bases of the paraoccipital processes.
28	Greatest breadth of the foramen magnum.
31	Least breadth between the horn sheaths in *Ovibos*. Least breadth between the horn cores in extinct ovibovines.
32	Minimum breadth of postorbital constriction.
33*	Least breadth across the dorsal surface of the orbit.
33A**	Breadth across midpoint of ventral surface of orbit.
34	Breadth immediately anterior to orbits.
35	Breadth across the facial tuberosities.
37G***	Greatest breadth across the premaxillae.
38	Greatest breadth across palate, measured from the labial surfaces of the toothrows.
42	Breadth between tips of the hornsheaths in *Ovibos*, and between the horncore tips in extinct ovibovines.
43	Maximum lateral breadth between horncores.

45	Dorso-ventral height of the horn sheath at base of horn for *Ovibos*. Dorso-ventral height of horn core at the base of horn for extinct muskoxen.
46	Maximum antero-posterior breadth of horn sheath at the base of the horn in *Ovibos*. Maximum antero-posterior breadth of the horn core at the base of the horn in extinct muskoxen.
Angle 1 (From McDonald and Ray, 1989)	The angle of flexion between the basioccipital and basisphenoid.
Angle 2	The angle formed by the intersection of the planes of the parietals and the occipital of the skull. Measured at the midline of the vertex of the skull.
Occlusal Breadth (OB)	The maximum breadth across the tooth (from labial to lingual surface) at the occlusal margin of the crown.
Occlusal Length (OL)	The maximum length of the tooth (from the anterior surface to posterior surface) at the occlusal margin of the crown.
Midcrown Breadth (BB	The maximum breadth across the tooth (from labial surface to lingual surface), at the basalmost available portion of tooth.
Midcrown Length (BL)	The maximum length of the tooth (from anterior face to posterior face), at the basalmost available portion of tooth.
Crown Height (CH)	The maximum height of the crown of the tooth, measured when the root was accessible.
Mandibular Height (MH)	The maximum height of the crown from the surface of the maxilla or mandible, measured when the tooth is in place in the jaw, and the root is inaccessible.
Posterior Orbital Breadth (New Measurment)	Breadth between the lateral most margins of the posterior edge of the protrusion of the orbits, measured from dorsal view.
Posterior Skull Length (New Measurement)	Distance from the midpoint of the "Orbital Breadth Index," to the occipital crest, measured from dorsal view.

*Measurement 33 Presented Here is a Different Measurement from von den Driesch's (1976) measurement 33

**Measurement is a Newly Proposed Measurement for Use with Muskoxen Crania

***Measurement 37G is the Same as 38 for *Ovis* from von den Driesch (1976)

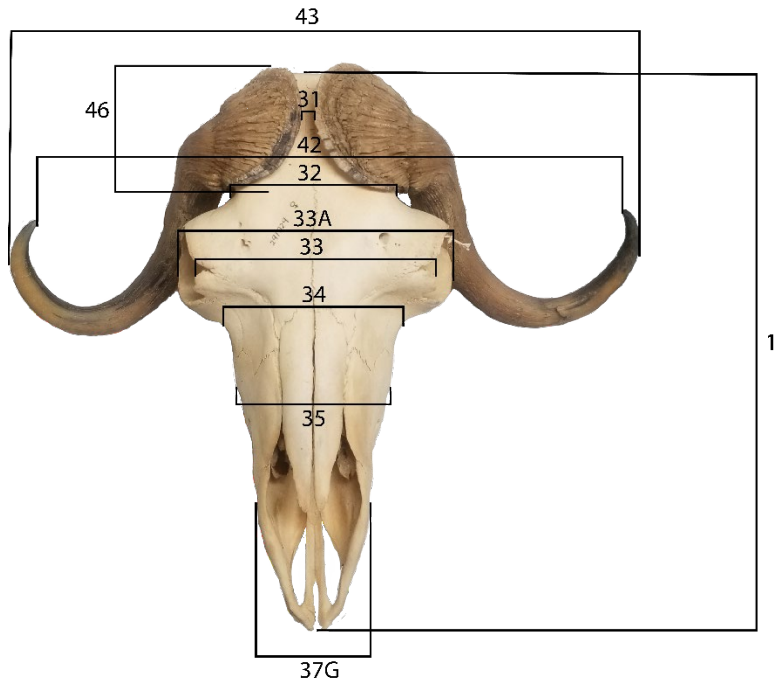

Figure 17. Collected measurements, dorsal view. USNM 291029

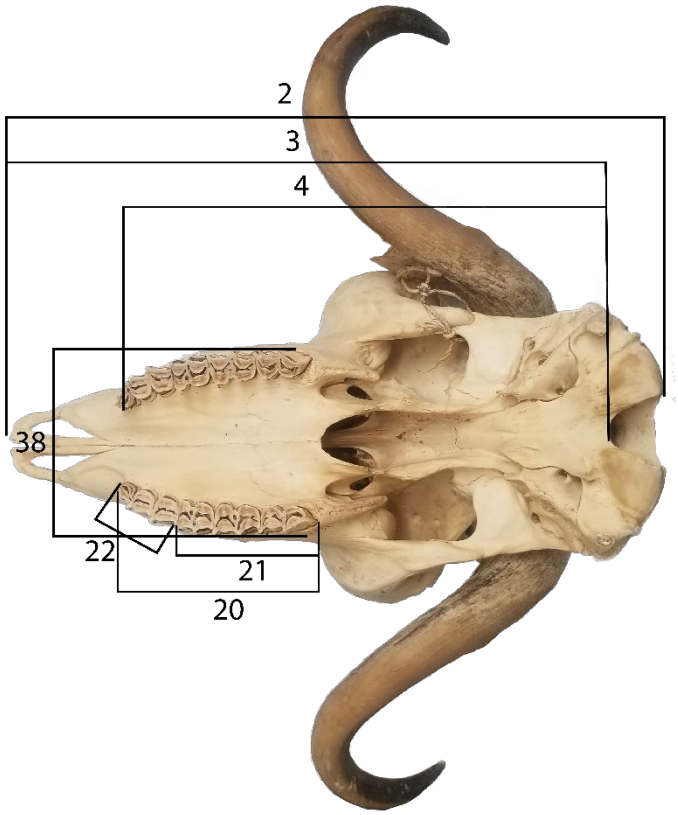

Figure 18. Collected measurements, ventral view. USNM 291029

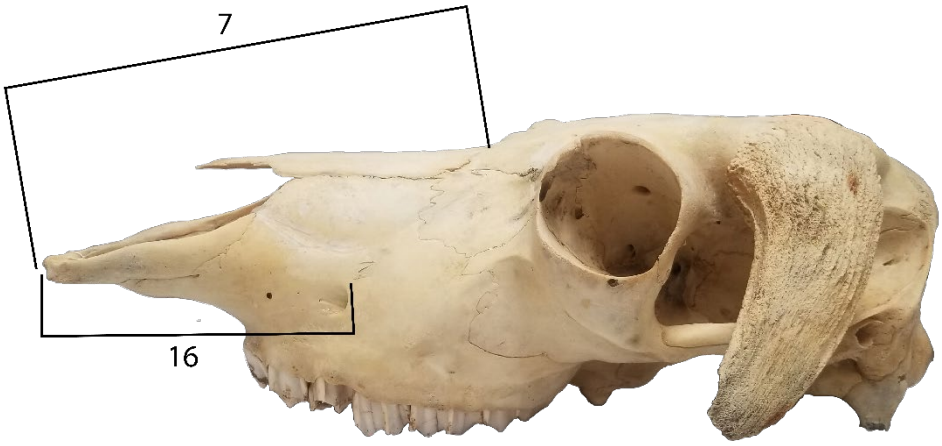

Figure 19. Collected measurements, left lateral view. USNM 399993

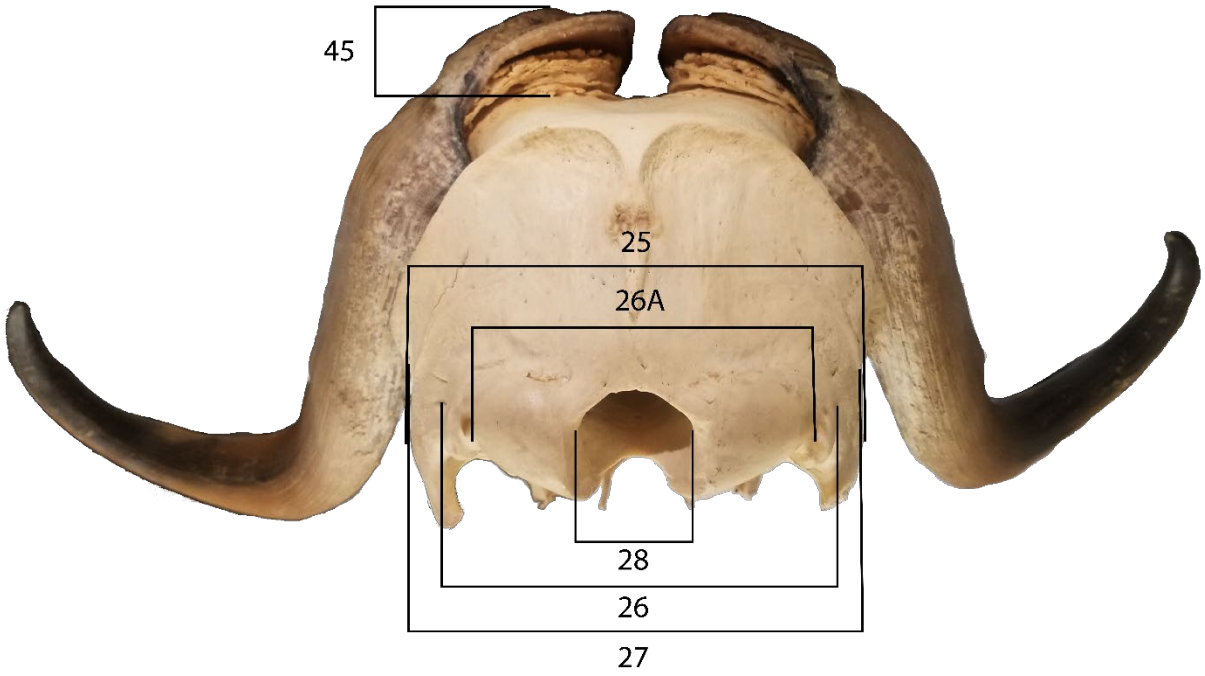

Figure 20. Collected measurements, posterior view. USNM 291029

Figure 21. Digital measurements from photographed and published skulls. The horizontal black line represents the Posterior Margin of the Orbits Breadth measurement. The vertical gray line represents the Posterior Skull Length measurement. USNM 291029, dorsal view

Measurements were scatterplotted in Microsoft Excel. Combinations of *Ovibos* and *Bootherium* measurements were plotted against each other with the goal of determining whether the measurements could be used to tell the genera apart. The mean and standard deviation were calculated in Microsoft Excel for promising measurements that were compared. Two sample F-tests were performed for selected measurements to compare the variances between the fossil sample and the *Ovibos* sample. If the variances were equal, a homoscedastic two samples T-test was performed, and if variances were unequal between the two samples a heteroscedastic two samples T-test was utilized.

Table 11. Muskox Specimen List. Specimens Included in Analysis, With Source of Measurements and Comments. Cranial Specimens from Nelson and Madsen (1987), McDonald and Ray (1989), and Richards and McDonald (1991). Identifications Here are Based on the Labels in Collections or Referenced Literature

Specimen	**Prior Identification**	**Group**	**Sex**	**Locality**	**Data Source**	**Comments**
USNM 291202	*Ovibos m. wardi*	Modern *Ovibos*	Male	Cornwallis, NW Territories, Canada	This Study	Skull
USNM 291025	*Ovibos moschatus*	Modern *Ovibos*	Female	Prince Patrick Island, NW Territories, Canada	This Study	Skull
USNM 291029	*Ovibos m. wardi*	Modern *Ovibos*	Female	Prince Patrick Island, NW Territories, Canada	This Study	Skull
USNM 256969	*Ovibos moschatus*	Modern *Ovibos*	Female	Locality Unknown	This Study	Skull
USNM 252504	*Ovibos m. wardi*	Modern *Ovibos*	Male	Locality Unknown	This Study	Skull
USNM 275099	*Ovibos m. wardi*	Modern *Ovibos*	Male	Devon Island, NW Territories, Canada	This Study	Skull
USNM 108722	*Ovibos m. moschatus*	Modern *Ovibos*	Male	Hudson Bay, NW Territories, Canada	This Study	Skull
USNM 399993	*Ovibos m. wardi*	Modern *Ovibos*	Female	Franklin District, NW Territories, Canada	This Study	Skull

USNM V 13696	*Symbos cavifrons*	Fossil unknown	Sex Unknown	American Falls, Idaho, United States	This Study	Isolated palate with teeth
USNM V 8574	*Bootherium bombifrons*	Fossil Male	Male	Union Township, Indiana, United States	This Study	Partial male cranium
USNM V 2556	*Symbos tyrelli*	Fossil *Bootherium*	Male	Klondike River, Dawson Area, Yukon, Canada	This Study	Partial male cranium
USNM V 23488	*Bootherium sargenti*	Fossil *Bootherium*	Female	Mooreland Swamp, Grand Rapids, Michigan, United States	This Study	Partial cranium, cast, *Bootherium sargenti* holotype
USNM V 372807	*Symbos cavifrons*	Fossil *Bootherium*	Male	Alaska, United States	This Study	Male partial cranium
USNM V 215066	*Bootherium bombifrons*	Fossil *Bootherium*	Female	Big Bone Lick, Kentucky, United States	This Study	Partial cranium, cast, *Bootherium bombifrons* holotype
USNM V 23577	*Symbos cavifrons*	Fossil *Bootherium*	Male	Saltville, Virginia, United States	This Study	Partial male cranium
USNM V 23264	*Bootherium*	Fossil *Bootherium*	Female	Saltville, Virginia, United States	This Study	Female partial cranium
USNM V 437774	*Bootherium bombifrons*	Fossil unknown	Sex Unknown	New Bern, North Carolina, United States	This Study	Isolated m3

USNM V 533996	*Bootherium*	Fossil unknown	Sex Unknown	Horry County, South Carolina, United States	This Study	Isolated M3
USNM V 23787	*Symbos* sp.	Fossil unknown	Sex Unknown	In Ocean, 40 miles NE of Cape Charles, Virginia, United States	This Study	Partial mandible with p4-m3
USNM V 636245	Unknown	Fossil unknown	Sex Unknown	Saltville, Virginia, United States	This Study	(Voucher Specimen) Isolated M2
ETMNH 15423	Ovibovine indet.	Fossil unknown	Sex Unknown	Saltville, Virginia, United States	This Study	Isolated P4-M2
King Leo LP4	*Bootherium*	Fossil unknown	Sex Unknown	King Leo Pit Cave, Harrison County, Indiana, United States	Richards and McDonald, 1991	Associated with other teeth
King Leo RP4A	*Bootherium*	Fossil unknown	Sex Unknown	King Leo Pit Cave, Harrison County, Indiana, United States	Richards and McDonald, 1991	Associated with other teeth
King Leo RP4B	*Bootherium*	Fossil unknown	Sex Unknown	King Leo Pit Cave, Harrison County, Indiana, United States	Richards and McDonald, 1991	Associated with other teeth
King Leo RM2	*Bootherium*	Fossil unknown	Sex Unknown	King Leo Pit Cave, Harrison County, Indiana, United States	Richards and McDonald, 1991	Associated with other teeth
King Leo RM3	*Bootherium*	Fossil unknown	Sex Unknown	King Leo Pit Cave, Harrison County, Indiana, United States	Richards and McDonald, 1991	Associated with other teeth

King Leo Lp2	*Bootherium*	Fossil unknown	Sex Unknown	King Leo Pit Cave, Harrison County, Indiana, United States	Richards and McDonald, 1991	Associated with other teeth
King Leo Rp2	*Bootherium*	Fossil unknown	Sex Unknown	King Leo Pit Cave, Harrison County, Indiana, United States	Richards and McDonald, 1991	Associated with other teeth
King Leo Lp3	*Bootherium*	Fossil unknown	Sex Unknown	King Leo Pit Cave, Harrison County, Indiana, United States	Richards and McDonald, 1991	Associated with other teeth
King Leo Lm1	*Bootherium*	Fossil unknown	Sex Unknown	King Leo Pit Cave, Harrison County, Indiana, United States	Richards and McDonald, 1991	Associated with other teeth
King Leo Lm2	*Bootherium*	Fossil unknown	Sex Unknown	King Leo Pit Cave, Harrison County, Indiana, United States	Richards and McDonald, 1991	Associated with other teeth
King Leo Rm2	*Bootherium*	Fossil unknown	Sex Unknown	King Leo Pit Cave, Harrison County, Indiana, United States	Richards and McDonald, 1991	Associated with other teeth
King Leo Rm3	*Bootherium* sp.	Fossil unknown	Sex Unknown	King Leo Pit Cave, Harrison County, Indiana, United States	Richards and McDonald, 1991	Associated with other teeth
INSM 71.3.70	*Bootherium* sp.	Fossil *Bootherium*	Male	Silver Creek Sand and Gravel Quarry, Clarksville, Indiana, United States	Richards and McDonald, 1991	Partial cranium
“MSP”	*Bootherium* sp.	Fossil *Bootherium*	Male	Madison County,	Richards and	Partial cranium

Bootherium				Indiana, United States	McDonald, 1991	
AMNH F:AM A-204-4254	*Symbos* sp.	Fossil *Bootherium*	Male	Little Eldorado Creek, Alaska, United States	McDonald and Ray, 1989	Partial cranium
UUVP 8540	*Symbos cavifrons*	Fossil *Bootherium*	Male	Unknown	Nelson and Madsen, 1987	Cranium
USNM 2555	*Scaphoceros*	Fossil *Bootherium*	Male	Bonanza Creek, Yukon, Canada	McDonald and Ray, 1989	Cranium
USNM 2324	*Bootherium nivicolens*	Fossil *Bootherium*	Female	Escholtz Bay, Alaska, United States	McDonald and Ray, 1989	Partial cranium
USNM 347315	*Bootherium*	Fossil *Bootherium*	Female	Oregon Inlet, Dare County, North Carolina, United States	McDonald and Ray, 1989	Partial cranium
AMNH F:AM 33124	*Symbos cavifrons*	Fossil *Bootherium*	Male	Upper Cleary Creek, Alaska, United States	McDonald and Ray, 1989	Cranium
AK Fish and Game Skull	*Ovibos*	Fossil *Ovibos*	Male	Unknown	Nelson and Madsen, 1987	Partial cranium
USNM 291028	*Ovibos*	Modern *Ovibos*	Male	Prince Patrick Island, NW Territories, Canada	McDonald and Ray, 1989	Cranium

Results

Cranial Measurements

Comparison of cranial characteristics was limited by the large number of fragmentary skulls available during the data collection process, which reflects the usual state of preservation of fossil muskox crania. Fortuitously, many of the fragmentary remains did have some overlapping, commonly preserved characters, including the foramen magnum, occipital condyles and the accessory surfaces of the occipital condyles. Unfortunately, these characters did not generally prove useful in differentiating the muskox genera with the collected measurements. When the measurements were plotted against each other in scatterplots, the result was often two loose groupings that overlapped with each other to varying degrees.

All specimens examined had enough of the horn core region present to determine an identification based on the work of McDonald and Ray (1989). When possible, their identifications of specimens were used, and the identifications of other specimens were reassessed. Based on horn core morphology of the specimens, one fossil muskox (Alaska Fish and Game Skull) was attributed to *Ovibos* in agreement with the source for that specimen (Nelson and Madsen 1987). All other fossil skulls and partial crania in this analysis were determined to belong to the genus *Bootherium.* The full specimen list can be found in Table 11. Means and sample sizes for select cranial measurements are provided in Table 12.

Definitive separation between *Ovibos* and *Bootherium* crania was achieved by plotting the breadth across the occipital condyles (26) against the minimum breadth of the postorbital constriction (32) (Fig. 22). This resulted in a clear pattern of two linear groupings. The minimum breadth of the postorbital constriction was similar between genera, with the *Bootherium* range completely encompassing the range seen in modern *Ovibos*. F-test results (Table 13) suggested

that the measurements had equal variances. The difference then, is present in larger *Bootherium* occipital condyle breadth. This was supported by the T test results confirming a difference in means between the occipital condyle breadth of the two groups (p = .0002), but not the postorbital constriction (p = .9313). Due to the difference in occipital condyles breadth, comparisons using this character are deemed useful for potentially distinguishing between *Ovibos* and fossil muskoxen like *Bootherium*. Similar, but less-striking results were achieved when comparing the breadth of the occipital condyles against foramen magnum breadth. Other comparisons of width measurements against width measurements (not including the occipital condyle breadth) resulted in mostly overlapping clusters.

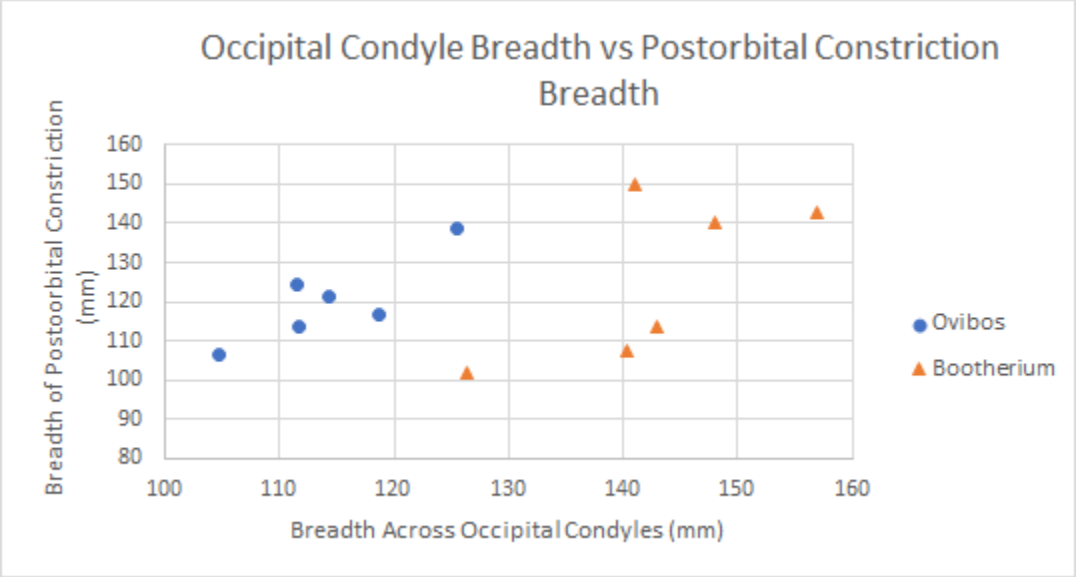

Figure 22. Comparison of measurements 26 and 32. Occipital condyle breadth (26) and postorbital constriction breadth (32) for modern *Ovibos* and fossil muskoxen previously identified as *Bootherium*

There is probably some significance to the data suggesting that the postorbital constriction in *Bootherium* is roughly the same width as seen in *Ovibos*. Although measurements were possible on extinct muskoxen missing their horn sheaths, it was more difficult to acquire

with calipers on modern *Ovibos* that retained horn sheaths. This was due to the manner in which the horn sheath spreads out over the skull in the modern muskox (as well as the more immediate downward path of the horns), thus making it difficult to position the calipers closely around the postorbital constriction. While it seems the current attempt to replicate this measurement in modern muskox specimens was flawed, these data were still recorded for specimens where it could be measured, obstructions preventing measurement on only two males. Because of the inaccurate nature of this measurement, another, more universal alternative to distinguish the crania of *Bootherium* and *Ovibos* was sought.

The similarity in the breadth of the posterior portion of the skull between *Bootherium* and *Ovibos* (proxy being postorbital constriction) warranted investigation into the claims that *Ovibos* orbits projected farther than those of *Bootherium* (Osgood 1905a). An index of orbital protrusion was created by measuring the breadth across the posterior margin of the lateral edge of the orbit, and then measuring the distance from the midline of that breadth to the posteriormost portion of the cranium to create a ratio. While not ideal as a proxy for skull width due to the character potentially being so variable on its own, this measurement and the subsequent posterior skull length measurement, were easily taken on a variety of modern and fossil muskox skulls from the literature using imageJ software.

Both measurements, and their ratio of posterior orbital breadth/posterior skull length were subjected to F-test and t-tests. The breadth across the orbits were supported as having equal variance, but a significant difference between the means between *Ovibos* and the fossil specimens was supported ($p = .0005$). An F-test supported the hypothesis of unequal variance between groups in posterior skull length ($p = .0453$), although the t-test resulted in no support for differences between the two groups ($p = .8536$). When the ratio was analyzed a difference in

variances was not supported, while a difference between the means of the two groups was strongly supported (p = .0000).

Table 12. Cranial Measurement Means and Sample Sizes. Comparison of Select *Ovibos* and Fossil Muskox Cranial Measurements with Means and Standard Deviations.

Measurement	***Ovibos* Mean (Std Dev)**	**Ovibos Sample Size**	**Fossil Mean (Std Dev)**	**Fossil Sample Size**
Posterior Orbital Breadth	257.16 (42.00)	10	200.57 (26.25)	13
Posterior Skull Length	168.98 (39.44)		171.56 (21.39)	
Cranial Ratio	1.55 (0.21)		1.17 (0.13)	
Postorbital Constriction Breadth (32)	120.18 (11.00)	6	120.91 (18.24)	9
Occipital Condyle Breadth (26)	114.48 (11.94)	8	144.48 (10.39)	7

Table 13. Cranial Measurement Statistical Test Results. Statistical Test Values for Cranial Comparisons of *Ovibos* and Fossil Sample Groups. Bolded Results Indicate Statistical Significance.

Measurement	**F-test (Probability)**	**T-test (Probability)**
Posterior Orbital Breadth	0.1209	**0.0005**
Posterior Skull Length	**0.0453**	0.8536
Cranial Ratio	0.1217	**0.0000**
Postorbital Constriction Breadth (32)	0.2804	0.9313
Occipital Condyle Breadth (26)	0.7500	**0.0002**

These analyses demonstrate proportional differences between the skulls of *Ovibos* and the *Bootherium* examined here. It has previously been claimed (Osgood 1905a) without statistical support that the orbits of *Ovibos* protrude more than those of *Bootherium*, and these results confirm that observation. Unequal variances between the two samples were not supported ($p = .1217$), while a difference in the means between the two groups was supported ($p = .0000$). The median of the *Bootherium* group lies entirely outside of the range of the *Ovibos* group (Fig. 23), while the median of the *Ovibos* group lies entirely outside the range of the *Bootherium* group. This suggests a real difference in the distribution of the groups and supports the observation that the values of the cranial elongation ratio are different between the genera.

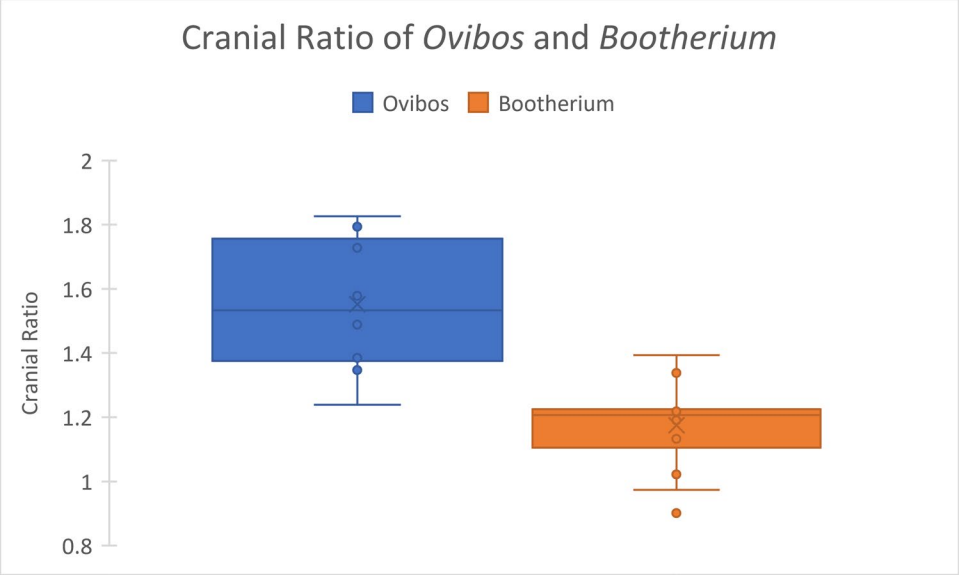

Figure 23. Comparison of cranial elongation ratio. Posterior margin of orbits breadth / posterior skull length for both *Ovibos* and *Bootherium* in this study

Comparison of the posterior skull length measurement to the occipital condyle breadth was also performed. Because it has long been demonstrated that occipital condyle width is well correlated with body mass in mammals (Martin 1980), this measurement may provide a better

alternative for cranial width than the breadth at the posterior margin of the orbits. As mentioned earlier, the posterior skull length was found to have a different level of variance in the modern and fossil groups, but not a significant difference between the means. The occipital condyle breadth was not supported as having a different level of variance between the groups but was supported as having a statistically significant difference in the means ($p = 0.0002$). These data support the notion that *Bootherium* had a greater breadth across the occipital condyles, but not necessarily greater length of the posterior portion of the cranium. This comparison suggests that *Bootherium* is a larger animal than *Ovibos* based on the larger occipital condyle breadth (Martin 1980) of the former, although a small sample of *Bootherium* crania with preserved occipital condyles impacts the confidence of this assessment.

A comparison between male and female skulls of the genera (Fig. 24) revealed no absolute trends. In both muskox genera, males tended to have longer posterior portions of the skull than females. This was apparent in *Ovibos*, though this genus also had a smaller female sample size. In both cases however, there were large females whose posterior portions of the skull were almost as long as those of the largest males. A larger sample size may be needed to assess the level of variation and patterns of this measurement between the sexes of both muskoxen, but the conservative interpretation is that posterior skull length is not correlated with sex in either genus. If present, horn sheath or horn core morphology can be used to distinguish female from male in adult muskoxen. Male *Ovibos* and *Bootherium* each have thicker, larger horns whose medial margins are closer together than in females, or fuse medially in the case of the latter, in the center of the skull (Allen 1913; McDonald and Ray 1989).

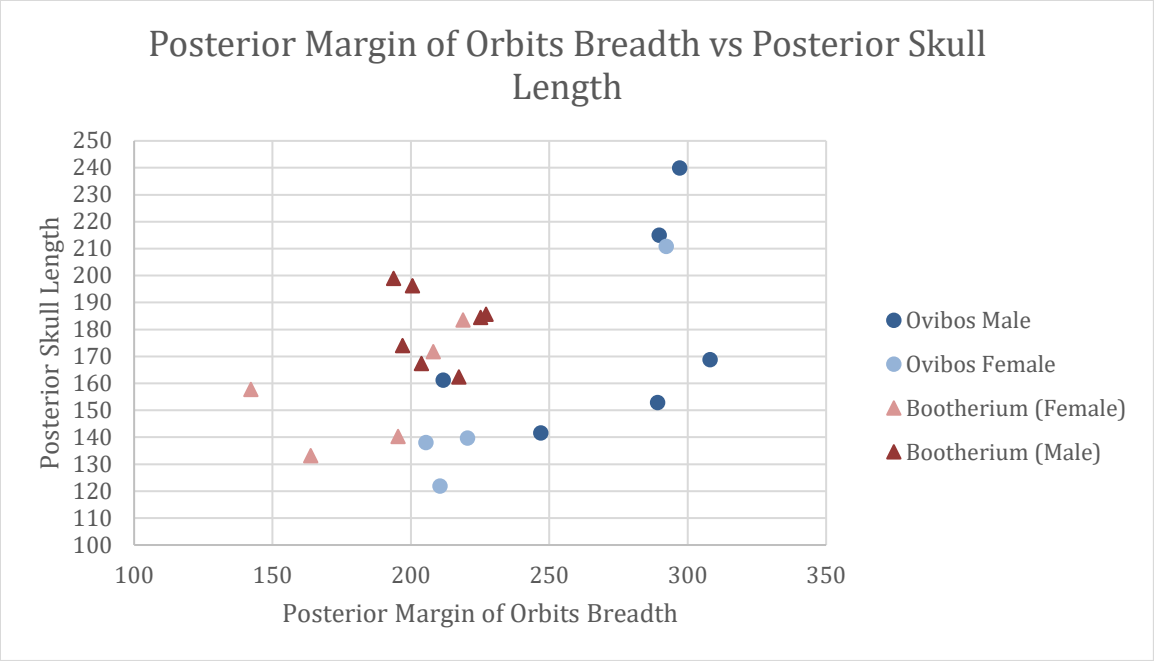

Figure 24. Comparison of posterior margin of orbits breadth and posterior skull length. Comparison of posterior margin of orbits breadth and the posterior skull length for both male and female modern *Ovibos* and *Bootherium (=Symbos)* in this study

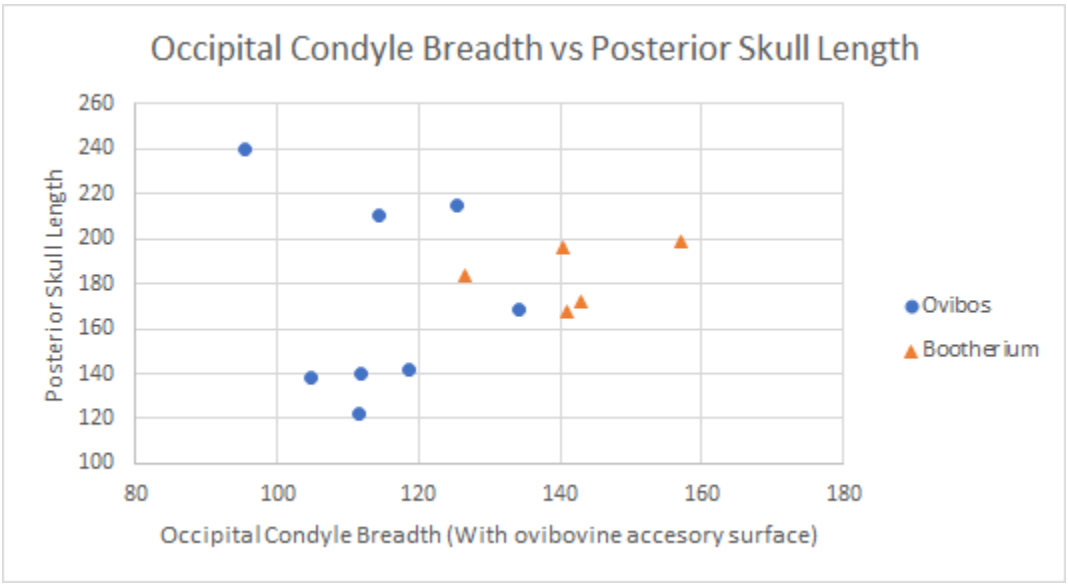

Figure 25. Comparison of occipital condyle breadth and posterior skull length. Comparison of occipital condyle breadth (26) and posterior skull length for modern *Ovibos* and fossil muskoxen in this study

Tooth Measurements

Tooth measurements proved to be provisionally useful in distinguishing between the muskox teeth, and thus more useful for identification than the cranial measurements that were collected. When comparing molars, fossil teeth were proportionally wider than modern *Ovibos* teeth when basal length (BL) was plotted against basal breadth (BB). This trend was apparent in all molars to some degree and includes both upper and lower molars. Though this trend is consistent within the dataset (Tables 14 and 15), the number of modern comparative *Ovibos* individuals is still low, and it is possible that this sample may not accurately reflect the morphological variation present in *Ovibos* teeth. Moreover, it is possible that the addition of more fossil teeth would cause disruptions in these patterns if added teeth represented taxa new to the analysis, or if the current sample of fossil muskox teeth does not adequately capture the total variability of represented taxa.

A small sample of premolars previously measured and identified as *Bootherium bombifrons* were available for comparison, from the King Leo Pit Cave (Harrison County, Indiana) sample of Richards and McDonald (1991). When the basal lengths of the teeth were plotted against the basal breadth, there was no proportional difference supported between *Bootherium* and *Ovibos* premolars. However, the upper fourth premolar, and the lower second, third, and fourth premolars of these *Bootherium* all plotted as distinct from *Ovibos* in size, as they were much larger in the former. Separation was less pronounced in the upper fourth premolar than in the lower teeth, but all plotted *Bootherium* premolars seemed to follow the trend of being roughly the same proportions, but larger in overall size. The upper second and third premolars of *Bootherium* were not readily available during the process of data collection, and thus are not compared to those of *Ovibos*.

Table 14. Dental Measurement Means and Sample Sizes. Comparison of *Ovibos* and Fossil Muskox Dental Measurements with Means and Standard Deviations.

Tooth	Measurement	Modern *Ovibos* Mean (Std Dev)	Modern *Ovibos* Sample Size	Fossil Unknown Mean (Std Dev)	Fossil Unknown Sample Size
M1	Length	19.03 (2.40)	16	22.54 (3.18)	2
	Breadth	20.21 (1.00)		25.90 (3.07)	
	B/L Ratio	1.08 (0.14)		1.14 (0.01)	
M2	Length	27.32 (3.81)	16	30.04 (1.17)	4
	Breadth	20.74 (2.09)		29.41 (1.39)	
	B/L Ratio	0.78 (0.16)		0.98 (0.08)	
M3	Length	33.66 (1.37)	16	39.20 (2.59)	4
	Breadth	18.13 (1.93)		29.65 (4.27)	
	B/L Ratio	0.54 (0.06)		0.76 (0.12)	
m1	Length	21.47 (1.30)	16	25.69 (0.72)	2
	Breadth	15.36 (0.74)		19.70 (2.54)	
	B/L Ratio	0.72 (0.05)		0.77 (0.12)	
m2	Length	25.86 (1.30)	16	28.66 (3.57)	3
	Breadth	16.65 (1.03)		23.33 (1.00)	
	B/L Ratio	0.65 (0.06)		0.82 (0.13)	
m3	Length	39.34 (1.96)	16	48.16 (4.25)	3
	Breadth	15.38 (1.43)		21.51 (0.43)	
	B/L Ratio	0.39 (0.03)		0.45 (0.03)	

There was a clear proportional separation in the M1 group (Fig. 26) between the unknown fossil sample and *Ovibos* sample, with greater breadth in the unknown specimens compared to *Ovibos* specimens. While both fossil specimens were longer than even the longest *Ovibos* tooth, they were only slightly so, and a larger sample size might reveal length overlap. A breadth overlap between the groups would require a significant change in the proportions of any additional fossil muskox M1s relative to length and seems unlikely. While the means of both the length and breadth of the two groups were determined to be significantly different, the ratio of

breadth/length was not. Despite this, there is a clear separation between these groups in terms of breadth, and it seems unlikely that either of these fossil M1s represent fossil *Ovibos*, based on this dataset.

Table 15. Dental Measurement Statistical Test Results. Statistical Test Values for Dental Comparisons of *Ovibos* and Fossil Sample Groups. Bolded Results Indicate Statistical Significance.

Measurement	F-test Value (Probability)	T-test (Probability)
M1 Length	0.166	**0.007**
M1 Breadth	0.711	**0.000**
M1 B/L Ratio	0.083	0.587
M2 Length	0.076	0.182
M2 Breadth	0.545	**0.000**
M2 B/L Ratio	0.300	**0.023**
M3 Length	0.078	**0.000**
M3 Breadth	**0.029**	**0.010**
M3 B/L Ratio	**0.049**	**0.031**
m1 Length	0.819	**0.000**
m1 Breadth	**0.008**	0.249
m1 B/L Ratio	**0.047**	0.665
m2 Length	**0.011**	0.306
m2 Breadth	0.821	**0.000**
m2 B/L Ratio	0.065	**0.001**
m3 Length	0.052	**0.000**
m3 Breadth	0.169	**0.000**
m3 B/L Ratio	0.857	**0.018**

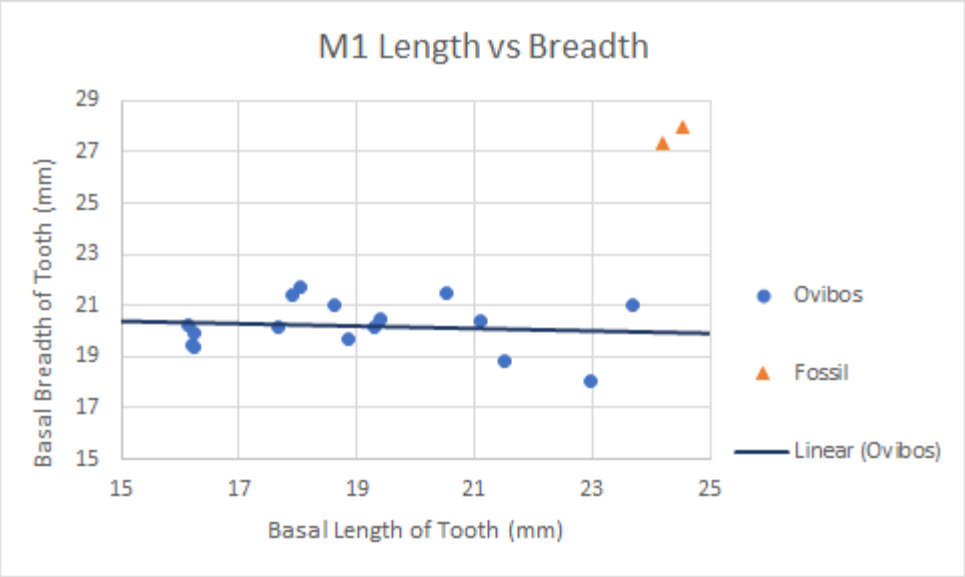

Figure 26. Basal length vs breadth of M1s. Specimens represent modern *Ovibos* and fossil muskox M1s in this study

Within the M2 group (Fig. 27), separation between the fossils and modern *Ovibos* was once again clear. While there was no overlap between the breadths of the groups, the lengths did overlap. The lengths of the fossil teeth tended to be clustered around the maximum lengths of the *Ovibos* teeth, the *Ovibos* teeth were negatively skewed so that outliers tended to be shorter, and the bulk of the specimens tended to be towards the longer end of their range. Because the two groups overlapped well in length but not at all in breadth, it seems unlikely that these fossil teeth represent *Ovibos*. While the means of the lengths of the two groups were not significantly different, both the breadths and the ratio of breadth/length were, further supporting this distinction between *Ovibos* and sampled fossil muskoxen.

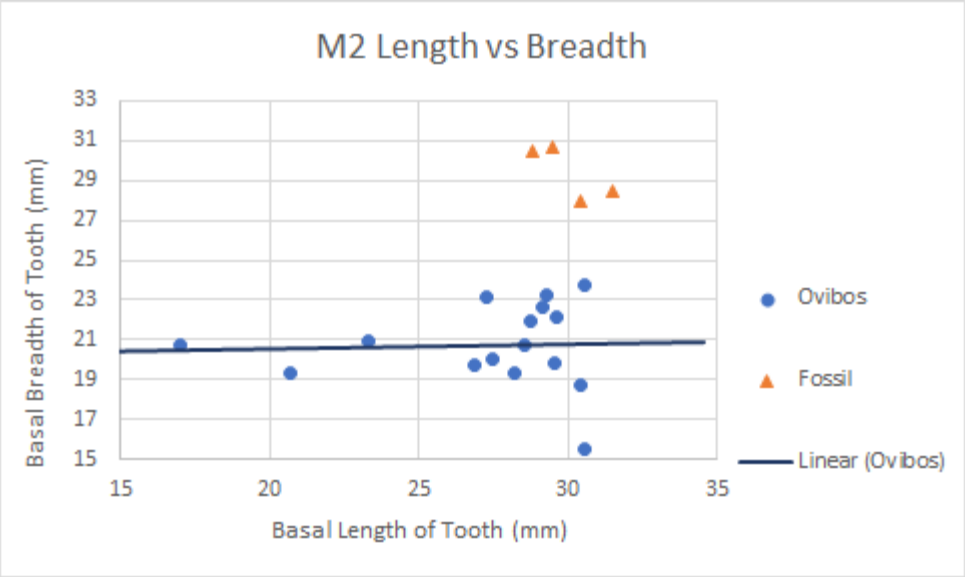

Figure 27. Basal length vs breadth of M2s. Specimens represent modern *Ovibos* and fossil muskox M2s in this study

For the M3 group, separation was still apparent when graphed, albeit less clearly so than in the first or second upper molars (Fig. 28). While the breadth of the fossil muskox and *Ovibos* samples once again did not overlap at all, there was a slight overlap in length. The length of the fossil muskoxen teeth tended to be longer than in the *Ovibos* teeth, and both the differences in length and breadth of the two groups were statistically significant. While this would at first seem to simply suggest a larger size for the fossil muskoxen teeth, the ratio of breadth/length was also significantly different, with the fossil forms being consistently broader for their size than the *Ovibos* teeth. This represents an interesting dichotomy between the graphic separation being less distinct than in the M1 or M2 samples, but the statistical separation being more robust due to significant differences in length, breadth and the ratio between them. Given this evidence, it is inappropriate to assign any of the fossil muskoxen teeth to *Ovibos*.

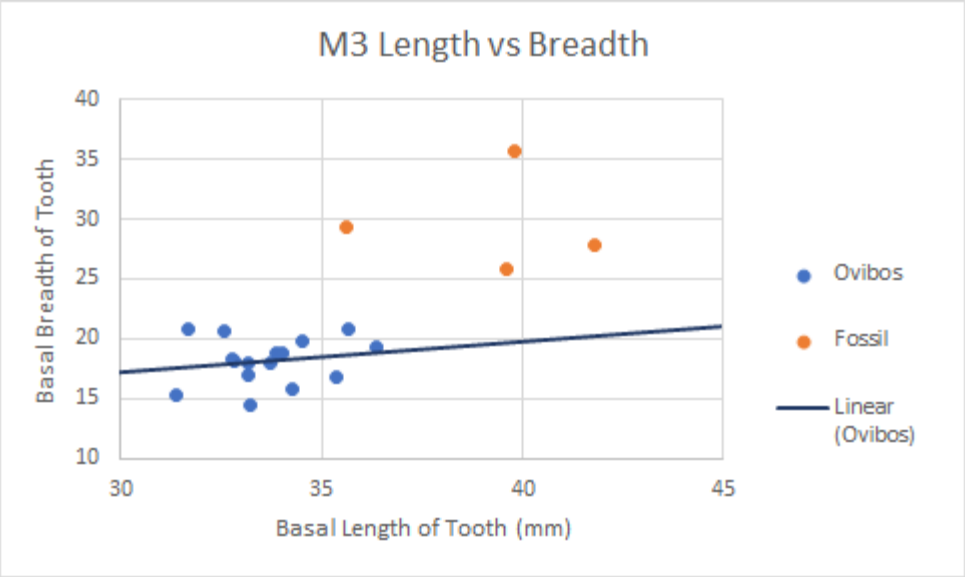

Figure 28. Basal length vs breadth of M3s. Specimens represent modern *Ovibos* and fossil muskox M3s in this study

Within the m1 group (Fig. 29), there was graphic separation between both the lengths and the breadths of *Ovibos* and the fossil muskoxen sample. The breadth separation was noticeably smaller than in other tooth groups, although the length separation was readily apparent. Statistically, a separation was not well defined. While the difference between means of the lengths of the two groups was significant, this was not the case for breadth or the breadth/length ratio. This was the only sample where variances between the length, breadth, and breadth/length ratio were all unequal, which could have impacted statistical analysis of these samples. Of particular interest in comparing these samples is the less broad fossil tooth, which was reported as a *Bootherium* Lm1 by Richards and McDonald (1991). Given its closeness in breadth and position to the regression line for the *Ovibos* teeth, it is possible that this could represent a fossil *Ovibos* tooth, though this hypothesis would necessitate a much greater dataset to be tested.

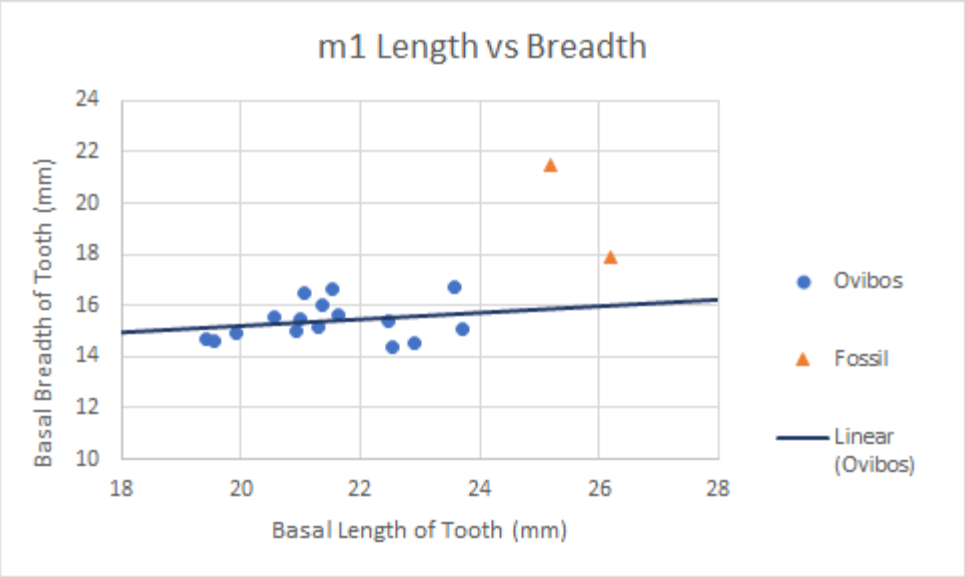

Figure 29. Basal length vs breadth of m1s. Specimens represent modern *Ovibos* and fossil muskox m1s in this study

For the m2 group (Fig. 30), there was a clear graphical separation of the extant *Ovibos* and sampled fossil muskox teeth. While there was no overlap between the breadths of the groups, there was overlap between the lengths. Interestingly, the m2 sample of fossil muskoxen teeth appear to show similar variability in length to that of the *Ovibos* m2s, with a large overlap between the ranges of the groups. Following the graphical trend, there was no statistical support for a difference in means between the lengths of the two groups, but both breadth and the breadth/length ratio were significantly different.

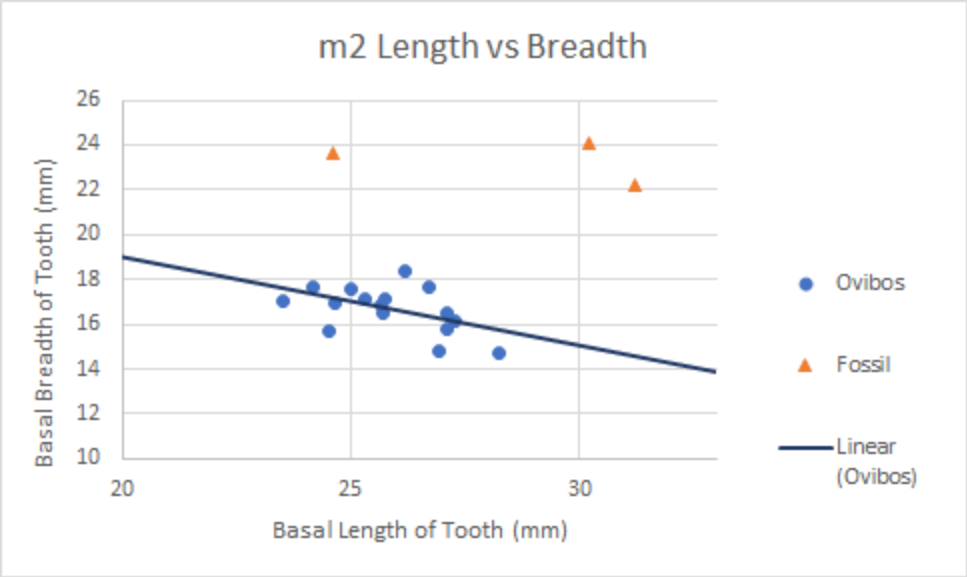

Figure 30. Basal length vs breadth of m2s. Specimens represent modern *Ovibos* and fossil muskox m2s in this study

Within the m3 group (Fig. 31), there was a strong graphical distinction between both the lengths and breadths of the teeth between the two groups. There was no overlap between the lengths or breadths of either group, and the results of the Student's t tests supported the means of length, but not breadth as being different between the fossil and *Ovibos* teeth. While it might at first just appear to be a size relationship where the fossil teeth are bigger, this is not supported by the significant difference in ratios between the two groups, with the fossil teeth tending to be wider proportionally than the *Ovibos* m3s.

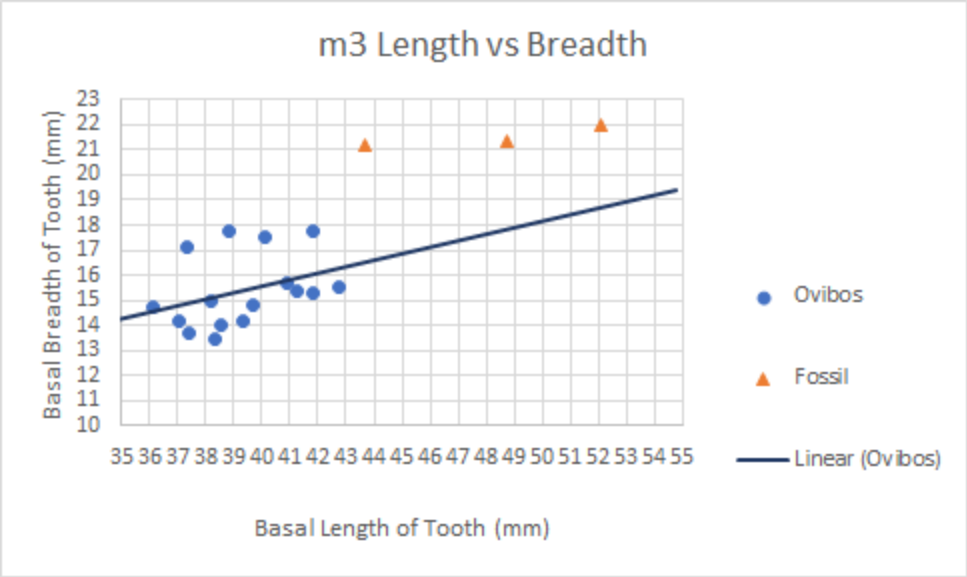

Figure 31. Basal length vs breadth of m3s. Specimens represent modern *Ovibos* and fossil muskox m3s in this study

Given that *Bootherium* and *Ovibos* are the only muskoxen genera known from the southeastern United States, and that almost all of the fossil teeth (with one exception addressed below) appear to be from two distinct groupings, it is most parsimonious to suggest that the fossil muskox teeth represent *Bootherium*. These analyses suggest that it is possible to differentiate isolated molars of *Bootherium* and modern *Ovibos* independent of size. Most groups of molars (all except M1 and m1) suggested that *Bootherium* had a greater raw and proportional breadth than *Ovibos*. While length was sometimes statistically supported as longer, this was not always the case, and when length was supported as different between the fossil and *Ovibos*, the ratio of breadth/length was also found to be different. The results of the lower first molars did not support this trend, though the reason for this will be explored below. As a general rule however, these results indicate that each molar of the fossil sample tends to be either as long or longer than

the longest in *Ovibos* and is also both absolutely and proportionally wider than the same tooth in *Ovibos*.

Of course, this examination is not without weaknesses. This is a relatively small dataset and will need to be augmented with additional modern *Ovibos* and fossil muskoxen teeth. Additionally, most of the fossil teeth are being assigned to *Bootherium* based on this being the most likely candidate based on known distributions and material, but that necessarily limits the geographic scope in which these trends may be useful for identification. Caution should be used when applying this dataset to identify fossil musk ox teeth in locations where there is the potential for presence of other fossil ovibovines, which were not included in this dataset (notably *Euceratherium* and *Soergelia*).

Discussion

Identification of Fossil Muskoxen from Saltville and the Eastern US

When examining the trends differentiating the modern *Ovibos* and unknown fossil muskoxen teeth, potential identification must be carefully considered. As mentioned previously, there are five ovibovine genera known to have occurred in North America. *Praeovibos*, *Ovibos*, *Soergelia*, *Euceratherium* and *Bootherium*.

Praeovibos appears unlikely to occur at Saltville but cannot fully be excluded as a potential identification. Although this genus is known to have inhabited a wider variety of habitats than modern *Ovibos* (Mol and Reumer 1999), including woodland habitats that may have been similar to Saltville, their range is thus far limited exclusively to the Beringian portion of the continent. Thus, their presence at Saltville would invoke a major range extension for *Praeovibos*. While this is not out of the realm of possibility, it seems an unlikely outcome given

how well the Pleistocene fauna of North America has been documented. Therefore, this genus is not considered a likely candidate for the fossil unknown teeth but should not be ruled out entirely.

While the range of *Ovibos* is thus far limited to being slightly north of Saltville (McDonald and Davis 1989), there is some evidence that the conditions they favor may have been present as far south in the Appalachians as Saltville, although the precise timing of these permafrost occurrences are unknown (Clark and Ciolkosz 1988, Nelson et al. 2007; French and Millar 2014). Given this combination of features it seems plausible that *Ovibos* could be found at Saltville, and therefore it should be considered as a potential identification for unknown fossil remains.

Euceratherium is a large ovibovine that has not been reported from Saltville, Virginia, or eastern North America. While the forward curving horns of this genus would be difficult to confuse with *Praeovibos*, *Ovibos*, or *Bootherium*, their range within North America is thus far strictly limited to southwestern North America (Campos et al. 2010). Thus, their potential occurrence in the Saltville paleofauna seems unlikely because the extensive Pleistocene fossil record of eastern North America lacks this taxon.

Soergelia is another large ovibovine with characteristic horn morphology. The horncores of this genus are known to open in a v-shaped pattern and, like *Euceratherium*, curve forwards (Kurtén and Anderson 1980; Cregut-Bonnoure and Dimitrijevic 2006). While specimens have been reported from the Yukon, Texas, and Kansas, they are not common and there are no reports east of Kansas. Additionally, while the range extension required to place *Soergelia* at Saltville is not as large as required for *Praeovibos* or *Euceratherium*, it is important to note that within North America *Soergelia* has only been found in Irvingtonian aged deposits and may have gone

extinct long before the latest Pleistocene Saltville fauna (Eschelman and Hager 1984). Thus, it seems unlikely to be present at Saltville unless extraordinary evidence for its occurrence is found.

Unlike the other ovibovines considered, *Bootherium* has already been confirmed to be present in the Saltville paleofauna. These records are clear and unambiguous, and represent individuals of both sexes (Ray et al. 1967; McDonald and Ray 1989). Thus, they are a plausible identification for unknown fossil ovibovine remains from Saltville.

Cranial identification for ovibovines is heavily researched, and the advances in this area by McDonald and Ray (1989) have allowed for straightforward identification of North American ovibovines, provided that the horncore region or the occipital region of the skull are present. All skulls observed from Saltville within this thesis are confirmed to belong to *Bootherium bombifrons* based on horn core and frontal region morphology. Fossil ovibovine crania from Saltville examined in this study include USNM 23577 and USNM 2326, both of which are partial crania containing the horncore region. USNM 23577 represents a male of the species based on the deep exostosis and horn core morphology, and the USNM 23264 represents a female based on the smooth frontal surface and horncores that project strongly laterally prior to curving ventrally.

While it is straightforward to differentiate crania of different muskoxen genera if the horncores are included, other taxon-specific anatomical features are less defined for the ovibovine group. Isolated teeth from across the United States have been attributed to *Bootherium* (some of which are included in this study), but few quantitative analyses of these dentitions have taken place. Unfortunately, no examples of teeth directly measured by this study were associated with diagnostic cranial material. Thus, while the crania used were easily identifiable to genus,

any fossil ovibovine teeth were necessarily treated as fossil unknown specimens. While fossil unknown ovibovine specimens from Saltville and the eastern United States seem most likely to be *Bootherium*, it is assumed within this study that *Bootherium* teeth will cluster together into one group, and not form multiple groups. Based on specimen observations made prior to data collection, as well as Osgood's (1905a) initial description of the *Bootherium* teeth, it was hypothesized that teeth attributable to this genus may group as proportionally broader than the teeth of *Ovibos*.

With one possible exception, this was the trend observed in the fossil unknown sample. All of the fossil unknown specimens were teeth, or multiple teeth with an associated dentary. These results showed a consistent and clear trend of these fossil ovibovines clustering into a single group of differing breadth, separate from *Ovibos*. The analyses returned statistical support for a difference in breadths between the modern *Ovibos* and fossil ovibovines for M1, M2, M3, m2 and m3, suggesting that the teeth included in the fossil ovibovine sample did not belong to *Ovibos*.

Fossil ovibovine specimens from Saltville included ETMNH 15423 and one tooth within USNM V 636245. ETMNH 15423 (Table. 3.1) is an associated series of cheek teeth from P4 to M2. The two molar teeth plotted at similar breadths to other fossil ovibovine teeth, as broader than those of the modern *Ovibos* sampled. This was also the case for an M3 that was a part of USNM V 636245, which was the broadest of all M3's sampled. Because the most plausible identifications for these teeth are currently *Ovibos* and *Bootherium*, and these teeth plotted significantly and consistently away from those of the former, these specimens most likely represent *Bootherium*.

While the primary target of identification in this study were fossil ovibovines from Saltville, this dataset also afforded the opportunity to assess the identification of ovibovine teeth from the King Leo Pit Cave locality in Harrison County, Indiana. Measurements of these teeth were published by Richards and McDonald (1991), wherein they were all identified as *Bootherium*. This study treated them as fossil unknowns due to the lack of diagnostic skull material associated with them. While this site is much closer to the known fossil range of *Ovibos*, and closer to the range of *Soergelia*, all but one of these teeth plotted with the fossil ovibovines rather than the modern *Ovibos*. Because there did not appear to be multiple groups within the fossil ovibovine teeth, and *Bootherium* is the most plausible identification for the teeth from Saltville, this study supports the earlier identification of most of these isolated teeth as *Bootherium* (Richards and McDonald 1991).

However, there is one tooth from King Leo Pit Cave which appears anomalous. Richards and McDonald (1991) publish this tooth as a *Bootherium* left m1. While the breadth (17.90) of this fossil tooth is more than three standard deviations (stdev = 0.74) broader than the mean (15.36) of the modern *Ovibos* group, it is absolutely closer to this value than to the breadth (21.495) of the only other unknown fossil m1 in the sample (Fig. 32). The relationship for *Ovibos* seemed to be one of slightly increasing breadth relative to length for the m1. A tooth the length of this one would be within three standard deviations of the regression line for *Ovibos*, although that is not enough evidence to make a case for this tooth belonging to *Ovibos* rather than *Bootherium*. Two right fourth premolars assigned to *Bootherium* were recovered from the cave, meaning that there are, at minimum, two individual fossil muskoxen, if not more. Therefore, it is possible that the muskoxen from this cave are represented by *Bootherium* and another genus of late Pleistocene ovibovine, although a better morphological understanding of

Bootherium and other extinct ovibovine dentition would be needed to properly address that hypothesis. This is of importance, because King Leo Pit Cave would become the new southern-most occurrence for *Ovibos* in the eastern United States. Thus, I advocate for the identification of the King Leo Pit Cave left m1 tooth to be identified as Ovibovine indet., rather than being retained as *Bootherium*.

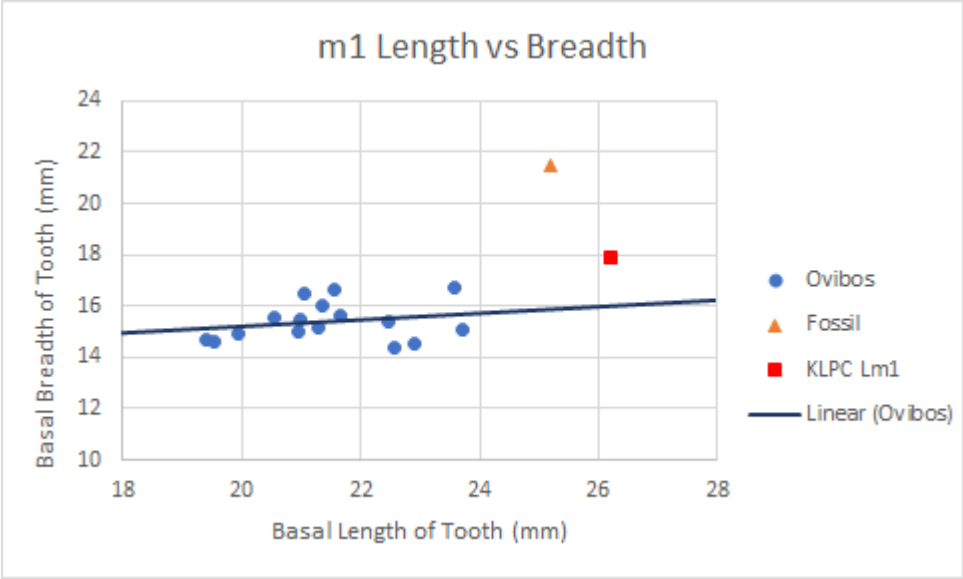

Figure 32. Basal length vs breadth of m1s, with focus on KLPC m1. Specimens represent modern *Ovibos* vs fossil muskoxen m1s, with the King Leo Pit Cave Lm1 from Richards and McDonald (1991) emphasized

Morphological Differences between Ovibos *and* Bootherium

Because all but one of the measured teeth are considered to be *Bootherium*, and all of the analyzed crania belonged to either this genus or *Ovibos*, a direct comparison between the two is made here. These comparisons provided insights into the non-horncore differences between the crania and teeth of *Ovibos* and *Bootherium* and will hopefully serve as a starting point for further

differentiation of these and other ovibovine taxa.

Differences in the molars of both genera were readily apparent when the basal breadth and widths of teeth were compared against each other. For all molars, the teeth identified as *Bootherium* are both absolutely and proportionally broader than the teeth of *Ovibos*. Differences in the means of basal breadth between modern *Ovibos* and fossil groups (interpreted to represent only *Bootherium*) were supported for all teeth except for the m1s. The m1 sample size consisted of only 2 specimens, and one of these appeared to be anomalous when compared to the patterns of all other measured molars.

Non-horn core cranial measurements proved somewhat less useful than dental measurements to differentiate the groups. While fragmentary skulls are the norm when working with ovibovine fossils, it is common to have large parts of the posterior portion of the skull, namely the occipital, frontal, and orbital regions. The most distinct character between the two genera was occipital condyle breadth (26). In all cases this measurement was absolutely larger in *Bootherium* so that the smallest breadth across the occipital condyles measured in *Bootherium* was slightly larger than in the largest *Ovibos*. There was no support for differences in variances of the measurement between the two ovibovine genera, but the means of each were statistically supported as different. While not necessarily useful on its own, this trait proved a potentially powerful tool for differentiating the two genera when combined with other measurements. For example, the breadth across the postorbital constriction was similar in both groups, with no statistical support for a difference in distributions or means between *Ovibos* and *Bootherium*. When this character is compared in a scatterplot against the occipital condyle breadth however, a clear visual separation between *Ovibos* and *Bootherium* is observed (Fig. 3.10).

Another morphological difference discovered between the two genera is in the shape of

the posterior portion of the skull (i.e., the part of the cranium posterior to the posterior margin of the orbits). Two measurements were digitally collected to examine the shape of this region of the skull (Fig. 3.1). A straight line from the posteriormost part of each orbit must be drawn, connecting the two points. This distance is measured as a proxy for posterior skull width and the midpoint of this line on the skull noted. Another line is drawn from the midpoint of the existing line straight back to the posteriormost margin of the skull. This line is measured as a proxy for posterior skull length. When a ratio is created from these measurements (posterior skull width / posterior skull length) a consistent difference was seen between *Ovibos* and *Bootherium* in that the ratios of the former were much higher than those of the latter. This is the result of the greater protrusion of the orbits in *Ovibos* than in *Bootherium*, and thus may not actually represent a difference in the cranium itself, so much as a difference in orbital protrusion. A significant difference between the means of the two groups was supported by the Student's t-test, however, so this comparison does appear to be capturing a real morphological difference.

One similarity worth highlighting is the lack of statistical support for the postorbital portion of the crania being longer (and thus larger) in *Bootherium* than in *Ovibos*. This suggests that *Bootherium* skulls may not be absolutely larger than that of *Ovibos*, as two large males and a large female all plotted as wider across the orbits and longer in the postorbital crania than the largest fossil muskoxen measured in this study. It is possible that the width of the cranium behind the orbits is a good indicator of overall size, but this measurement was not accessible for most male muskoxen crania that have been published due to the horncore in *Bootherium*, and the horn-sheaths in *Ovibos* covering the measurement area. Thus, other characteristics will need to be explored in order to aid in the identification of ovibovine cranial material lacking horncores, since comparison necessarily must be made against specimens containing horncores.

Study Limitations and Future Research

All but one of the fully measured crania in this study were limited to the posterior portion of the skull, and thus comparison with the facial region, which has been noted as different between the two groups (Osgood 1905a), is not possible with this dataset. Future research should prioritize measuring and figuring complete or relatively complete skulls of both male and female *Bootherium* if the difference between *Bootherium* and *Ovibos* are to be better understood.

Another important limitation of this study is that accessible surfaces are not always present in both modern and fossil groups. Important measurements, such as skull breadth posterior to the orbits, are obscured in many modern *Ovibos* specimens where horn sheaths grow over measurement landmarks. Further, due to the presence of extensive exostoses in the males of both *Ovibos* and *Bootherium*, any features which may have been present on the dorsal surface of the skull between the orbits and the occipital crest are absent. It is possible that the lack of potential characters may be complicating our understanding of variation in muskoxen when comparing fossil male individuals to fossil females, and this must be kept in mind when attempting to draw conclusions within this highly sexually dimorphic group.

Regarding *Ovibos*, there is a particular complication when attempting to study the skulls of modern specimens for comparative purposes. Many of these specimens are curated with attached horn sheaths obscuring characters and measurements around the horn cores. Because many fossil muskoxen only retain a sheath-less horncore, this makes a direct comparison of the horns of the animals difficult and renders direct comparison more difficult. An important step in future research will be the analysis of modern *Ovibos* horn cores without the sheath. Because removing horn sheaths from specimens is not an ideal solution, CT scanning and other advanced imaging techniques may be needed to address horn core morphology questions moving forward.

Conclusions

These analyses demonstrate novel methods for separating *Ovibos* from non-*Ovibos* specimens in eastern North America. If previous authors are correct, and *Bootherium* is the only other eastern taxon, then *Ovibos* and *Bootherium* teeth can be distinguished without using size alone as a character. As a general pattern, the molars of "*Bootherium"* are proportionally broader than those of *Ovibos*, and the data collected and reported herein should allow others to assess identification of isolated muskoxen teeth. Additionally, select cranial characteristics serve to differentiate the two genera. Both the breadth across the occipital condyles and the newly proposed cranial elongation ratio have statistical support for their ability to distinguish *Ovibos* from *Bootherium*.

In addition, these analyses support previous conclusions that at least two muskoxen genera occurred in eastern North America during the late Pleistocene. Despite this, there is no current evidence that *Ovibos* occurred further south than the southernmost (unfigured) occurrence at Big Bone Lick, Kentucky or than the published occurrence within Hamilton County, Ohio. If indeed *Bootherium* is the only other ovibovine taxon in eastern North America, then the studied fossil material from Saltville and other sites represents this taxon.

REFERENCES

Allen, JA. 1913. Ontogenetic and other variations in muskoxen, with a systematic review of the muskox group, recent and extinct. *Memoirs of the American Museum of Natural History* 1, 103-226

Barbour, EH. 1934. A new ovibovine*, Symbos convexifrons*, sp. nov. *The Nebraska State Museum Bulletin* 1, 295-298

Blainville, HM de. 1816. Sur plusieurs especes d;animoux mammiferes, de l'ordre des ruminans. *Bulletin des Sciences, par La Societe Philomatique de Paris*. 1816, 73-82

Blair TC, McPherson JG. 1992. The Trollheim alluvial fan and facies model revisited. *Geological Survey of America Bulletin* 104, 762-769

Blair TC, McPherson JG. 1998. Recent debris-flow processes and resultant form and facies of the Dolomite alluvial fan, Owens Valley, California. *Journal of Sedimentary Research* 68, 800-818

Bohlin, B. 1935. Cavicornier der Hipparion-fauna nord Chinas. *Palaentologica Sinica* 9, 1-166

Bover P, Llamas B, Thomson VA, Pons J, Cooper A, Mitchell, KJ. 2018. Molecular resolution to a morphological controversy: The case of North American fossil muskoxen *Bootherium* and *Symbos*. *Molecular Phylogenetics and Evolution* 129, 70-76

Brown, B. 1908. The Conard fissure, a Pleistocene bone deposit in northern Arkansas: With descriptions of two new genera and twenty new species of mammals. *Memoirs of the American Museum of Natural History* 9, 155-208

Bryant, ID. 1983. Facies sequences associated with some braided river deposits of Late Pleistocene age from southern Britain. *Special Publications of the International Association of Sedimentologists* 6, 267-275

Butts, C. 1933. Geologic map of the Appalachian valley with explanatory text. *Virginia Geological Survey Bulletin* 52

Campos, PF. Sher, A. Mead, JI. Tikhonov, A. Buckley, M. Collins, M. Willerslev, E. Gilbert, MTP. 2010. Clarification of the taxonomic relationship of the extant and extinct ovibovids, *Ovibos*, *Praeovibos*, *Euceratherium* and *Bootherium*. Quaternary Science Reviews 19, 2123-2130

Church, M. Jakob, M. 2020. What is a debris flood? *Water Resources Research* 56, e2020WR027144

Clark, GM. Ciolkosz, EJ. 1988. Periglacial geomorphology of the Appalachian highlands and interior highlands south of the glacial border — a review. *Geomorphology* 1, 191-220

Collinson, JD. 1978. Alluvial sediments. *In* Reading, H. G. (ed): *Sedimentary environments and facies*: Blackwell, Oxford, 15-60

Copper, BN. 1966. Geology of the salt and gypsum deposits in the Saltville area, Smyth and Washington counties. *In* Rau, J. L. (ed): *Second Symposium on Salt* 1: Northern Ohio Geological Survey, Cleveland, Ohio, 11-34

Cossman, M. 1907. Proposal to replace *Liops* with *Gidleya*. *Revue Critique de Paleozoologie* 1, 64

Costa, JE. 1994. Physical geomorphology of debris flows. In Costa, J. E. and P. J. Fleischer (ed): *Developments and applications of geomorphology*. Springer-Verlag Berlin, Heidelberg, p. 268-317

Cregut-Bonnoure, E. Dimitrijevic, V. 2006. *Megalovis balcanicus* sp. nov. and *Soergelia intermedia* sp. nov. (Mammalia, Bovidae, Caprinae), new Ovibovini from the Early Pleistocene of Europe. *Revue de Paleobiologie, Geneve* 25, 723-773

Dawkins, WB. 1867. *Ovibos moschatus* (Blainville). *Proceedings of the Royal Society of London* 15, 516-517

DeKay, JE. 1828. Notes on a fossil skull in the cabinet of the Lyceum, of the genus *Bos*, from the banks of the Mississippi; with observations on the American species of that genus. *Annals of the Lyceum of Natural History Museum of New York* 2, 280-291

Delcourt, HR. Delcourt, PA. 1988. Quaternary landscape ecology: Relevant scales in space and time. *Landscape Ecology* 2, 23-44

Domingo, MS. Martin-Perea, D. Domingo, L. Cantero, C. Cantalapiedra, JL, Yelo, BAG. Cano, ARG, Alcalde, GM. Fesharki, O. Fernandez MH. 2017. Taphonomy of mammalian fossil bones from the debris-flow deposits of Somosaguas-north (Middle Miocene, Madrid Basin, Spain). *Palaeogeography, Palaeoclimatology, and Palaeoecology* 465a, 103-121

Eaton, LS. Morgan, BA. Kochel, RC. Howard, AD. 2003. Role of debris flows in long-term landscape denudation in the central Appalachians of Virginia. *Geology* 31, 339-342

Feranec, RS. 2009. Implications of radiocarbon dates from Potter Creek Cave, Shasta County, California, USA. *Radiocarbon* 51, 931-936

Folk, RL. 1980. *Petrology of sedimentary rocks*. Hemphill Publishing Company, Austin, Texas 182 p.

France, CAM., Zelanko, PM. Kaufman, AJ. Holtz, TR. Carbon and nitrogen isotopic analysis of Pleistocene mammals from the Saltville quarry (Virginia, USA): Implications for trophic relationships. *Palaeogeography, Palaeoclimatology, and Palaeoecology* 249, 271-282

French, HM. Millar, SWS. 2014. Permafrost at the time of the last glacial maximum (LGM) in North America. *BOREAS* 43, 667-677

Frick, C. 1937. Horned ruminants of North America. *Bulletin of the American Museum of*

Natural History 69, 669 p.

Gause, ARJ. 2020. Paleoenvironmental reconstruction of Quaternary Saltville, Virginia, using ostracode autoecology. Master's Thesis, Department of Geosciences, East Tennessee State University, Johnson City, Tennessee, 81 p.

Gentry, AW. 2000. An ovibovine (Mammalia, Bovidae) from the Neogene of Stratzing, Austria. *Annalen des Naturhistorischen Museums in Wien* 102 A, 189-199

Geraads, D. Spassov, N. 2008. A new species of Criotherium (Bovidae, Mammalia) from the late Miocene of Bulgaria. *Hellenic Journal of Geosciences* 43, 21-27

Gidley, JW. 1906. A new ruminant from the Pleistocene of New Mexico. *Proceedings of the United States National Museum* 30, 393-396

Gill, T. 1872. Arrangement of the families of mammals with analytical tables. *Smithsonian Miscellaneous Collections* 11, 1-98

Gray, JE. 1872. *Catalogue of ruminant Mammalia (Pecora, Linnaeus) in the British Museum*. Taylor and Francis, London, England.

Groves, P. Shields, GF. 1996. Phylogenetics of the Caprinae based on cytochrome b sequence. *Molecular Phylogenetics and Evolution* 5, 467-476

Groves, P. Shields, GF. 1997. Cytochrome b sequences suggest convergent evolution of the asian takin and arctic muskox. *Molecular Phylogenetics and Evolution* 8, 363-374

Guilday, JE. 1977. Sabertooth cat, *Smilodon floridanus* (Leidy), and associated fauna from a Tennessee cave (40DV40) – the First American Bank site. *Journal of the Tennessee Academy of Science* 52, 84-94

Guthrie, RD. 1992. New paleoecological and paleoethological information on the extinct helmeted muskoxen from Alaska. *Annales Zoologici Fenneci* 28, 175-186

Harington, CR. 1961. History, distribution and exology of the muskoxen. Master's Thesis, Department of Geography, McGill University, Montreal, Quebec, Canada. 489 p.

Harington, CR. 1977. Pleistocene mammals of the Yukon territory. Doctoral Dissertation, Department of Zoology, University of Alberta, Edmonton, Alberta, Canada. 1060 p.

Harlan, R. 1825. *Fauna Americana: Being a description of the mammiferous animals inhabiting North America*. Anthony Finley, Philadelphia, Pennsylvania

Hassanin, A, Pasquet, E. Vigne, J. 1998. Molecular systematics of the subfamily Caprinae (Artiodactyla, Bovidae) as determined from cytochrome b sequences. Journal of Mammalian Evolution 5, 217-236

Hassanin, A. Ropiquet, A. Couloux, A. Cruaud, C. 2009. Evolution of the mitochondrial genome in mammals living at high altitude: New insights from a study of the tribe Caprini (Bovidae, Antilopinae). Journal of Molecular Evolution 68, 293-310

Hay, OP. 1915. Contributions to the knowledge of the mammals of the Pleistocene of North America. *Proceedings of the United States National Museum* 48, 515-575

Hay, OP. 1920. Descriptions of some Pleistocene vertebrates found in the United States. *Proceedings of the United States National Museum* 58, 83-146

Hein, FJ. 1984. Deep-sea and fluvial braded channel conglomerates: a comparison of two case studies. *Canadian Society of Petroleum Geologists Memoir* 10, 33-49

Heiri, O. Lotter, AF. Lemcke, G. 2001. Loss on ignition as a method for estimating organic and carbonate content in sediments: reproducibility and comparability of results. *Journal of Paleolimnology* 25, 101-110

Hesse, CJ. 1942. The genus *Bootherium*, with a new record of its occurrence. *Bulletin of the Texas Archeological and Paleontological Society* 14, 77-87

Hibbard, CW. Hinds, FJ. 1960. A radiocarbon date for a woodland musk ox in Michigan. *Papers of the Michigan Academy of Science, Arts, and Letters* 45, 103-111

Hicken, EJ. 1993. Fluvial facies models: a review of Canadian research. *Progress in Physical Geography* 17, 205-222

Holman, JA. McDonald, JN. 1986. A late Pleistocene herpetofauna from Saltville, Virginia. *Brimleyana* 12, 85-100

Jefferson, T. 1781. Notes on the state of Virginia. W. W. Norton and Co., New York, 315 p.

Karatson, D., Sztano, O. and T. Telbisz. 2002. Preferred clast orientation in volcaniclastic mass-flow deposits: application of a new photo-statistical method. *Journal of Sedimentary Research* 72, 823-835

Knotterus-Meyer, T. 1907. Uber das tranenbein der Huftiere. Vergleichend-anatomischer beitrag zur systematik der rezenten ungulata. *Archiv fur Naturgeschichte* 1907, 1-152

Kodama, Y. 1994. Downstream changes in the lithology and grain size of fluvial gravels, the Watarase River, Japan: Evidence of the role of abrasion in downstream fining. *Journal of Sedimentary Research* 64, 68-75

Kolfschoten, T van. Vervoort-Kerkhoff, Y. 1999. The Pleistocene and Holocene mammalian assemblages from the Maasvlakte near Rotterdam (The Netherlands) with special reference to the ovibovini *Soergelia minor* and *Praeovibos* cf. *P. priscus*. *Deinsea* 7, 369-381

Kulander, BR. Dean, SL. 1986. Structure and tectonics of central and southern Appalachian valley and ridge and plateau provinces, West Virginia and Virginia. *The American Association of Petroleum Geologists Bulletin* 70, 1674-1684

Kurtén, B. Anderson, E. 1980. Pleistocene mammals of North America. Colombia University

Press, New York, New York 442 p.

Lancaster, ST. Underwood, EF. Frueh, WT. Sediment reservoirs at mountain stream confluences: dynamics and effects of tributaries dominated by debris-flow and fluvial processes. *Geological Society of America Bulletin* 122, 1775-1786

Landler, L. Ruxton, GD. Malkemper, EP. 2019. The Hermans-Rasson test as a powerful alternative to the Rayleigh test for circular statistics in biology. *BMC Ecology* 19:30 8 p.

Lazaridus, G. Kostopoulos, DS. Lyras, G. Roussiakis, S. 2017. A new Late Miocene ovibovine-like bovid) Bovidae, Mammalia) from the Kassandra Peninsula (Chalkidiki, Northern Greece) and implications to the phylogeography of the group. *Palaontologische Zeitschrift* 91, 427-437

Leidy, J. 1852a. Remarks on two crania of extinct species of ox. *Proceedings of the Academy of Natural Sciences of Philadelphia* 6, 71

Leidy, J. 1852b. Memoir on the Extinct Species of American Ox. *Smithsonian Contributions to Knowledge* 5, 20 p.

Leidy, J. 1854. Remarks on the question of the identity of *Bootherium cavifrons* with *Ovibos moschatus* or *O. maximus*. *Proceedings of the Academy of Natural Sciences of Philadelphia* 7, 209-210

Lönnberg, E. 1900. On the structure and anatomy of the musk-ox. *Proceedings of the zoological Society of London* 1900, 686-718

Agostinelli, C. Lund, U. 2017. R package 'circular': circular statistics-0.4-93 https://r-forge.r-project.org/projects/circular/

MacPhee, RDE. Greenwood, AD. 2007. Continuity and change in the extinction dynamics of Late Quaternary muskox (*Ovibos*): Genetic and radiometric evidence. *Bulletin of*

Carnegie Museum of Natural History 39, 203-212

Martin, RA. 1980. Body mass and basal metabolism of extinct mammals. *Comparative Biochemistry and Physiology Part A* 66, 307-314

Martinez-Navarro, B. Sardella, R. Rook, L. Bellucci, L. Ros-Montoya, S. 2012. First occurrence of Soergelia (Ovibovini, Bovidae, Mammalia) in the Early Pleistocene of Italy. *Quaternary International* 267, 98-102

Matschie, P. 1898. Die systematische stellung von *Budorcas* Hodgson. Sitzungsberichte der Gesellschaft Natuforschender Freunde zu Berlin 1898, 30-32

McDonald, HG. Davis, RA. 1989. Fossil muskoxen of Ohio. *Canadian Journal of Zoology* 67, 1159-1166

McDonald, JN. 1984a. Paleoecological investigations at Saltville, Virginia. *Current Research in the Pleistocene* 1,77-78

McDonald, JN. 1984b. The Saltville, Virginia, locality: A summary of research and field trip guide. Symposium on the Quaternary of Virginia 1984, 45 p.

McDonald, JN. 1985a. Late Quaternary deposits and paleohydrology of the Saltville, Valley, Southwest Virginia. *Current Research in the Pleistocene* 2, 123-124

McDonald JN. 1985b. Valley-bottom stratigraphy of Saltville, Virginia and its paleoecological implications. *National Geographic Society Research Reports* 21, 191-296

McDonald, JN. 2000. An outline of the Pre-Clovis archeology of SV-2, Saltville, Virginia, with special attention to a bone tool dated 14,510 yr BP. *Jeffersonia* 9, 60 p.

McDonald, JN. Bartlett, CS. 1983. An associated musk ox skeleton from Saltville, Virginia. *Journal of Vertebrate Paleontology* 2, 453-470

McDonald, JN. Ray, CE. 1989. The autochthonous North America musk oxen *Bootherium*,

Symbos, and *Gidleya* (Mammalia: Artiodactyla: Bovidae). *Smithsonian Contributions to Paleobiology* 66, 77 p.

Miall, AD. 1977. A review of the braided-river depositional environment. *Earth-Science Reviews* 13, 1-62

Mol, D. Vos, J de. Reumer, JWF. 1999. *Praeovibos priscus* (Bovidae, Artiodactyla, Mammalia) from the North Sea and aspects of its paleoecology. In Reumer, J. W. F. and de Vos, J. (eds): Elephants have a snorkel! Papers in honour of Paul Y Sondaar. Deinsea, Rotterdam, Netherlands, p. 223-232

Needham, RS. Stuart-Smith, PG. 1987. Coronation hill U-Au mine, south Alligator Valley, Northern Territory: an epigenetic sandstone-type deposit hosted by debris-flow conglomerate. *Journal of Australian Geology and Geophysics* 10, 121-131

Nelson, BW. 1973 Mineralogy of the Maccrady Formation near Saltville, Virginia. *American Journal of Science* 273, 539-563

Nelson, KJP. Nelson, FE. Walegur, MT. 2007. Periglacial Appalachia: Paleoclimatic significance of blockfield elevation gradients, eastern USA. *Permafrost and Periglacial Processes* 18, 61-73

Nelson, ME. Madsen Jr, JH. 1987. Occurrence of the musk ox *Symbos cavifrons*, from southeastern Idaho and comments on the genus *Bootherium*. *The Great Basin Naturalist* 47, 239-251

Osgood, WH. 1905a. *Scaphoceros tyrrelli*, an extinct ruminant from the Klondike gravels. *Smithsonian Miscellaneous Collections* 48, 173-186

Osgood, WH. 1905b. *Symbos*, a substitute for *Scaphoceros*. *Proceedings of the Biological Society of Washington* 18, 223-224

Owen, R. 1856. Description of a fossil cranium of the musk-buffalo [*Bubalus moschatus*, Owen; *Bos moschatus* (Zimm & Gmel), Pallas; *Bos pallasii* DeKay; *Ovibos pallassii*, H. Smith & Bl.] from the "lower level drift" at Maidenhead, Berkshire. *Proceedings of the Geological Society of London* 12, 124-130

Peterson, OA. 1917. A fossil bearing alluvial deposit in Saltville Valley, Virginia. *Annals of the Carnegie Museum* 11, 469-474

Pettijohn, FJ. 1975. Sedimentary rocks 2nd edition. Harper and Row, New York, New York, 628 p.

Prothero, DR., and Schwab, F. 1966. *Sedimentary Geology. An introduction to sedimentary rocks and stratigraphy*. W. H. Freeman, New York, New York, 575 p.

Pycke, JR. 2010. Some tests for uniformity of circular distributions powerful against multimodal alternatives. *Canadian Journal of Statistics* 38, 80-96

Ray, CE. Cooper, BN. Benninghoff. WS. 1967. Fossil mammals and pollen in a late Pleistocene deposit at Saltville, Virginia. *Journal of Paleontology* 41, 608-622

Rhoads, SN. 1897. Notes on a living and extinct species of North American Bovidae. *Proceedings of the Academy of Natural Sciences of Philadelphia*. 49, 483-502

Richards, RL. McDonald, JN. 1991. New records of Harlan's muskox (*Bootherium bombifrons*) and an associated fauna from the Late Pleistocene of Indiana. *Proceedings of the Indiana Academy of Science* 99, 211-228

Richardson, J. 1852. The zoology of the voyage of H.M.S. Herald, under the command of Captain Henry Kellett, R. N., C. B. during the years 1845-51. Lovell Reeve, Longon, England. 171 p.

Rogers, RR. 2005. Fine-grained debris flows and extraordinary vertebrate burials in the Late

Cretaceous of Madagascar. *Geology* 33, 297-300

Saula, E. Mato, EE. Puigdefabregas, C. 2002. Catastrophic debris-flow deposits from an inferred landslide-dam failure, Eocene Berga Formation, eastern Pyrenees, Spain. *Special Publications of the International Association of Sedimentologists* 32, 195-209

Schlunegger, F. Garefalakis, P. 2018. Clast imbrication in coarse-grained mountain streams and stratigraphic archives as indicator of deposition in upper flow regime conditions. *Earth Surface Dynamics* 6, 743-761

Schneider, CA. Rasband, WS. Eliceiri, KW. 2012. NIH to ImageJ: 25 years of image analysis. *Nature methods* 9, 671-675

Schubert, BW. Wallace, SC. 2009. Late Pleistocene giant short-faced bears, mammoths, and large carcass scavenging in the Saltville Valley of Virginia, USA. *BOREAS* 38, 482-492

Schultz, CB. Tanner, LG. Whitmore Jr, FC. Ray, LL. 1963. Paleontologic investigations at Big Bone Lick State Park, Kentucky: A preliminary report. *Science* 142, 1167-1169

Scott, KM. Yuyi, W. 2004. Debris flows – geologic process and hazard illustrated by a surge sequence at Jiangjia ravine, Yunnan, China. US Geological Survey Professional Paper 1671, 26 p.

Semken, HA. Miller, BB. Stevens. JB. 1964. Late Wisconsin woodland musk ox in association with pollen and invertebrates from Michigan. *Journal of Paleontology* 38, 823-835

Shi, Q. 2013. New species of *Tsaidamotherium* (Bovidae, Artiodactyla) from China sheds new light on the skull morphology and systematics of the genus. Science China Earth Sciences 57, 258-266

Shi, Q. He, W. Chen, S. 2014. A new species of Shaanxispira (Bovidae, Artiodactyla) from the upper Miocene of China. *Zootaxa* 3794, 501-513

Shi, R. Sun, Y. Teng, L. Liu, Z. 2015. Complete mitochondrial genome of red goral (*Naemorhedus baileyi*) and a complete estimate of the phylogenetic relationships in Caprinae. *Mitochondrial DNA Part A* 27, 2721-2722

Silverstein, R. 2017. A paleontological analysis of Late Pleistocene Proboscidea from Saltville, Virginia: taphonomy, systematic paleontology, and paleobiology. Master's Thesis, East Tennessee State University, Johnson City, Tennessee, 73 p.

Simpson, EMB. 2019. Paleoecology and land-use of Quaternary megafauna from Saltville, Virginia. Master's Thesis, Department of Geosciences, East Tennessee State University, Johnson City, Tennessee, 96 p.

Smith, ND. 1970. The braided stream depositional environment: comparison of the Platte River with some Silurian clastic rocks, north-central Appalachians. *Geological Society of America Bulletin* 81, 2993-3014

Sohn, YK. Rhee, CW. Kim, BC. 1999. Debris flow and hyperconcentrated flood-flow deposits in an alluvial fan, northwestern part of the Cretaceous Yongdong Basin, central Korea. *Geology* 107, 111-132

Solounias, N. 1981. The Turolian Fauna from the island of Samos, Greece with special emphasis on the hyaenids and the bovids. *Contributions to Vertebrate Evolution* 6, 1-232

Stock, C. Furlong, EL. 1927. Skull and skeletal remains of a ruminant of the *Preptoceras-Euceratherium* group from the McKittrick Pleistocene, California. *University of California Bulletin of the Department of Geological Sciences* 16, 409-434

Stoval, JW. 1937. *Euceratherium bizzelli*, a new ungulate from Oklahoma. *Journal of Paleontology* 11, 450-455

Vander Linden, A. Dumont, ER. 2019. Ultraspecific male combat behaviour predicts

morphology of cervical vertebrae in ruminant mammals. *Proceedings of the Royal Society B* 286, 20192199

von den Driesch, A. 1976. A guide to the measurement of animal bone from archaeological sites. *Peabody Museum Bulletin* 1, 138 p.

Watson, TL. 1907. Mineral resources of Virginia. The Virginia Jamestown Exposition Commission, Lynchburg, Virginia, 618 p.

West, AR. 2016. Multidisciplinary investigations on the origins and evolution of the extinct ungulate order Notoungulata (Mammalia: Placentalia) and the extinct muskox genus *Bootherium* (Mammalia: Artiodactyla: Bovidae). Doctoral Dissertation, Colombia University, New York, New York, 353 p.

Whisonant, RC. 1996. Geology and the Civil War in southwestern Virginia: The Smyth County salt works. *Virginia Minerals* 42, 21-30

Wieczorek, GF. Mossa, GS. Morgan, BA. 2004. Regional debris-flow distribution and preliminary risk assessment from severe storm events in the Appalachian Blue Ridge Province, USA. *Landslides* 1, 53-59

Wistar, C. 1818. An account of two heads found in the morass, called the Big Bone Lick, and presented to the Society, by Mr. Jefferson. *Transactions of the American Philosophical Society* 31, 375-380

Yagashita, K. 1997. Paleocurrent and fabric analyses of fluvial conglomerates of the Paleogene Noda group, northeast Japan. *Sedimentary Geology* 109, 53-71

Yong Technology Inc. 2020. Georose 0.5.1-rose plot software. http://www.yongtechnology.com/download/georose

Zimmerman, EAW. 1780. *Geographische geschichte des menschen und der allgemein*

verbreiteten vierfussingen theire. 2, 496 p. Weygan, Leipzig, Germany

APPENDIX: Muskoxen Cranial and Dental Raw Measurements

Specimen	Identification	Measurement 1	Measurement 2	Measurement 3	Measurement 4	Measurement 7	Measurement 16 L/R	Measurement 20 L/R	Measurement 21 L/R	Measurement 22 L/R	Measurement 25	Measurement 26	Measurement 26A	Measurement 27	Measurement 28	Measurement 31	Measurement 32	Measurement 33	Measurement 33A	Measurement 34	Measurement 35	Measurement 37	Measurement 38	Measurement 42	Measurement 43	Measurement 46 L/R	Measurement 45 L/R	Posterior Protrusion of Orbit	Posterior Cranial Length	Cranial Elongation Ratio	Angle 1	Angle 2
USNM 291202	*Ovibos m. wardi*	289.72	478.4	451.4	333.435	250.115	157.975 / 147.895	136.85 / 136.545	87.98 / 87.975	51.51 / 51.95	183.23	125.53	104.485	169.025	34.045	8	138.655	224.535	261.96	130.66	144.25	107.75	121.55	555.675	570.635	117.865 / 113.32	214.725 / 214.1	289.72	215.03	1.347	151	143.5
USNM 291025	*Ovibos moschatus*	292.305	434.75	402.84	246.665	228.76	148.7 / 147.935	130.09 / 130.855	85.45 / 85.5	56.7 / 56.7	157.99	114.345	98.005	137.265	38.295	11.195	131.165	178.505	221.105	133.875	131.36	80.52	115.035	496.545	441.82	99.71 / 25.1	91.77 / 100.62	292.305	210.79	1.387	166.5	122.5
USNM 291029	*Ovibos m. wardi*	210.565	430.18	401.245	298.145	221.985	147.785 / 147.115	135.85 / 135.78	84.955 / 85.03	52.055 / 55.565	153.655	111.485	99.585	136.34	37.74	9.59	124.585	176.225	216.355	109.71	124.745	79.355	111.175	469.235	508.59	31.185 / 27.645	103.21 / 94.93	210.565	121.845	1.728	152	118
USNM 256968	*Ovibos moschatus*	230.505	457.54	416.77	309.915	238.94	153.2 / 146.12	130.57 / 133.335	82.07 / 79.955	48.04 / 52.305	154.615	111.72	105.935	128.46	38.78	16.015	113.52	173.34	212.495	111.2	110.41	78.98	112.905	410.345	447.525	34.99 / 27.385	91.195 / 91.42	230.505	139.72	1.578	155.5	118.5
USNM 252504	*Ovibos m. wardi*	246.95	449.02	417.955	318.39	227.44	140.95 / 146.275	139.545 / 137.695	85.45 / 85.42	54.05 / 55.775	162.3	118.64	108.59	135.715	43.96	9.37	116.61	194.81	235.695	119.26	136.93	83.065	116.27	582.43	594.39	52.685 / 62.03	157.235 / 170.75	246.95	141.61	1.744	146.5	119.5
USNM 275090	*Ovibos m. wardi*	308.145			340.92			142.43 / 138.54	86.545 / 90.05	49.735 / 55.445	162.665	134.05	112.31	149.69	39.455	8.975		207.79	244.1	130.86	145.415		121.13	645.07	629.135	95.905 / 101.965	198.2 / 209.48	308.145	168.775	1.826	135	107.5
USNM 108722	*Ovibos m. moschatus*	297.125	434.07	389.49	310.53	219.19	121.14 / 122.905	132.785 / 131.59	86.335 / 84.72	52.375 / 48.79	182.62	95.4	117.22	149.505	34.375	10.665		198.115	236.035	150.01	137.91	86.98	111.555	295.215	321.445	101.015 / 108.115	215.32 / 211.38	297.125	239.885	1.239	139	110
USNM 399993	*Ovibos m. wardi*	205.485	407.74	381.555	282.35	211.05	134.7 / 134.925	136.165 / 138.37	88.69 / 86.98	57.26 / 53.37	141.005	104.685	91.46	120.8	36.445	98.405	106.535	147.815	193.095	101.35	115.315	74.9	100.69	216.145	222.08		61.055 / 57.15	205.485	138.075	1.488	151.5	119
USNM V 13606	*Symbos cavifrons (=Bootherium)*						/ 173.665		/ 109.28	69.14 / 67.745																							
USNM V 8574	*Bootherium bombifrons*	239.145									206.665	156.925	134.615	190.78	35.92	0	142.795	217.44	242.035	120.18					509.955	73.46 / 74.985	111.675 / 110.475	239.145	198.79	1.203	135.5	
USNM V 2516	*Symbos tyrrell (=Bootherium)*											140.37		157.38	40.09	39.075	107.56									60.72 / 63.665	109.225 / 106.31	200.56	196.215	1.022	156	149
USNM V 23488	*Bootherium sargenti*															277.18	198.125	162.705						498.025	550.77	66.98 / 72.025	76.78 / 80.315	195.425	140.235	1.394		
USNM V 372807	*Symbos cavifrons (=Bootherium)*															101.525	117.525								283.615	69.405 / 68.44	95.125 / 101.95	193.76	198.995	0.974		87.5
USNM V 215066	*Bootherium*											126.45	106.35		41.215	139.615	101.96							492.93	436.66	61.83 / 69.135	71.75 / 72.5	218.82	183.575	1.192	142	127.5
USNM V 23577	*Symbos cavifrons (=Bootherium)*										228.83	151.63	134.81	192.775	45.58	44.76									387.76	87.785 / 81.375	136.93 / 117.7				144.5	151.5
USNM V 23264	*Bootherium*										194.815	143.015	121.645		46.095	74.66	113.71							512.11	538.155	76.905 / 77.14	94.49 / 98.605	208.14	171.735	1.212		136.5
USNM V 23787	*Unknown*								120.705 /																							
USNM V 636245-1	*Unknown*																															
INSM 71.1.70	*Bootherium*										216	141	152	195	39.4		150		264						554			201.85	167.325	1.218	149	117
"MSP" Bootherium	*Bootherium*											148			46.4		140														148	128
AMNH F-AM A-20404254	*Symbos (=Bootherium)*																											225.18	184.445	1.221		
UUVP 8540	*Symbos cavifrons (=Bootherium)*																											227.215	185.705	1.224		
ANSP 994 = USNM 215066	*Bos bombifrons (=Bootherium)*																											175.56	147.505	1.190		
USNM 2501	*Scaphiceros tyrrelli (=Bootherium)*																											217.34	162.385	1.338		
USNM 2324	*Bootherium miocenus*																											163.78	133.17	1.230		
USNM 347215	*Bootherium*																											142.185	117.735	0.991		
AMNH F-AM 33124	*Symbos cavifrons (=Bootherium)*																											197.035	173.995	1.132		
AK Fish and Game Skull	*Ovibos moschatus*																											289.145	161.17	1.794		
USNM 291028	*Ovibos moschatus*																											211.675	152.85	1.385		

Specimen	Identification	P2 OB L/R	P3 OB L/R	P4 OB L/R	M1 OB L/R	M2 OB L/R	M3 OB L/R	P2 OL L/R	P3 OL L/R	P4 OL L/R	M1 OL L/R	M2 OL L/R	M3 OL L/R	P2 BB L/R	P3 BB L/R	P4 BB L/R	M1 BB L/R	M2 BB L/R	M3 BB L/R	P2 BL L/R	P3 BL L/R	P4 BL L/R	M1 BL L/R	M2 BL L/R	M3 BL L/R	P2 CH L/R	P3 CH L/R	P4 CH L/R	M1 CH L/R	M2 CH L/R	M3 CH L/R	P2 MH L/R	P3 MH L/R	P4 MH L/R	M1 MH L/R	M2 MH L/R	M3 MH L/R
USNM 291202	Ovibos m. wardi	10.73 / 10.925	14.97 / 15.22	15.37 / 18.2	18.88 / 19.1	20.375 / 20.21	17.515 / 16.685	15.095 / 16	19.305 / 18.545	20.35 / 19.66	24.725 / 22.395	30.31 / 29.895	34.245 / 35.155	12.04 / 10.95	16.695 / 16.345	18.24 / 18.57	19.46 / 19.385	21.925 / 20.9	15.74 / 16.815	14.885 / 14.355	12.645 / 13.43	14.095 / 13.39	16.19 / 16.25	28.725 / 23.295	34.275 / 35.365							18.26 / 14.285	16.045 / 15.39	17.925 / 18.955	20.205 / 19.225	20.08 / 18.6	14.955 / 16.055
USNM 291025	Ovibos moschatus	11.33 / 10.375	15.685 / 14.82	16.8 / 16.105	20.51 / 20.015	19.85 / 20.64	16.11 / 17.89	18.305 / 17.565	19.735 / 19.485	19.765 / 19.42	24.515 / 24.685	30.96 / 31.345	32.21 / 32.39	11.34 / 12.245	17.81 / 17.68	18.105 / 18.825	21.44 / 20.155	22.65 / 22.1	18.78 / 18.75	14.885 / 15.36	16.265 / 17.18	15.01 / 14.605	17.92 / 19.29	29.145 / 28.58	33.86 / 34.015							17.625 / 17.85	14.845 / 16.08	18.315 / 17.335	16.32 / 19.975	20.53 / 20.25	15.075 / 13.98
USNM 291029	Ovibos m. wardi	10.43 / 10.685	14.245 / 14.35	13.985 / 16.545	20.395 / 19.45	20.09 / 19.415	16.7 / 16.46	15.96 / 16.345	19.525 / 19.07	17.11 / 18.79	24.285 / 24.07	29.795 / 29.595	31.785 / 33.13	12.965 / 13.05	19.155 / 17.615	19.78 / 17.25	20.175 / 19.72	19.835 / 20.745	16.875 / 18.04	15.055 / 16.07	15.125 / 17.31	15.655 / 16.4	17.685 / 18.86	29.51 / 28.505	33.145 / 32.8							14.23 / 11.13	15.2 / 12.485	16.155 / 15.525	17.39 / 16.34	14.56 / 15.435	12.705 / 12.565
USNM 256969	Ovibos moschatus	10.3 / 11.035	14.775 / 16.24	16.76 / 16.405	20.645 / 19.02	21.24 / 20.755	15.525 / 18.445	17.39 / 19.64	19.06 / 18.77	20.525 / 19.78	25.95 / 20.87	28.635 / 25.68	32.355 / 31.02	11.45 / 11.435	15.805 / 15.87	17.705 / 17.505	20.24 / 19.94	19.36 / 20.775	20.855 / 20.565	14.58 / 12.335	18.065 / 17.485	13.035 / 13.315	16.13 / 16.225	20.7 / 17.01	31.69 / 32.58	16.44 / 10.885	19.655 / 20.245	20.15 / 17.255	18.895 / 12.085	16.99 / 11.365	25.93 / 20.16						
USNM 252504	Ovibos m. wardi	9.535 / 9.53	14.94 / 14.205	16.505 / 16.505	19.455 / 19.4	18.48 / 19.43	14.34 / 14.9	15.29 / 13.785	18.715 / 17.5	20.095 / 20.64	21.505 / 24.77	29.96 / 28.18	31.945 / 31.155	11.85 / 12.26	15.245 / 15.04	17.105 / 18.165	20.465 / 21	20.085 / 21.775	17.905 / 19.78	13.99 / 11.615	16.275 / 18.92	16.12 / 17.53	19.405 / 23.685	27.475 / 30.535	33.605 / 34.53							11.82 / 13.05	12.405 / 19.665	15.15 / 14.34	17.675 / 17.42	17.555 / 13.97	13.4 / 11.44
USNM 275099	Ovibos m. wardi	/ 10.735	14.91 / 15.165	15.9 / 17.29	17.325 / 17.93	19.845 / 20.73	18.3 / 18.68	/ 15.39	18.81 / 18.435	19.99 / 18.625	23.12 / 23.07	31.075 / 30.15	33.7 / 34.07	/ 11.1	16.515 / 16.71	18.945 / 19.005	21.69 / 20.985	23.285 / 23.145	20.815 / 19.215		15.81 / 13.265	14.71 / 13.07	18.03 / 18.615	29.285 / 27.275	35.66 / 36.365							15.93 / 13.405	17.68 / 16.985	15.06 / 14.48	16.655 / 14.53	13.365 / 12.195
USNM 108722	Ovibos m. moschatus	13.87 / 11.25	14.54 / 16.295	15.805 / 16.665	19.96 / 19.195	19.085 / 18.97	18.24 / 17.955	13.48 / 15.53	16.97 / 17.78	17.685 / 19.165	26.48 / 25.82	28.63 / 29.765	31.525 / 30.845	11.67 / 13.27	15.58 / 15.79	16.495 / 16.3	21.49 / 20.42	19.75 / 19.325	17.92 / 18.235	12.63 / 14.29	16.185 / 14.605	14.87 / 14.535	20.53 / 21.095	26.88 / 28.18	33.16 / 32.78							12.37 / 17.275	13.17 / 18.585	16.025 / 18.765	19.84 / 19.19	18.755 / 18.385	16.75 / 15.265
USNM 399693	Ovibos m. wardi	9.413 / 10.545	12.685 / 14.15	14.385 / 12.785	16.73 / 17.41	18.14 / 17.875	14.08 / 12.44	13.445 / 15.07	16.71 / 17.535	19.78 / 18.225	25.6 / 23.67	33.125 / 32.12	31.765 / 29.65	11.755 / 13.285	15.04 / 16.105	16.29 / 17.97	18.025 / 18.815	15.535 / 18.715	14.425 / 15.325	14.505 / 14.49	16.5 / 16.79	21.785 / 16.56	22.985 / 21.525	30.525 / 30.42	33.21 / 31.37							15.09 / 17.545	15.955 / 16.575	18.675 / 14.59	18.795 / 17.355	18.115 / 16.34	13.45 / 14.02
USNM V 13696	Symbos cavifrons				26.36 /	32.11 / 24.785	/ 23.46				30.58 /	38.44 / 36.98	/ 39.485				27.995 /	30.72 / 30.495	/ 25.84					24.55 /	29.465 / 28.8	/ 39.61			21.485 /	31.33 / 31.84	/ 28.29						
USNM V 533096	Bootherium						19.74 /						36.225 /						29.27 /							35.615 /					46.05 /						
USNM V 636245-1	Unknown						27.94 /						43.56 /						35.695 /							39.8 /					29.005 /						
ETMNH 19793	Unknown				/ 16.24						/ 26.79						/ 18.875							/ 22.375					/ 18.875								
ETMNH 15423-A	Bootherium				/ 18.67						/ 22.335						/ 24.49							/ 17.775					/ 30.46								
ETMNH 15423-B	Bootherium					/ 21.985						/ 31.425						/ 27.33							/ 24.19					/ 30.46							
ETMNH 15423-C	Bootherium						/ 21.01						/ 35.92						/ 28.455						/ 31.49						/ 39.985						
King Leo LP4	Bootherium															24.3 /						19.1 /															
King Leo RP4A	Bootherium															/ 21.7						/ 19.8															
King Leo RP4B	Bootherium															/ 24.2						/ 20.6															
King Leo RM2	Bootherium																	/ 28						/ 30.4													
King Leo RM3	Bootherium																		/ 27.8						/ 41.8												

Specimen	Identification	p2 OB L/R	p3 OB L/R	p4 OB L/R	m1 OB L/R	m2 OB L/R	m3 OB L/R	p2 OL L/R	p3 OL L/R	p4 OL L/R	m1 OL L/R	m2 OL L/R	m3 OL L/R	p2 BB L/R	p3 BB L/R	p4 BB L/R	m1 BB L/R	m2 BB L/R	m3 BB L/R	p2 BL L/R	p3 BL L/R	p4 BL L/R	m1 BL L/R	m2 BL L/R	m3 BL L/R	p2 CH L/R	p3 CH L/R	p4 CH L/R	m1 CH L/R	m2 CH L/R	m3 CH L/R	p2 MH L/R	p3 MH L/R	p4 MH L/R	m1 MH L/R	m2 MH L/R	m3 MH L/R
USNM 291202	*Ovibos m. wardi*	6.185 /	8.395 / 9.225	11.695 / 12.98	14.835 / 14.235	16.315 / 14.835	14.575 / 14.095	8.385 /	15.96 / 14.86	20.395 / 19.2	23.345 / 23.84	28.225 / 28.29	42.31 / 41.04	7.225 / 5.09	9.71 / 10.09	12.44 / 12.77	14.665 / 15.02	16.96 / 16.83	15.665 / 15.545	8.58 / 5.435	11.375 / 11.01	17.805 / 17.495	19.405 / 20.945	24.645 / 25.665	40.87 / 42.775							9.715 /	10.96 / 11.635	21.58 / 16.585	22.395 / 16.95	20.8 / 18.835	18.69 / 17.32
USNM 291025	*Ovibos moschatus*	5.295 / 5.85	9.3 / 8.195	12.32 / 13.27	14.87 / 15.27	14.2 / 14.955	12.475 / 13.16	7.83 / 7.915	14.27 / 15.185	21.665 / 20.835	24.405 / 24.54	28.32 / 28.66	40.89 / 40.93	6.88 / 5.91	9.99 / 9.095	13.145 / 12.62	16.46 / 16.635	17.56 / 17.67	15.355 / 15.27	9.4 / 9.57	12.82 / 14.11	18.705 / 19.37	21.065 / 21.55	24.99 / 26.72	41.235 / 41.835	10.395 / 11.765							12.875 / 12.13	20.23 / 14.485	20.32 / 16.665	19.41 / 18.535	19.12 / 16.67
USNM 291029	*Ovibos m. wardi*	4.97 / 5.475	8.52 / 8.36	12.165 / 12.2	14.765 / 14.57	15.28 / 14.515	13.2 / 13.255	11.08 / 10.36	14.885 / 15.065	19.235 / 19.16	24.305 / 22.21	27.33 / 25.65	38.655 / 39.095	7.385 / 7.225	9.405 / 9.32	12.835 / 12.7	15.38 / 15.615	16.48 / 15.72	14.84 / 14.395	8.71 / 8.1	12.635 / 12.02	18.24 / 18.805	22.465 / 21.65	27.12 / 24.505	39.67 / 39.33							9.87 / 6.44	11.46 / 8.485	14.175 / 15.08	17.87 / 16.705	17.51 / 18.07	16.505 / 15.68
USNM 256969	*Ovibos moschatus*	5.35 / 5.775	9.505 / 8.67	12.58 / 13.78	15.405 / 14.82	15.67 / 17.215	14.55 / 14.5	7.645 / 9.71	15.06 / 15.195	17.53 / 20.06	22.885 / 22.88	26.555 / 23.88	40.99 / 38.59	6.96 / 6.865	10.24 / 9.414	13.32 / 13.26	14.915 / 14.58	17.635 / 17.035	17.77 / 17.095	8.515 / 7.365	14.62 / 12.275	16.39 / 17.275	19.935 / 19.545	24.16 / 23.53	38.845 / 37.295	11.375 / 6.68	13.9 / 10.135	13.18 / 11.98	14.435 / 12.48	15.225 / 9.965	16.465 / 17.365						
USNM 252504	*Ovibos m. wardi*	3.905 / 4.845	8.875 / 8.67	11.985 / 11.91	15.37 / 15.555	15.185 / 14.915	12.5 / 12.585	5.115 / 6.51	16.205 / 15.46	18.07 / 18.38	24.54 / 25.01	29 / 27.73	36.39 / 35.95	7.15 / 6.695	9.805 / 9.785	13.71 / 13.31	15.105 / 15.455	17.09 / 16.535	14.71 / 14.205	7.87 / 7.965	13.845 / 13.425	19.085 / 17.345	21.295 / 20.985	25.75 / 25.68	38.15 / 37.04							6.955 / 6.135	11.005 / 10.95	14.39 / 13.775	19.295 / 16.895	18.845 / 15.625	15.93 / 18.2
USNM 275099	*Ovibos m. wardi*	6.995 / 6.605	9.56 / 9.51	11.565 / 11.88	15.47 / 14.635	15.47 / 15.415	15.645 / 16.155	9.8 / 7.945	14.57 / 14.745	19.385 / 18.935	23.36 / 22.255	26.465 / 27.81	41.685 / 42.675	6.555 / 6.22	9.65 / 8.975	12.855 / 12.2	15.995 / 15.585	18.38 / 17.16	17.5 / 17.775	8.71 / 8.405	13.11 / 12.235	18.125 / 18.11	21.37 / 20.56	26.165 / 25.315	40.135 / 41.825	6.705 / 5.845	/ 8.35						8.5 /	13.965 / 13.48	18.54 / 14.27	15.985 / 14.905	15 / 13.685
USNM 108722	*Ovibos m. moschatus*	4.75 / 4.235	8.21 / 7.585	10.875 / 10.9	14.005 / 14.225	13.11 / 14.175	13.54 / 12.405	11.23 / 11.72	15.42 / 14.92	19.67 / 18.6	24.71 / 24.84	28.79 / 27.935	37.26 / 34.795	7.51 / 7.5	9.645 / 8.98	12.49 / 12.77	16.725 / 15.085	15.775 / 16.17	13.71 / 14.96	8.785 / 8.64	13.82 / 12.84	18.875 / 18.025	23.565 / 23.7	27.115 / 27.265	37.4 / 38.15	/ 12.09	/ 13.2					12.93 /	14.005 /	16.685 / 14.67	19.075 / 18.05	19.71 / 22.315	16.855 / 18.545
USNM 399993	*Ovibos m. wardi*	4.73 / 4.84	6.945 / 7.51	10.095 / 10.9	12.46 / 12.825	13.365 / 12.425	11.165 / 10.47	8.815 / 8.53	14.74 / 14.58	19.805 / 20.045	25.17 / 24.955	31.985 / 31.585	37.8 / 38.195	7.315 / 6.61	8.56 / 8.45	12.25 / 12.37	14.58 / 14.38	14.76 / 14.71	13.49 / 14.04	7.665 / 7.73	12.465 / 12.935	18.135 / 19.675	22.92 / 22.555	26.92 / 28.24	38.3 / 38.52							8.975 / 10.25	13.175 / 12.785	16.44 / 16.965	20.1 / 120.995	21.57 / 21.035	19.85 / 20.275
USNM V 437774	*Boatherium bombifrons*						/ 17.745						/ 44.4						/ 21.205						/ 43.655					/ 54.89						
USNM V 467587	*Boatherium bombifrons*						/ 22.33						/ 30.27						/ 23.485						/ 35.75					/ 27.695						
USNM V 23787	*Unknown*			16.215 /	18.665 /	17.815 /	18 /			28.525 /	28.085 /	36.99 /	49.73 /			18.785 /	21.495 /	23.68 /	21.33 /			19.99 /	25.185 /	24.585 /	48.715 /			29.62 /	25.3 /	47.92 /	57.275 /			17.715 /	15.335 /	22.23 /	21.58 /
USNM V 636245-2	*Unknown*				20.5 /						39.715 /						31.325 /						29.93 /						41.505 /								
King Leo Lp2	*Boatherium*													11.5 /						12.2 /																	
King Leo Rp2	*Boatherium*													/ 11.6						/ 12.5																	
King Leo Lp3	*Boatherium*														14.6 /						19.6 /																
King Leo Lm1	*Boatherium*																17.9 /						26.2 /														
King Leo Lm2	*Boatherium*																	22.2 /						31.2 /													
King Leo Rm2	*Boatherium*																	/ 24.1						/ 30.2													
King Leo Rm3	*Boatherium*																		/ 22						/ 52.1												

VITA

NICKOLAS A. BRAND

Education:	M.S. Geosciences, East Tennessee State University, Johnson City, Tennessee, 2021
	B.S. Geology, Appalachian State University, Boone, North Carolina, 2018
Professional Experience:	Graduate Assistant, East Tennessee State University, College of Arts and Science, 2018-2020
	Field Chief, East Tennessee State University, Department of Geosciences, 2019
	Collections Intern, East Tennessee Museum of Natural History and Gray Fossil Site, 2019
Presentations:	Brand NA. Widga C. Schubert BW. 2020. Musk ox measurements: Differentiating the teeth and crania of the fossil woodland musk ox *Bootherium* from the tundra musk ox *Ovibos*. Digital Poster. Society of Vertebrate Paleontology.
	Brand NA. Haugrud SJ. 2019. Breaking clay: Testing the efficacy of hydrogen peroxide aided screenwashing at the Pliocene Gray Fossil Site. Association for Materials and Methods in Paleontology. Oral Presentation.

Brand NA. Heckert AB. Foster JR. Hunt-Foster RK. 2017. The microvertebrate fossil assemblage of the Upper Cretaceous (Campanian-Maastrichtian) Williams Fork Formation, western Colorado. Society of Vertebrate Paleontology. Poster.

Brand NA. Heckert AB. Foster JR. Hunt-Foster RK. 2017. The Upper Cretaceous (Campanian-Maastrichtian) J&M site: The microvertebrate fossil assemblage of the Williams Fork Formation, N.W. Colorado. Southeastern Association of Vertebrate Paleontology. Oral Presentation.

Honors and Awards:

Presidential Scholarship, Department of Environmental Science and Public Policy, George Mason University, 2020

McCarty Student Travel Grant, Association for Materials and Methods in Paleontology, 2019